Timber Structure

Inspection and maintenance planning of timber structures concerning climate change implementing reinforcement learning

Sasipa Vichitkraivin

5765668

Course:

Building Technology Graduation Studio

MSc Architecture, Urbanism and Building Sciences

Mentor:

First Mentor: Prof. Dr. Mauro Overend, Structural Design

Second Mentor: Dr. Charalampos Andriotis, Computational Intelligence

Special Advisor: Dr. Ming Shan Ng (Charmaine), Timber Structure

TU Delft

Contents

1

Introduction

Problem statement

Wood, a timeless and versatile material, has played a pivotal role in constructing structures across diverse cultures throughout history. It is employed in heritage structures featuring wood-wood connections that can date back hundreds or thousands of years (van Nimwegen & Latteur, 2023).

As a hygroscopic material, timber exhibits sensitivity to environmental factors such as light, temperature, and moisture. Moreover, it is susceptible to biological factors including fungi and insects. This leads to a gradual decline in both physical and mechanical characteristics, adversely impacting the stability and safety of wooden structures (Xin et al., 2022). The increasing effects of climate change pose a significant challenge to the long-term performance and structural integrity of timber elements in construction, particularly in historical buildings. The evolving climatic conditions can lead to complex changes in the mechanical properties of timber, necessitating a proactive approach to inspection and maintenance planning.

Traditional methods of assessing timber structures have not been shown to adapt to the dynamic nature of climate change impacts on this hydro-sensitive material. Moreover, current practices require time-consuming processes and mainly rely on the individual experiences and skills of inspectors. Recognizing the potential effectiveness of machine learning, there is an opportunity to leverage this technology to develop a nuanced understanding of the evolving condition of timber structures. This proactive approach has the potential to significantly enhance timber inspection processes and optimize maintenance planning.

This master's thesis addresses the intricate relationship between climate change, timber sensitivity, and the maintenance challenges in traditional construction. The central focus is on leveraging machine learning methodologies to create an optimized maintenance model tailored to the unique characteristics of timber. By harnessing the power of machine learning, this research aims to enhance the accuracy and efficiency of inspection planning, allowing for timely interventions to preserve the structural integrity and longevity of timber structures in the face of climate-induced variations. The proposed model will not only contribute to the field of timber engineering but will also provide a scalable and adaptable solution for sustainable construction practices in the context of evolving climate patterns.

Research Questions

As per the problem statement, the main research question is articulated. To address the main research question, several subordinate research questions are posed as outlined below.

Main research question:

"How can machine learning consider climate change effects to inform inspection and maintenance for timber structures?"

Sub-Research questions:

- What are the key factors that significantly influence timber structural degradation and what are their processes?
- How does climate change impact timber degradation factors and how does it result in the alteration in the mechanical properties of timber?
- What are the current inspection and maintenance methods of historical timber structures?
- Which machine learning (ML) model is most suitable for assessing timber strength and planning the maintenance needs of timber structures?
- How can the ML model be optimized to provide accurate and reliable planning?
- How can the model planning be validated and evaluated?
- What measures can be taken to ensure the interpretability of the machine learning models for practical application in maintenance planning?

Research framework

Designing machine learning models that can be effectively applied to predict inspection and maintenance planning for timber structures while considering the impact of climate change on the mechanical properties of timber.

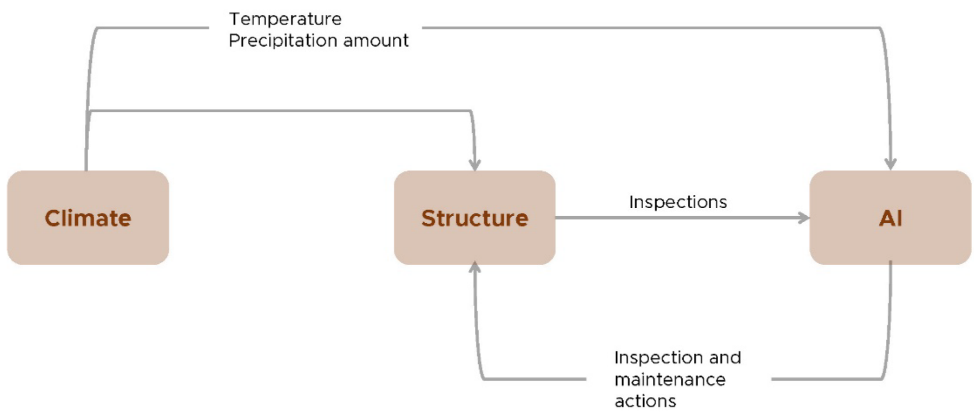

Figure 1.1: Dynamic Policy Framework under climate change (Own work)

Methodology

The research objective is to set up a framework that cooperates with the climate alteration, degradation of timber structures, and optimal inspection & maintenance planning. The making of inspection & maintenance plans relies on the climate scenarios and structural conditions. The framework that is set up will be implemented in the selected case study. The outcome policies will be compared with the traditional expert-based heuristic policies as an evaluation. In the end, the results gained from the framework will be analyzed to answer the research questions and will lead to the conclusion and further discussion.

The outline and workflow of this research can be elaborated as follows:

1. **Background Knowledge and Relevant Data Collection:**
   Conduct an extensive literature review on the scope of timber mechanical properties, its deterioration factors and process, climate change and its effects on timber, inspection and maintenance methods, dynamic policy framework set up under the specific conditions, and the possible machine learning methods that can be implemented into the framework. The sources are obtained from both online platforms and printed books.

2. **Framework Strategy Planning:**
   The information and data that are acquired from the literature review will be utilized to establish the framework. The framework is structured into three primary stages to establish the optimal sequence of inspection and maintenance actions. Initially, it involves setting up the physical model of the structural components. Following this, the Decentralized Partially Observable Markov Decision Process (Dec-POMDP) is configured. The final stage focuses on determining the optimal policy. This framework integrates climate scenarios and the stochastic deterioration of various structural elements to facilitate these decisions.

3. **Case Study Selection and Structural Analysis:**

A case study is selected based on the information available in the historical inspection and maintenance records in the archive section at the Kyoto Institute of Technology in Kyoto, Japan. This case study will be analyzed in the Finite Element Model. Its results will be utilized to set up the structural deterioration model which is one of the essential parts of the Dec-POMDP framework.

4. **Machine Learning Framework Execution:**
   The framework will be applied based on the selected case study information. Then, the Multi-Agent Reinforcement Learning (MARL) will be executed to solve the Dec-POMDP framework.

5. **Evaluation and Discussion:**
   The benchmark of the framework is set concerning the traditional method namely, expert-based heuristic policies where the outcome policies will be discussed and analyzed. In addition, the policies considering climate change different from the original policies will be, too, analyzed and discussed in terms of their effectiveness. Eventually, the conclusions will be drawn, the limitations will be stated, and the potential further studies will be suggested.

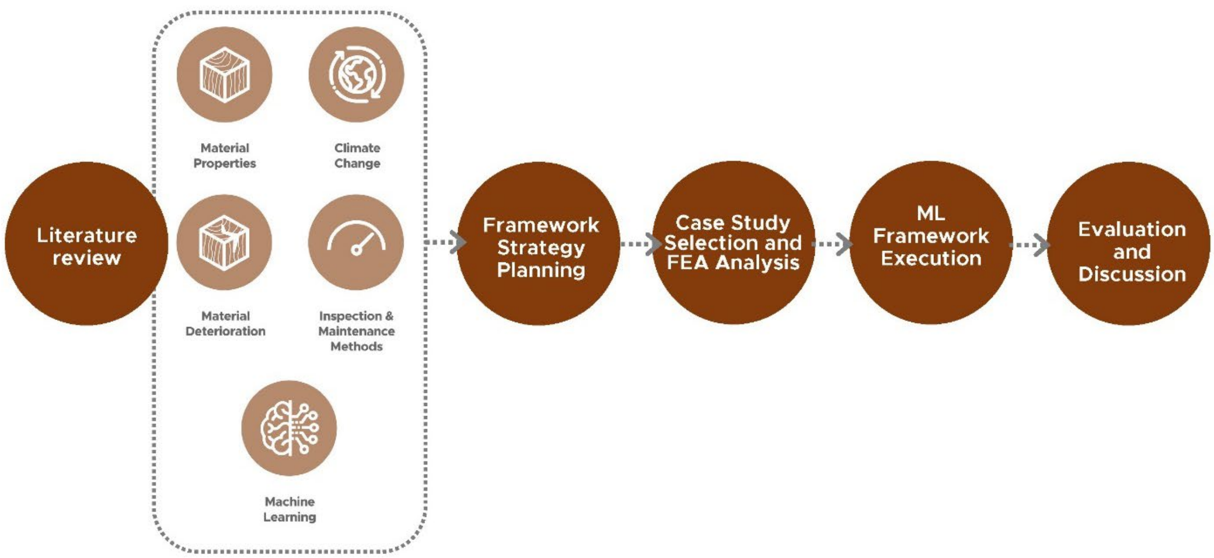

Figure 1.2: Research outline and workflow (Own work)

Research methods

The methodologies employed in this study encompass a comprehensive approach, integrating various research techniques to ensure a thorough investigation of the subject matter. These methods include a literature review, data collection from archival records, interviews, onsite visits, and consultation with mentors.

1. **Literature Review:**

This initial step involves a systematic review of existing literature, serving as a foundational element of the research. The literature review aids in narrowing down the scope of the study by identifying key areas and concepts pertinent to the research questions. It provides essential background information and helps frame the subsequent stages of the research.

2. **Data Collection from Archival Records**:
   Considering the need to select a case study based on the availability of information, this research method is crucial. The Kyoto Institute of Technology houses a significant archive with extensive data on the inspection and maintenance of historical timber structures in Japan. This archival information is instrumental for the study, offering a rich source of historical data.

3. **Interviews:**
   To further detail the specific methods used in the inspection and maintenance of timber structures, interviews are conducted. These are particularly vital as the archival records often lack comprehensive details about the processes involved. Engaging with professionals from companies that specialize in these maintenance activities provides deeper insights, helping to bridge the information gap identified in the historical records.

4. **Onsite Visits:**
   Observing the actual buildings where maintenance work has been performed offers practical insights that are not always apparent in the documentation. These visits allow for the examination of physical evidence and traces of maintenance procedures, enhancing the understanding of the practical applications and outcomes of the theoretical methods discussed in the literature and archives.

5. **Mentorship and Guidance:**
   The research process is overseen and guided by three main mentors, each expert in a distinct aspect relevant to the study: structural integrity, timber construction, and computational analysis. Their expertise provides a multidimensional perspective on the research, ensuring a balanced approach and enhancing the scientific rigor of the study.

This combination of diverse research methods supports a holistic exploration of the topic, enabling a well-rounded understanding of both theoretical and practical elements involved in the inspection and maintenance of historical timber structures.

2

Literature Review

Theories

1. Mechanical properties of timber
2. Climate change
    - Illustrative climate scenarios
    - Timber Deterioration and the Effect of Climate Change on Timber Structure
3. Methods of timber monitoring, testing, and grading
4. Optimal inspection and maintenance policies
    - IMP-MARL method: Multi-agent reinforcement learning (MARL) for large-scale Infrastructure Management Planning (IMP)

1. Mechanical properties of timber

Timber is an orthotropic material which means its mechanical properties are dependent on the direction of the grain. The directions of three mutually perpendicular axes are Longitudinal (L), Radial (R), and Tangential (T) (Gedeon, 1999).

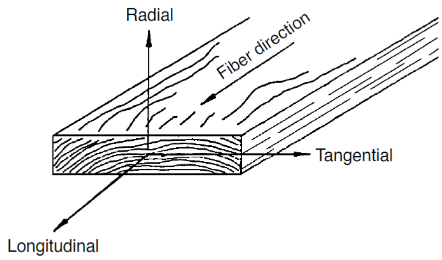

Figure 2.1: Three principal axes of wood concerning grain direction and growth rings (Gedeon, 1999)

$\sigma_L >> \sigma_R > \sigma_T$

Strength of Timber

Timber can withstand various types of stresses being central to its utility in construction and manufacturing. The strength of timber refers to the stress measured from the maximum force exerted at the point of failure, or at a specific strain level, such as 2% strain when pressure is applied perpendicular to the wood fibers. This measure provides critical insight into the load-bearing capacity and resilience of the wood under different conditions.

The evaluation of timber's strength is primarily categorized based on the speed of the applied load, distinguishing between static and dynamic strength. Static strength pertains to the timber's resistance to loads that increase gradually, leading to failure at a slower rate. This type of strength test replicates conditions where timber is subjected to sustained weight or pressure, mirroring common scenarios in building structures. In contrast, dynamic strength is concerned with the wood’s response to swiftly changing or repeated loads. Examples include the impact of bending forces or the stresses of cyclical loads as evaluated in tests like the Wöhler test for fatigue. These dynamic conditions are crucial for assessing the performance of timber in environments where it is exposed to shocks or oscillating forces (Niemz et al., 2023).

Additionally, the direction of the load relative to the wood's natural grain also significantly impacts its strength. Timber's strength varies when forces are applied in different directions—longitudinal (along the grain: L), radial (R), and tangential (T) as previously mentioned. The types of strength characterized in these contexts include tensile strength, which measures the force required to pull the wood apart; compressive strength, which gauges the wood's ability to resist compression; bending strength; shear strength, which involves sliding layers of wood over each other; splitting strength, which tests the wood's resistance to being split apart; and torsional strength, concerning its ability to withstand twisting forces.

Beyond these primary categories, timber’s strength properties also extend to its capacity to hold fasteners such as nails and screws — referred to as nail and screw pull-out resistance. This characteristic is crucial for applications involving connections and joints in construction. Furthermore, the hardness and abrasion resistance of timber are essential factors in determining its suitability for flooring and other surfaces subject to wear. Each of these strength properties plays a vital role in defining the appropriate uses of timber in various engineering and architectural applications, ensuring safety, durability, and performance.

Failure Criteria of Timber

In assessing the strength of timber as a construction material, the basic principles outlined in EN 1995-1-1 Eurocode 5 are pivotal. According to this standard, the stress in a timber component is calculated as the ratio of force to the cross-sectional area (σ = Force / Area). When this stress exceeds the intrinsic strength of the timber, the component is deemed to have failed, as it cannot sustain the load without risk of damage or structural failure. Additionally, the bending strength of timber is evaluated through the bending moment when bending moment (σ_m) = Moment (M) $\times$ y / I, where ' y ' represents the distance from the neutral axis to the fiber furthest from it, and ' I ' is the moment of inertia of the cross-section. If this bending moment surpasses the Modulus of Rupture (MOR), which is the maximum stress the material can withstand in static bending, the component is also considered failed.

In terms of design considerations, Ultimate Limit States (ULS) focus on ensuring the safety of people and the structure itself, calculating forces from design loads that include safety factors of 1.35 for permanent actions (dead loads: G_k) and 1.5 for variable actions (live loads: Q_k). Thus, the loads that are taken into consideration $= 1.35G_k + 1.5Q_k$. Conversely, Serviceability Limit States (SLS) is concerned with the structure's functionality, user comfort, and aesthetic integrity under normal usage. SLS criteria necessitate a distinction between reversible and irreversible conditions, verifying aspects like deformations, vibrations, and potential damage that could impair the structure's appearance, durability, or functionality. This comprehensive approach ensures that timber structures are both safe and effective for their intended uses, adhering to stringent standards for load-bearing and user interaction.

2. Climate change

Climate refers to the long-term patterns of weather conditions in a specific region or globally. It can be described as the statistic of weather in terms of the mean and variation of relevant factors, for example, seasonal temperature, rainfall averages, and wind patterns. Climate change is the long-term alteration of the climate, as defined by the World Meteorological Organization (WMO), for a time of 30 years (IPCC, 2023b).

Illustrative Climate Scenarios

This study relies on climate projection data sourced from Coupled Model Inter-comparison Projects (CMIP6), a compilation of global climate models under the auspices of the World

Climate Research Program. CMIP6 data serves as a cornerstone of the IPCC's Sixth Assessment Report, providing insights into future climate trends. The Intergovernmental Panel on Climate Change (IPCC), a United Nations committee, is tasked with evaluating climate change science, and proposing projections of future climate change per the different scenarios.

Climate scenarios embedded within this dataset are the Shared Socio-economic Pathways (SSPs), each denoted as SSPx-y. These pathways represent a spectrum of socio-economic trajectories ('x') alongside levels of radiative forcing ('y') in watts per square meter, or W m-2 projected for the year 2100. They were designed to encapsulate diverse challenges related to climate mitigation and adaptation.

This project's analysis adopts illustrative scenarios based on SSPs. These scenarios integrate socio-economic assumptions, climate mitigation efforts, land use changes, and air pollution controls. They are shown in the levels of GHG emissions in the table below (IPCC, 2023a).

SSPx-y	GHG emissions scenarios	Description
SSP1-2.6	Low	limit warming to 2°C (>67%)
SSP2-4.5	Intermediate	limit warming to 3°C (>50%)
SSP3-7.0	High	limit warming to 4°C (>50%)
SSP5-8.5	Very high	limit warming to 4°C (>50%)

Table 2.1: Scenarios and pathways across AR6 Working Group reports

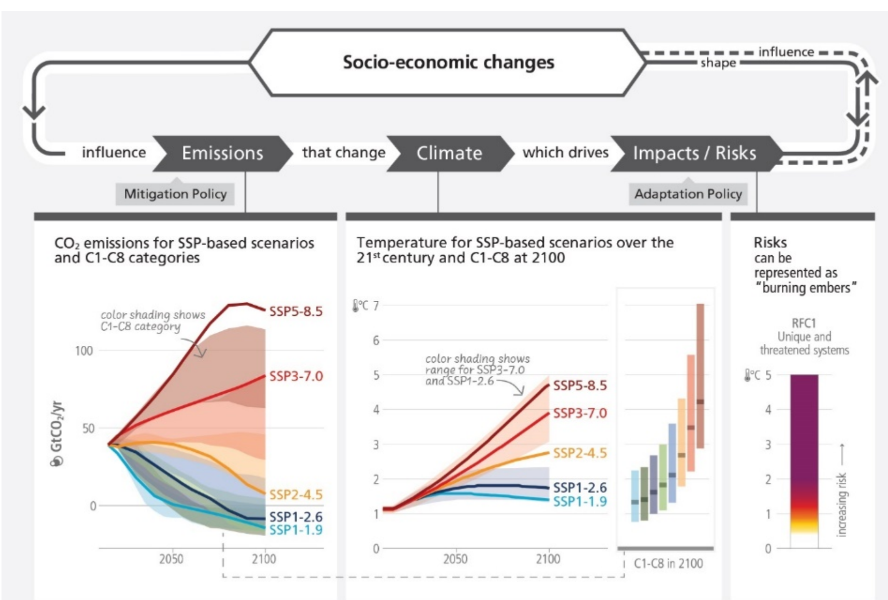

Figure 2.2: AR6 integrated assessment framework on future climate, impacts, and mitigation (IPCC, 2023a)

The Climate Change Knowledge Portal (CCKP), provided by the World Bank Group, offers climate scenarios for various countries, including Japan, based on the previously mentioned analysis.

Each scenario is represented through data projected over five distinct periods: historical reference (1950-2014), 2020 to 2039, 2040 to 2059, 2060 to 2079, and 2080 to 2099. This portal displays information on several climate metrics such as the average maximum (90th percentile), minimum (10th percentile), and mean (median) surface air temperatures, as well as precipitation levels.

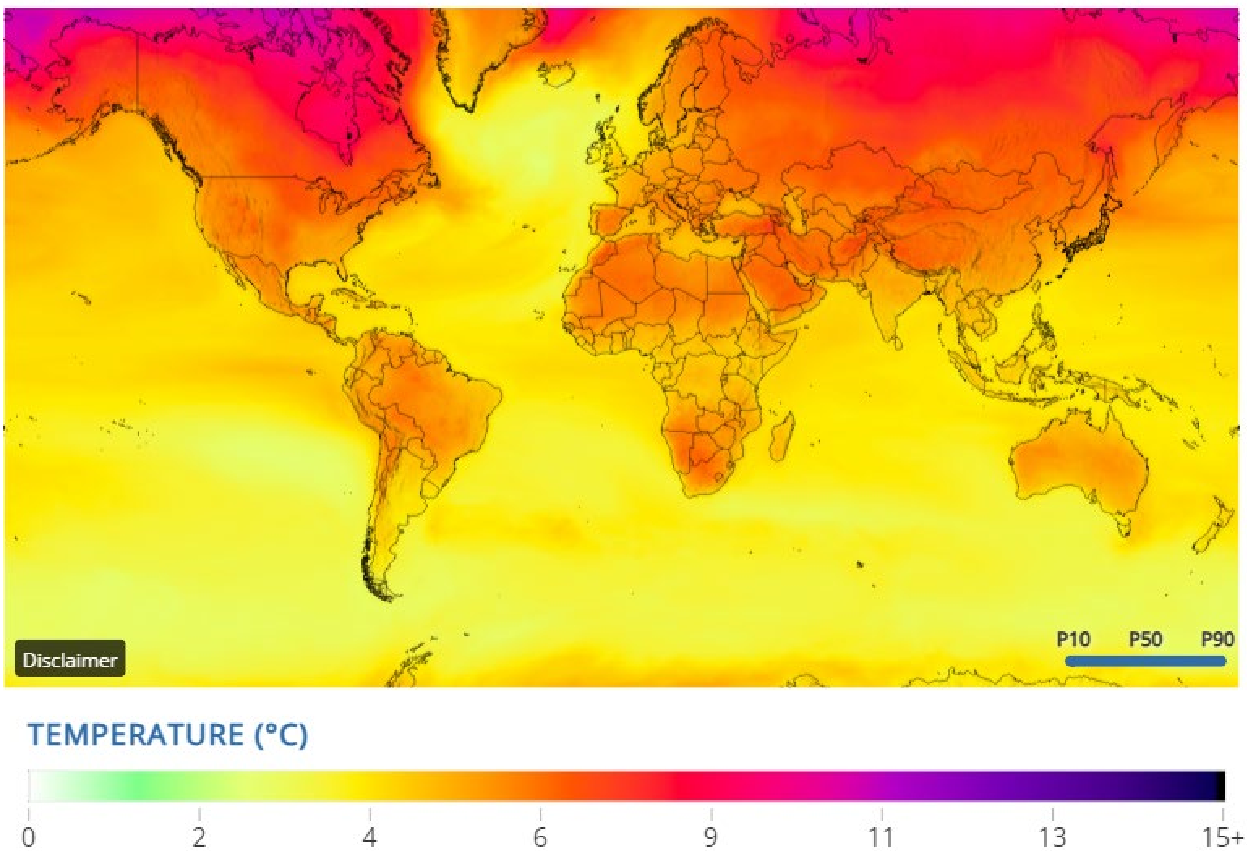

Figure 2.3: Projected Average Mean Surface Air Temperature Anomaly for 2080-2099 (Annual) globally; (Ref. Period: 1950-2014), SSP5-8.5, Multi-Model Ensemble (source: https://climateknowledgeportal.worldbank.org/country/japan/climate-data-projections)

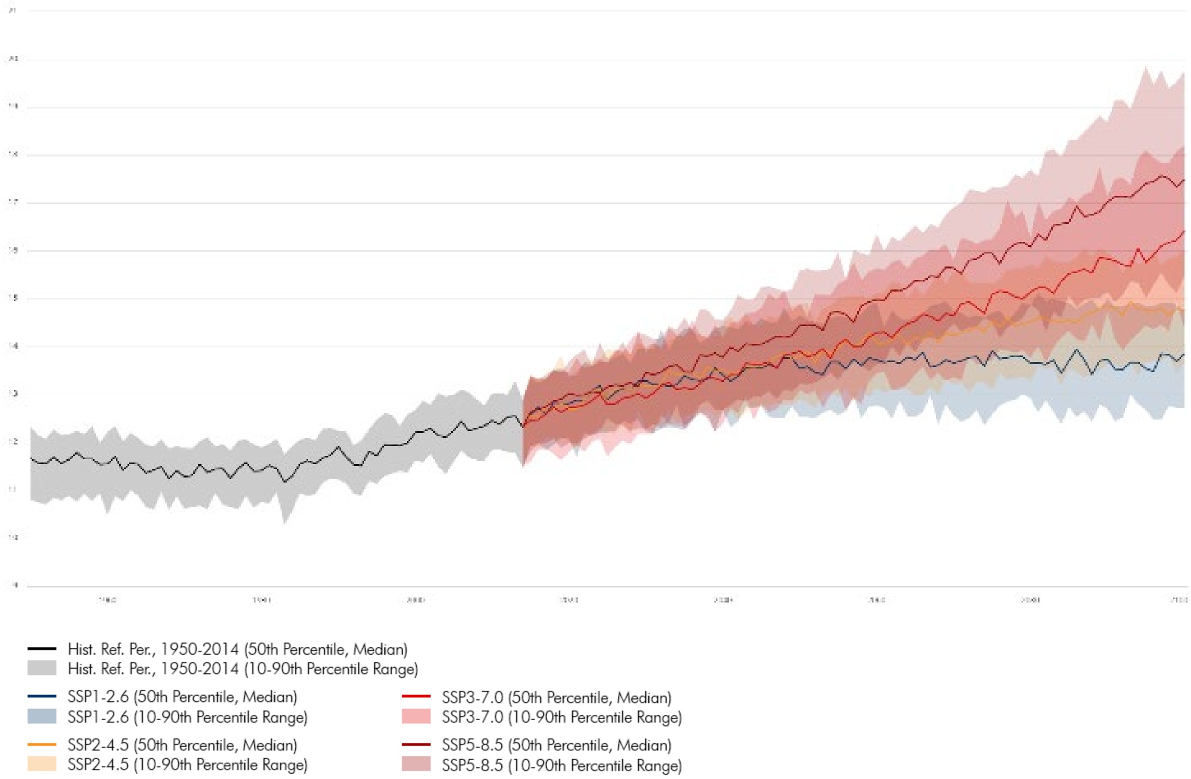

Figure 2.4: Projected Average Mean Surface Air Temperature Japan; (Ref. Period: 1950-2014), Multi-Model Ensemble (source: https://climateknowledgeportal.worldbank.org/country/japan/climate-data-projections)

	1951-1960	1961-1970	1971-1980	1981-1990	1991-2000	2001-2010	2011-2020	2021-2030	2031-2040	2041-2050	2051-2060	2061-2070	2071-2080	2081-2090	2091-2100
Jan	-0.55 °C	-0.83 °C	-0.71 °C	-0.62 °C	-0.42 °C	0.02 °C	0.41 °C	0.78 °C	1.31 °C	1.71 °C	2.36 °C	3.07 °C	3.49 °C	4.46 °C	4.96 °C
Feb	-0.56 °C	-0.82 °C	-0.93 °C	-0.72 °C	-0.59 °C	0.05 °C	0.43 °C	0.83 °C	1.18 °C	1.82 °C	2.29 °C	3.03 °C	3.66 °C	4.21 °C	4.90 °C
Mar	-0.56 °C	-0.74 °C	-0.87 °C	-0.70 °C	-0.44 °C	0.10 °C	0.31 °C	0.78 °C	1.35 °C	1.62 °C	2.58 °C	2.96 °C	3.62 °C	4.32 °C	4.92 °C
Apr	-0.61 °C	-0.72 °C	-0.79 °C	-0.72 °C	-0.26 °C	0.06 °C	0.23 °C	0.68 °C	1.27 °C	1.73 °C	2.21 °C	2.77 °C	3.22 °C	3.81 °C	4.62 °C
May	-0.64 °C	-0.68 °C	-0.69 °C	-0.71 °C	-0.35 °C	0.04 °C	0.24 °C	1.01 °C	1.39 °C	1.72 °C	2.28 °C	3.00 °C	3.52 °C	4.34 °C	4.80 °C
Jun	-0.65 °C	-0.89 °C	-0.78 °C	-0.88 °C	-0.41 °C	0.01 °C	0.31 °C	1.01 °C	1.43 °C	1.74 °C	2.27 °C	3.16 °C	3.67 °C	4.42 °C	4.76 °C
Jul	-0.75 °C	-0.85 °C	-0.96 °C	-0.87 °C	-0.54 °C	-0.02 °C	0.57 °C	0.95 °C	1.16 °C	1.69 °C	2.26 °C	3.06 °C	3.68 °C	4.36 °C	5.13 °C
Aug	-0.72 °C	-0.95 °C	-0.90 °C	-0.89 °C	-0.51 °C	-0.05 °C	0.50 °C	0.86 °C	1.46 °C	1.87 °C	2.49 °C	3.12 °C	3.75 °C	4.56 °C	5.36 °C
Sep	-0.85 °C	-1.02 °C	-1.09 °C	-0.78 °C	-0.48 °C	0.03 °C	0.46 °C	1.03 °C	1.42 °C	1.97 °C	2.50 °C	3.37 °C	3.83 °C	4.96 °C	5.67 °C
Oct	-0.78 °C	-0.95 °C	-0.84 °C	-0.76 °C	-0.44 °C	0.04 °C	0.34 °C	0.97 °C	1.57 °C	1.93 °C	2.62 °C	3.30 °C	4.21 °C	5.00 °C	5.55 °C
Nov	-0.80 °C	-0.90 °C	-0.82 °C	-0.71 °C	-0.45 °C	0.06 °C	0.34 °C	0.74 °C	1.14 °C	1.81 °C	2.46 °C	3.02 °C	3.90 °C	4.57 °C	5.50 °C
Dec	-0.73 °C	-0.94 °C	-0.78 °C	-0.66 °C	-0.45 °C	-0.01 °C	0.22 °C	0.68 °C	1.19 °C	1.90 °C	2.44 °C	3.20 °C	3.64 °C	4.59 °C	4.98 °C

Figure 2.5: Projected Average Mean Surface Air Temperature (Anomaly) in Japan; (Ref. Period: 1950-2014), SSP5-8.5, Multi-Model Ensemble (source: https://climateknowledgeportal.worldbank.org/country/japan/climate-data-projections)

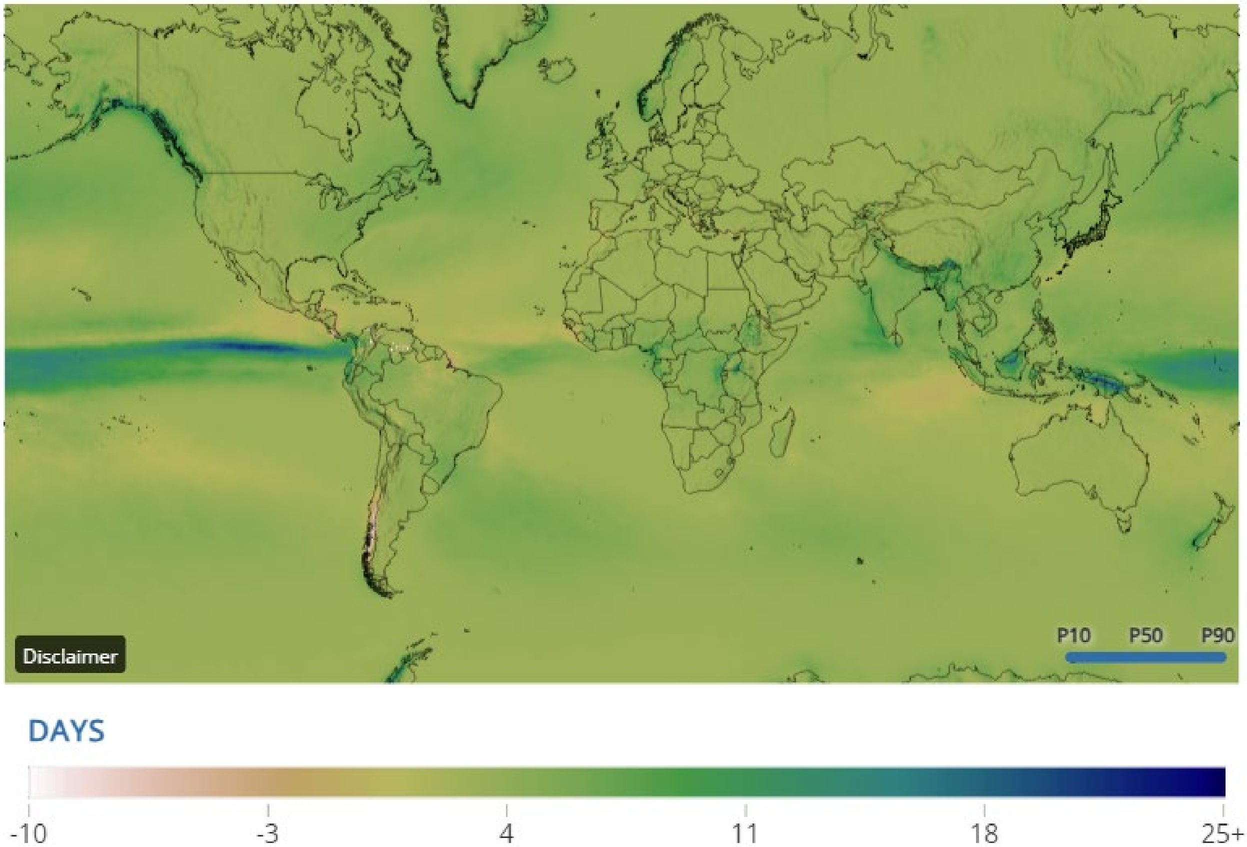

Figure 2.6: Projected Number of Days with Precipitation >20mm Anomaly for 2080-2099 (Annual) globally; (Ref. Period: 1950-2014), SSP5-8.5, Multi-Model Ensemble (source: https://climateknowledgeportal.worldbank.org/country/japan/climate-data-projections)

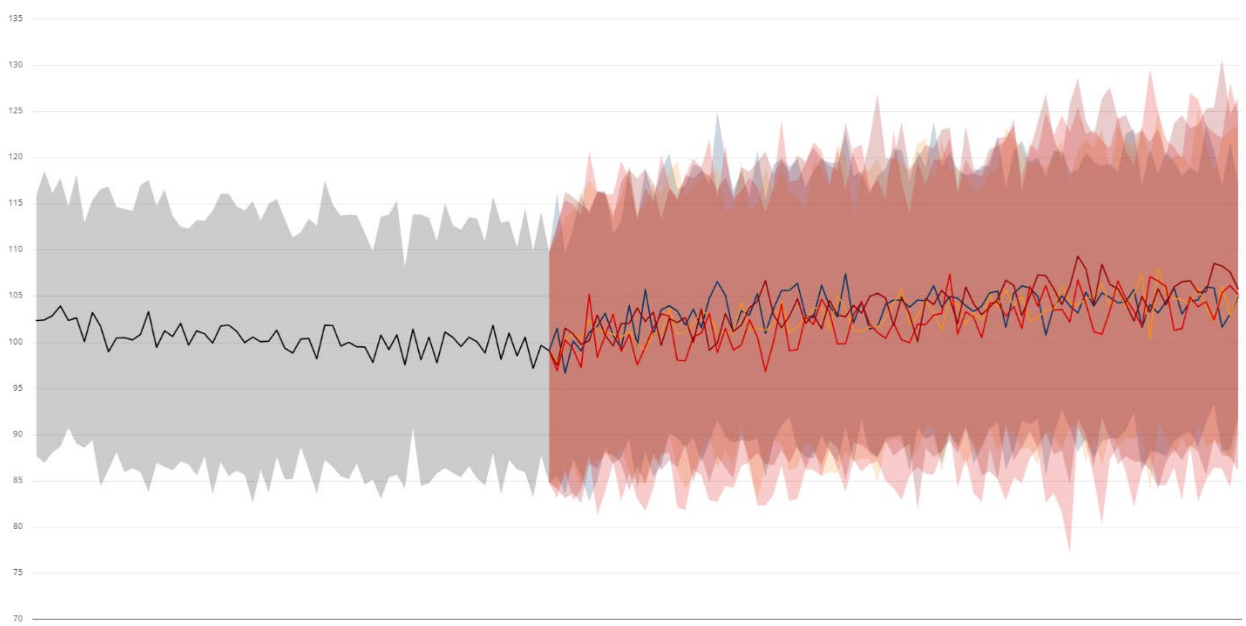

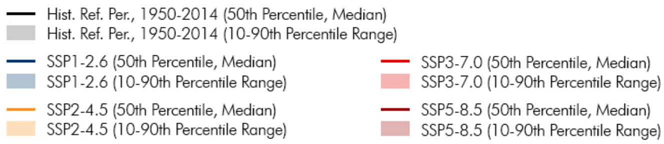

Figure 2.7: Projected Number of Days with Precipitation >20mm Japan; (Ref. Period: 1950-2014), Multi-Model Ensemble (source: https://climateknowledgeportal.worldbank.org/country/japan/climate-data-projections)

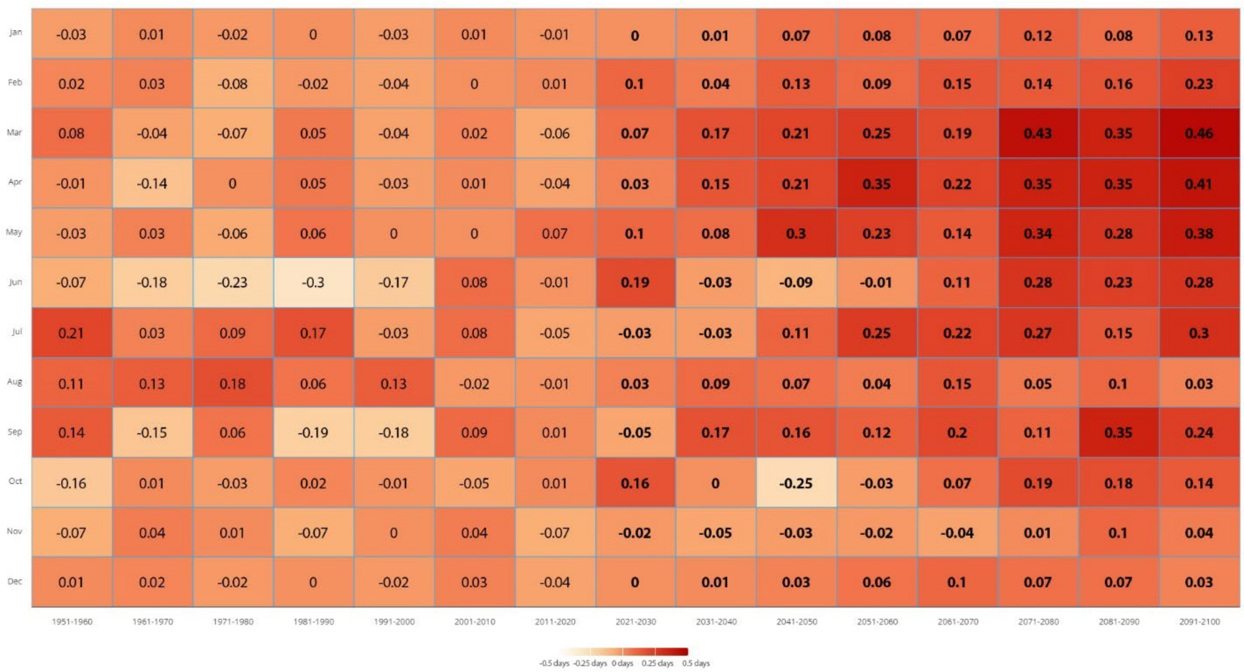

Figure 2.8: Projected Number of Days with Precipitation >20mm Anomaly Japan; (Ref. Period: 1950-2014), SSP5-8.5, Multi-Model Ensemble (source: https://climateknowledgeportal.worldbank.org/country/japan/climate-data-projections)

Timber Deterioration and Effect of Climate Change on Timber Structure

As wood is a biological substance, it is subject to degradation over time. The relevant characteristics and factors leading to the decline or deterioration of timber structures can be classified into three categories (Verbist et al., 2019).

1. Biologic Degradation

1.1 Fungi

Three types of fungi—sap stain, mold, and decay fungi—can lead to wood degradation and decay. While sap stain and mold fungi generally only discolor the wood's surface, affecting its appearance, decay fungi significantly impact the wood's physical and chemical properties, weakening its structural integrity (Verbist et al., 2019).

C.H. Wang et al. (2008) conducted extensive experiments in Australia, developing service life models to predict timber decay from these fungi, applicable to various locations. These models categorize decay based on the timber's exposure: direct ground contact, above-ground but exposed to weather, and being protected within the building envelope. In this research, the timber structure above ground and in the building envelope decay models will be in focus.

Timber structure installed above-ground decay model:

This model is defined by two key parameters: the initial delay before decay starts, and the rate of decay. It accounts for various factors in predicting the progression of decay, including the type of wood, the annual duration of moisture exposure from rainfall, whether the wood surface is painted, the size and alignment of the timber, and the specific geometrical configurations of the wood assembly. The model is described as follows:

$$d_t = \begin{cases} ct^2 & \text{if } t \le t_{d_0}; \\ (t - t_{lag})r & \text{if } t > t_{d_0}. \end{cases} \tag{1.1}$$

In which

$$t_{d_0} = t_{lag} + \frac{d_0}{r} \tag{1.2}$$

$$c = \frac{d_0}{t_{d_0}^2} \tag{1.3}$$

And the decay lag (t_{lag} in years) can be explained by

$$t_{lag} = 8.5r^{-0.85} \tag{1.4}$$

The decay rate, r is received from:

$$r = k_{wood}k_{climate}k_p k_t k_w k_n k_g \tag{1.5}$$

When k_{wood} = wood parameter, $k_{climate}$ = climate parameter

k_p = paint parameter, k_t = thickness parameter

k_w = width parameter, k_n = fastener parameter

k_g = geometry parameter.

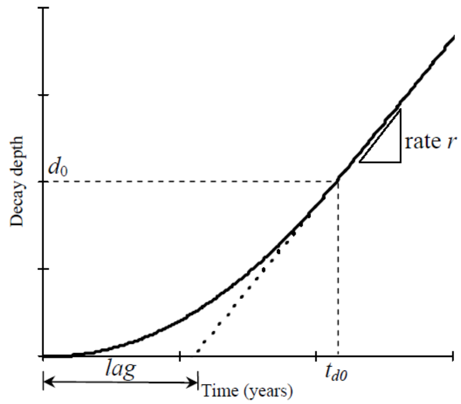

Figure 2.9: The graph depicting the idealized progress of decay depth over time (C.H. Wang, 2008a)

The $k_{climate}$ value (Climate parameter) can be acquired by the Scheffer Climate Index which can be calculated by:

$$\text{Scheffer Index} = \sum_{Jan}^{Dec} \frac{(T-2)(D-3)}{16.7}$$

(Carll, 2009)

When T = mean average temperature (monthly) in °C

D = mean number of days per month with the precipitation amount of 0.25 mm or more

The decay rate (r), which directly varies per $k_{climate}$ value, will change based on the temperature and precipitation days alteration under the different climate change scenarios.

Timber structure protected in the building envelope decay model:

$$d_t = \begin{cases} 0 & \text{if } t \le lag \\ (t - lag)r & \text{if } t > lag \end{cases} \qquad (2.1)$$

In which

$$lag = 8.5r^{-0.85} \qquad (2.2)$$

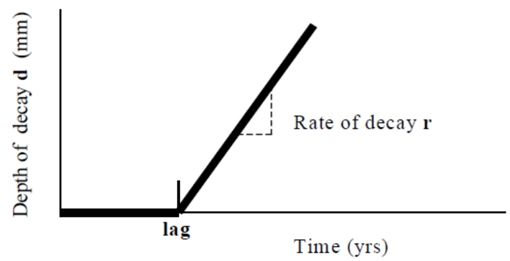

Figure 2.10: The graph depicting the idealized progress of decay depth over time (C.H. Wang, 2008b)

The decay rate, *r* is received from:

$$r = k_{wood}\, k_{geometry}\, k_{climate} \tag{2.3}$$

When k_{wood} = wood parameter $k_{climate}$ = climate parameter

$k_{geometry}$ = geometry parameter concerning the orientation and layout of the structural component.

Different from the previous model, $k_{climate}$ in this case can be acquired by the time of wetness value (t_{wet}):

$$k_{climate} = \begin{cases} 0.15 t_{wet}^{0.5} & \text{if } t_{wet} \text{ is in days/yrs;} \\ 0.03 t_{wet}^{0.4} & \text{if } t_{wet} \text{ is in hrs/yrs.} \end{cases} \tag{2.4}$$

In the case of the roof structural elements, t_{wet} can be shown in:

$$t_{wet} = \sum_{i}^{N} (\alpha t_{rain,\ V \geq 4m/s} - t_{delay})_i$$
$$\text{with } (\alpha t_{rain,\ V \geq 4m/s} - t_{delay})_i > 0 \tag{2.5}$$

The decay rate (*r*), which changes following $k_{climate}$ value, will vary based on the alteration in the number of days of precipitation under the different climate change scenarios.

1.2 Insects

Wood-boring beetles and termites, the most common pests in aboveground timber buildings, thrive in temperatures above 20°C and humidity over 60%. They infest damp areas like basements and attics due to condensation, poor damp-proofing, or leaks from gutters or pipes (Verbist et al., 2019).

However, the decay processes per these species of insects are not clearly described, additionally, this research focuses on the structures above ground. This factor will not be included in the consideration.

2. Chemical and physical agents

2.1 Weathering

Weather factors consider various aspects including UV radiation, Temperature, and Moisture & Humidity.

UV radiation

The impact of UV and solar radiation on the degradation of wood's mechanical properties remains inconsistent across studies. For instance, research by Sharratt et al. (2009) indicates that accelerated UV exposure can lead to a significant reduction in the strength of Scots pine wood strips, with a decrease of 20-40% reported. Nasir et al. (2021) conducted experiments on four different wood species, observing not only significant color changes in weathered wood but also alterations in its mechanical properties.

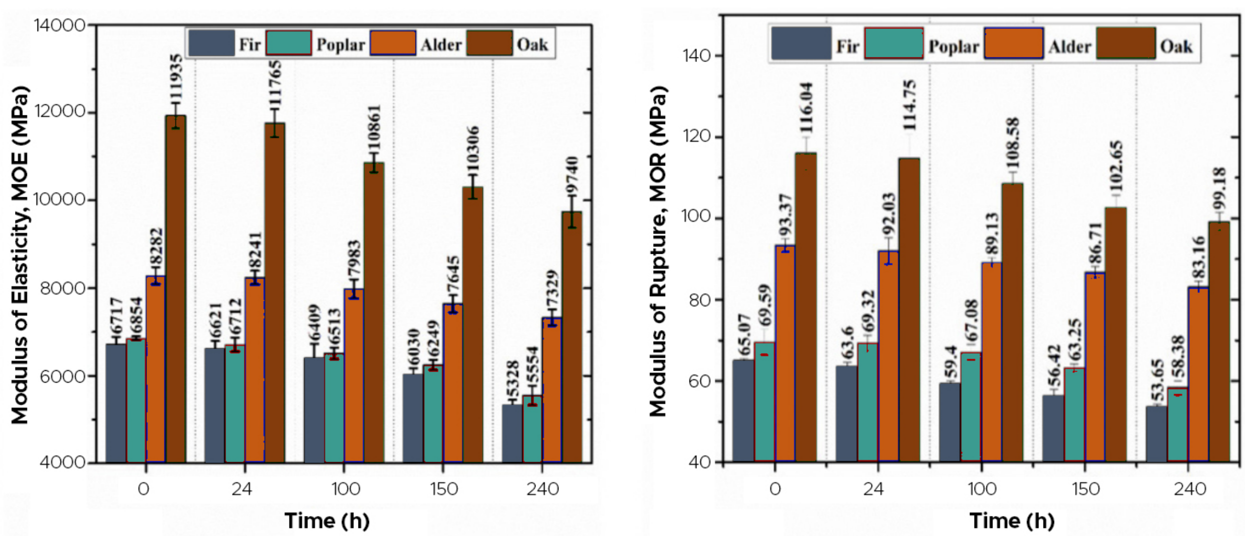

Figure 2.11: The variation of MOE and MOR in weathered wood samples (Nasir et al., 2021)

Conversely, György Papp (2005) found that UV radiation primarily affects the aesthetic appearance of timber, with minimal impact on its structural integrity.

Aside from these findings, the specific variations in UV radiation due to climate change remain unclear. Consequently, this research will not consider the effects of UV radiation on timber, focusing instead on other environmental factors that influence wood degradation.

Moisture and Humidity

Timber is a hygroscopic material that strives to reach equilibrium with its surrounding climate, reacting to daily and seasonal changes in temperature and relative humidity (RH). These fluctuations impact its moisture content (MC), leading to potential twisting and distortion of the wood.

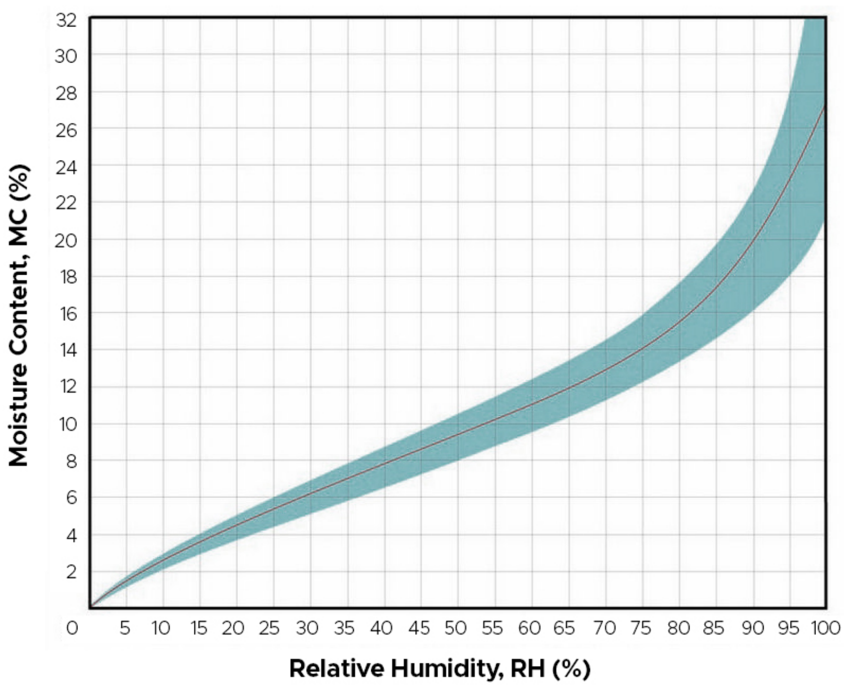

Figure 2.12: The relationship between relative humidity (RH) and wood moisture content (wood MC) (source: https://workshopcompanion.com/KnowHow/Design/Nature_of_Wood/2_Wood_Movement/2_Wood_Movement.htm)

The moisture content significantly influences the wood's strength, which varies based on its proximity to the Fiber Saturation Point (FSP). The FSP, typically between 25% and 35% MC for many wood types, marks the threshold at which free water in the wood has been fully dissipated and below which wood begins to swell and shrink (Csébfalvi & Len, 2020).

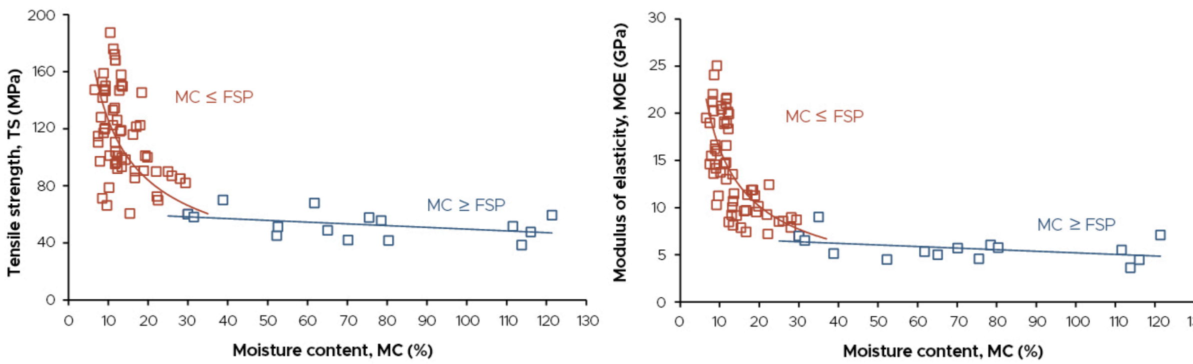

Figure 2.13: Relations between moisture content and mechanical parameters from pine wood (Roszyk, 2013)

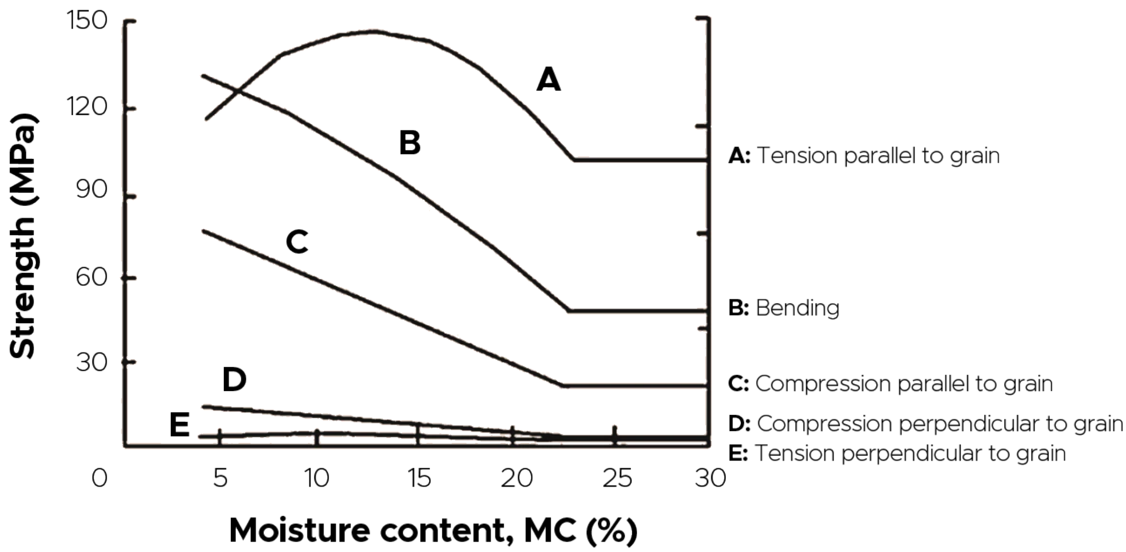

Figure 2.14: Relations between moisture content and mechanical parameters from pine wood (Niemz et al., 2023)

The Equilibrium Moisture Content (EMC) is where the wood's moisture levels align with the ambient environment, usually stabilizing between 10% and 15% MC in controlled settings. Moisture content can be measured with a portable moisture meter. Wood strength decreases as moisture content approaches the FSP and increases as it drops below this point, although shrinkage can counteract this strength gain by weakening wood fibers.

Repeated drying and wetting cycles can cause significant deformation in timber, impairing its mechanical and functional integrity, and making it unsuitable for construction and use. These cycles also lead to timber cracking—manifesting as shakes, checks, splits, or loosened grains—which, while generally having a minor impact on mechanical performance, can exacerbate biological deterioration, fostering fungi and insect growth (Aghayere A, 2007; Verbist et al., 2019).

Given the above traits, climate change influences temperature and humidity trends, which in turn affect the mechanical strength of timber. However, data on relative humidity for various climate scenarios in Japan is limited. Additionally, predicting fluctuations in moisture content over the years is challenging. Therefore, relative humidity will not be included in the timber deterioration model of this research.

Temperature

The impact of temperature on timber's strength properties can be divided into two categories: reversible effects and irreversible effects.

Reversible Effects (Immediate effect)

Typically, the mechanical properties of wood tend to decline with heating and improve with cooling. Below about 150°C, and at a stable moisture content, these properties change in a roughly linear manner with temperature. This alteration in properties due to rapid heating or cooling, followed by immediate testing at that temperature, is known as an immediate effect. At temperatures under 100°C, this immediate effect is largely reversible, meaning the properties will revert to their original values if the temperature is quickly changed back to its initial state (Gedeon, 1999).

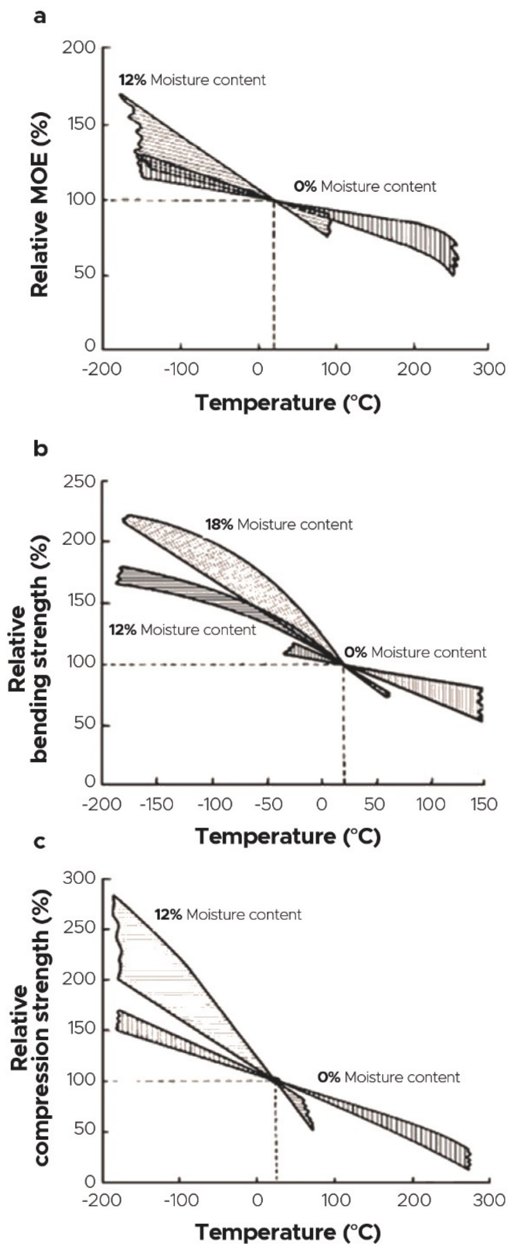

Figure 2.15: Temperature impact on various wood properties (Gedeon, 1999)

For dry lumber, which has a moisture content of about 12%, strength changes are minimal when temperatures fluctuate between -29°C and 38°C. In the case of green lumber, which contains more moisture, strength tends to decline with rising temperature. Nonetheless, between temperatures of approximately 7°C and 38°C, these alterations in strength are potentially not critically different from those observed at normal room temperature (Gedeon, 1999).

Irreversible Effects

The rising temperature can cause permanent effects in the aspect of wood weight loss and declining wood strength. The factors that impact these degradations include types and dimensions of wood, wood MC value, temperature, and duration of exposure. The geometry and size of the wood are critical when assessing temperature effects. For instance, in short-term exposures, the internal sections of a large piece of wood may not reach the surrounding medium's temperature, thus experiencing less strength reduction compared to the outer sections. Yet, the type of mechanical stress applied, such as bending, can make the outer layers more critical since they bear the most stress and generally determine the piece's overall strength. This makes the lower temperatures of the inner parts less relevant under such conditions (Gedeon, 1999).

During prolonged exposures where the wood is consistently subjected to high temperatures, it is likely that the entire piece will stabilize at the medium's temperature, resulting in uniform strength degradation across the piece, irrespective of its size or how it is stressed. However, in typical building scenarios, wood may not experience the extreme daily temperature fluctuations of the surrounding air; therefore, long-term effects should consider the cumulative temperature exposure of the most crucial structural elements.

Higher temperatures, especially during processes like steaming, coupled with weight loss, significantly diminish wood's modulus of elasticity and impact bending strength, as well as its compressive strength after being redried (Niemz et al., 2023).

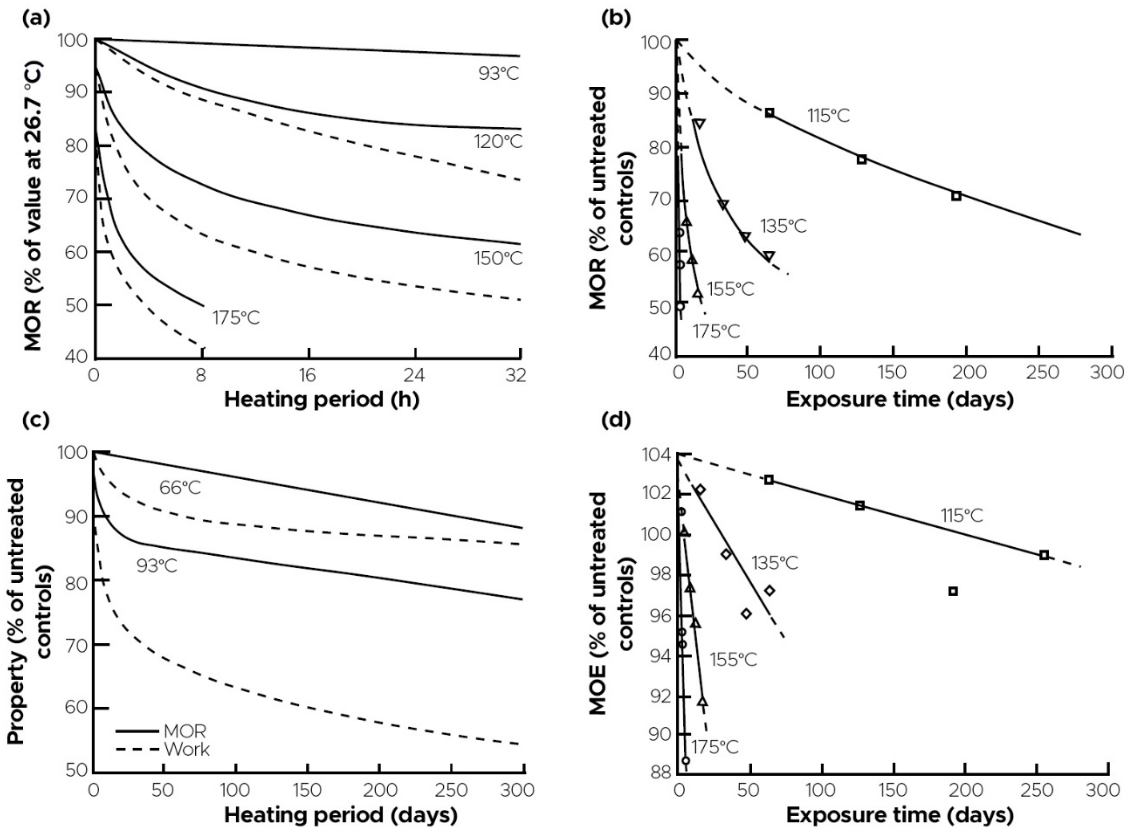

Figure 2.16: Temperature's permanent impact on various wood properties (Gedeon, 1999)

Nevertheless, the temperature ranges mentioned in the study are too extreme to be included in this research.

2.2 Fire

Although untreated timber structures are generally recognized for their fire resistance, wood is combustible and can degrade chemically when exposed to high temperatures, typically starting between 280 and 300°C. This leads to the formation of a char layer, which, while being a better insulator than the original wood, possesses significantly weaker mechanical properties. Historically, charring has been used to enhance the durability of timber against moisture, making the wood more stable under varying moisture conditions. According to Eurocode 5, in designing fire-exposed timber structures, the charred portion should not be counted towards structural integrity, requiring a reduction in the effective cross-section of timber elements. Charring rates vary from 0.5 to 0.8 mm/min depending on the type and density of the wood. Following severe fire damage, immediate steps must be taken to preserve any remaining timber structures by minimizing water penetration and facilitating drying through adequate ventilation (Cruz et al., 2015).

Nevertheless, in the scope of this research, the degradation according to fire will not be included in consideration.

3. Methods of timber monitoring, testing, grading, inspection, and maintenance

There are various ways to grade timber structures, the three main testing/evaluations are Non-destructive Testing/Evaluation (NDT/NDE), Semi-destructive Testing/Evaluation (SDT/SDE), and Destructive Testing.

Non-destructive Testing/Evaluation (NDT/NDE)

- Visual inspection
- Moisture Content Measurement
- Ultrasonic Testing
- Resistance Micro drilling
- Pulse Echo Sonic Tomography
- Acoustic Emission Testing
- Thermal Imaging
- X-ray and Gamma-ray Radiography
- Magnetic Resonance Imaging (MRI)

Semi-destructive Testing/Evaluation (SDT/SDE)

- Drilling Resistance Measurement
- Incremental Boring
- Ultrasonic Testing
- Radiography
- Resistance Drilling
- Pilodyn Testing
- Stress Wave Timing (SWT)
- Pull-out Tests

Destructive Testing

- Bending and Flexural Testing
- Compression Testing
- Tensile Testing
- Shear Testing
- Impact Testing
- Compression Perpendicular to Grain
- Density and Moisture Content Determination
- Chemical Analysis
- Microscopic Examination

For heritage buildings, evaluations are primarily conducted using non-destructive and semi-destructive methods. However, per the nature of timber which contains high variability and non-linearity, the data concerning timber's properties and NDT parameters are typically presented in statistical terms. Furthermore, since natural aging has a complex effect on timber members of ancient buildings, combined various Non-destructive testing/evaluations (NDT/NDE) are needed for more accurate results (Xin et al., 2022).

4. Machine Learning method

Machine learning encompasses a variety of methods designed to enable machines to learn from and make predictions or decisions based on data. These methods are broadly categorized into supervised learning, where the model is trained on labeled data (input-output pairs), enabling it to predict the output from new inputs; unsupervised learning, which deals with finding hidden patterns or intrinsic structures in input data that is not labeled; and reinforcement learning, where an agent learns to make decisions by performing actions and receiving feedback in the form of rewards or penalties. This feedback helps the agent learn the strategy, or policy, that will maximize its long-term rewards.

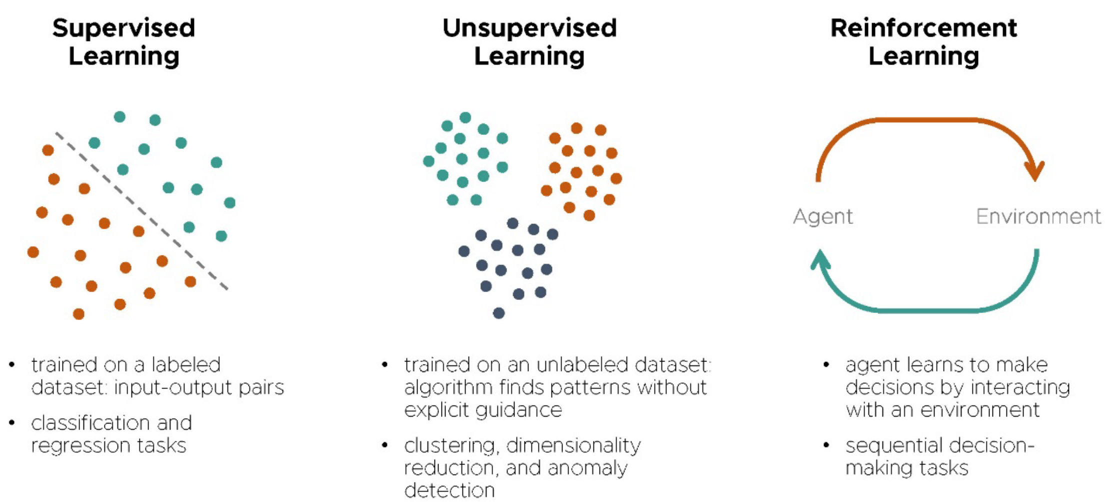

Figure 2.17: Different machine learning methods (Own work)

For this study of developing an optimal inspection and maintenance plan for historical timber structures, reinforcement learning is particularly suited. In recent times, advancements in reinforcement learning have demonstrated a capability to surpass traditional expert-driven heuristic maintenance strategies for intricate engineering systems. For instance, research conducted by Andriotis et al. (2019) illustrates the effectiveness of the Deep Centralized Multi-Agent Actor-Critic (DCMAC) framework. This approach outperforms traditional methods by offering more effective life-cycle management for large systems with multiple components and complex dimensional spaces, achieving superior results compared to optimized conventional policies. Another example is the study by Leroy et al. (2023) benchmarks cooperative Multi-Agent Reinforcement Learning (MARL) methods against expert-based heuristic policies revealing that MARL, particularly Centralized Training with Decentralized Execution (CTDE) methods, significantly outperforms heuristic policies in terms of scalability and performance in high-dimensional and complex IMP environments.

Markov Decision Processes (MDPs)

The foundation of many reinforcement learning applications is the Markov Decision Process (MDP), a mathematical framework used to model decision-making situations where outcomes are partly random and partly under the control of a decision-maker. MDPs are characterized by a set of states $s \in S$, actions $A(s)$, transition probabilities $P(s'|s, a)$ that define the likelihood of moving from state s to state s' given action, and rewards $R(s, a, s')$ that quantify the benefit of taking certain actions in specific states. Additionally, MDPs incorporate a discount factor γ, which is a value between 0 and 1 that weighs the importance of future rewards compared to immediate rewards, influencing the agent's strategy toward short-term or long-term benefits. In other words, MDPs can be defined by the tuple: $< S, A, R, P, \gamma >$. The policy $\pi(a|s)$, a crucial component of MDPs, dictates the action a to be taken when in state s. This policy aims to maximize the expected sum of discounted rewards over time, guiding the agent toward the most beneficial outcomes as defined by the model.

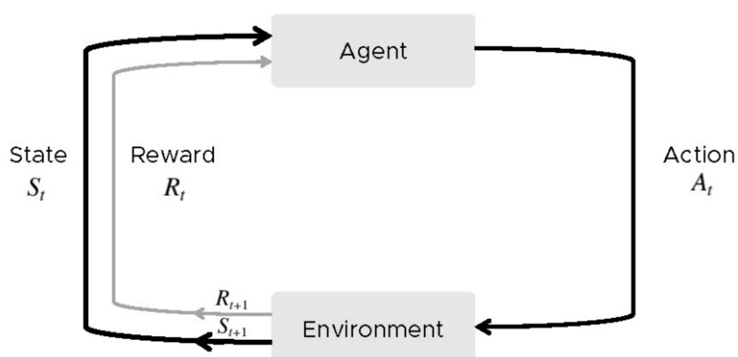

Figure 2.18: Interaction between agent and environment (Richard S. Sutton, 2018)

The objective in solving an MDP is to find a policy π that maximizes the expected sum of discounted rewards, known as the value function $V^{\pi}(s)$, defined for a policy π as:

$$V^{\pi}(s) = \mathbb{E}\left[\sum_{t=0}^{\infty} \gamma^t R(s_t, a_t, s_{t+1}) | s_0 = s, \pi\right]$$

where $\mathbb{E}$ denotes the expected value, assuming the agent follows policy π starting from state s.

Partially Observable Markov Decision Processes (POMDPs)

In many real-world problems, however, the agent cannot directly observe the underlying state of the system. These scenarios are modeled as Partially Observable Markov Decision Processes (POMDPs), where the agent must make decisions based on incomplete and possibly noisy observations of the state. POMDPs extend MDPs by including a set of observations $o \in O$ that provides partial information about the state and an observation function $Z(o|s', a)$ which specifies the probability of receiving observation o after taking action a and landing in state s'. This function models the uncertainty about the state given the observations. This complicates the decision-making process as the agent must infer the most probable state of the environment from the observations received. POMDP can be described by a tuple: $< S, A, R, P, \gamma, O, Z >$.

To manage this complexity, the agent maintains a belief state, which is a probability distribution over all possible states based on past actions and observations. This belief state represents the agent's current understanding of the probability of being in each possible state. When an action is taken, the belief state is updated through a prediction step based on the transition probabilities $P(s'|s, a)$, reflecting the likelihood of transitioning to each possible new state s' from a current estimated state s under action a. Subsequently, upon receiving an observation o, the belief state is further refined using the observation function $Z(o|s', a)$. This updates the belief to incorporate the new information provided by the observation, adjusting the probability distribution to better reflect which states are more likely given the observed outcome (Richard S. Sutton, 2018). The updated belief state is calculated using the formula:

$$b'(s') = \frac{Z(o|s', a) \sum_{s \in S} P(s'|s, a) b(s)}{\sum_{s'' \in S} Z(o|s'', a) \sum_{s \in S} P(s''|s, a) b(s)}$$

Here, $b(s)$ is the prior belief state, and $b'(s')$ is the updated belief state after observing o. This update ensures that the agent's decisions remain informed by the most current assessment of the environment's state, despite the inherent uncertainties. The normalization ensures that the updated beliefs form a valid probability distribution.

The optimal value function $V^*(b)$ guides the selection of the best action to take from any given belief state. It quantifies the maximum expected cumulative discounted reward that can be achieved, starting from any belief state b and following the best strategy. The value function essentially serves as a compass that helps the agent navigate through the decision space, where each decision is complicated by the uncertainty of partial observations and the need to operate based on probabilistic beliefs rather than certain knowledge. The optimal policy derived from the value function uses the updated belief states to make decisions that maximize the expected utility, balancing immediate rewards with the benefits of future actions, as modulated by the discount factor γ.

Computing the optimal value function in a POMDP is challenging due to the need to consider a continuous space of belief states and the dynamics of belief updates based on actions and observations. The Bellman equation for POMDPs, which underlies the computation of $V^*(b)$, is given by:

$$V^*(b) = \max_{a \in A} \left[\sum_{s \in S} b(s)R(s, a) + \gamma \sum_{o \in O} P(o|b, a)V^*(b') \right]$$

The term $\sum_{s \in S} b(s)R(s, a)$ calculates the expected immediate reward for taking action a in the belief state b, while the term $\gamma \sum_{o \in O} P(o|b, a)V^*(b')$ accounts for the expected discounted future rewards.

This ongoing cycle of action, observation, and belief update, guided by the optimal value function, is crucial for effective decision-making in environments characterized by uncertainty and partial observability. It allows the agent to "guess" the current state of the system with the best possible accuracy based on incomplete information, thereby enabling more informed and strategically advantageous decisions.

Reinforcement Learning (RL)

Reinforcement Learning (RL) is a framework in machine learning where an agent learns to make decisions by interacting with an environment to achieve a goal. Unlike other forms of machine learning, in RL, the agent is not taught the correct actions to take. Instead, it must discover them by trying different strategies and learning from the outcomes of its actions, typically represented through rewards. This method mirrors the way humans and animals learn from the consequences of their actions over time, making it particularly effective for complex decision-making tasks that require a sequence of decisions.

The core idea behind reinforcement learning is the concept of the agent-environment interaction loop. In this loop, the agent takes an action in the environment, the environment responds to the action by presenting a new state and providing a reward, and the agent then makes the next decision. This cycle continues until a terminal state is reached, which might represent the completion of a task or an episode. The key components of this interaction include the state (what is currently observable about the environment), the action (what the agent can do), and the reward (feedback from the environment indicating the value of the action taken). The cumulative reward, or return, from a series of actions is formalized as:

$$G_t = \sum_{k=0}^{\infty} \gamma^k R_{t+k+1}$$

Where G_t is the total cumulative reward from time step t, R_{t+k+1} is the reward received at time $t+k+1$, and γ is the discount factor ($0 \leq \gamma \leq 1$) that weighs the importance of future rewards relative to immediate ones.

The objective of an RL agent is to learn a policy — a mapping from states of the environment to actions — that maximizes the cumulative reward over time. This policy could be deterministic, where a state directly maps to an action, or stochastic, where a policy provides probabilities of selecting possible actions from a given state. Learning the optimal policy often involves evaluating the consequences of actions based on the long-term return, not just the immediate reward. This optimization can be mathematically represented using the Bellman equation for the state-value function:

$$V^{\pi}(s) = \sum_{a\in A} \pi(a|s) \sum_{s',r} p(s',r|s,a)[r + \gamma V^{\pi}(s')]$$

This equation illustrates how the value of a state under a policy is recursively determined by the immediate rewards and the discounted value of subsequent states.

Several algorithms exist for implementing RL, ranging from simple table-based methods like Q-learning, which utilizes the update rule

$$Q^{*}(s,a) = \sum_{s',r} p(s',r|s,a)[r + \gamma \max_{a'} Q^{*}(s',a')]$$

to sophisticated deep learning approaches like Deep Q-Networks (DQN) and policy gradient methods. These algorithms differ primarily in how they estimate the value of actions taken in given states and how they update the policy based on the estimated values. Policy gradient methods, for instance, optimize the policy directly by adjusting the policy parameters θ in the direction that maximizes the expected return, as given by the policy gradient theorem:

$$\nabla_{\theta} J(\theta) = \mathbb{E}_{\pi_{\theta}}\left[\sum_{t=0}^{\infty} \gamma^{t} \nabla_{\theta} \log \pi_{\theta}(a_t|s_t) Q^{\pi}(s_t,a_t)\right]$$

RL has been successfully applied to a variety of complex tasks that require a sequence of decisions, such as playing video games at a superhuman level, autonomous driving, robotic control, and more. One of the key challenges in RL is the trade-off between exploration (trying new actions to discover their effects) and exploitation (using known actions that yield high rewards). Additionally, in environments like POMDPs where the agent does not fully observe the underlying state, the agent must operate under uncertainty, which complicates the learning process and the design of effective policies.

Multi-Agent Reinforcement Learning environments for large-scale Infrastructure Management Planning (IMP-MARL)

MDPs and POMDPs offer a robust framework for decision-making in engineering systems management. These methods leverage offline knowledge about the environment to develop detailed policies for systems where state and action spaces are manageable in size (Andriotis & Papakonstantinou, 2019).

In practice, MDPs and POMDPs are particularly effective for smaller systems with well-defined parameters. They allow decision-makers to model uncertainties and dynamics systematically, providing a clear strategy for operational actions. This is especially useful in environments where conditions can be closely monitored and predicted.

However, the application of MDPs and POMDPs becomes challenging when dealing with large, multi-component systems. In such cases, the number of possible states and actions increases exponentially with each additional component, leading to what is known as the "curse of dimensionality." This complexity makes it impractical to directly apply traditional MDP or POMDP approaches due to the vast computational resources required (Andriotis & Papakonstantinou, 2019).

Additionally, the dynamics of the environment in large systems are often complex and cannot be easily encapsulated in simple models. Instead, they might only be understood through advanced, computationally intensive numerical simulations. This necessity further complicates the decision-making process, as obtaining timely and accurate data to feed into the decision models becomes a significant challenge.

The outlined challenges with MDPs and POMDPs in managing large multi-component systems can be effectively addressed through Decentralized Partially Observable Markov Decision Processes (Dec-POMDPs) and Multi-Agent Reinforcement Learning for Infrastructure Management Planning (IMP-MARL). These methodologies refine the approach to infrastructure management planning by integrating cooperative multi-agent systems to optimize decision-making processes under uncertainty.

Decentralized Partially Observable Markov Decision Processes (Dec-POMDPs)

Dec-POMDPs offer a robust framework for distributed decision-making where multiple agents operate independently but are evaluated on a collective outcome. In this structure, each agent has limited knowledge about the state of the environment and must base its decisions on local observations. The agents' actions are coordinated through a shared policy that aims to maximize collective rewards over time. This approach is particularly beneficial in scenarios where the system's state cannot be fully observed by any single agent, and decisions must be made based on incomplete and decentralized information (Leroy et al., 2023).

A Dec-POMDP is defined by the tuple $< S, Z, U, n, O, R, P, \gamma >$:

Where S represents the set of possible states in the environment, and Z is the observation space. The environment state at any given time t is denoted by $s_t \in S$. Each of the n agents, indexed from 1 to n, perceives an observation $o_t^a \in Z$ based on the observation function $O : S \times \{1, ..., n\} \rightarrow Z$, which maps the state and agent index to an observation. Agents choose actions $u_t^a \in U_a$, where U_a is the action space for agent a, and the collective actions form the joint action space $U = U_1 \times ... \times U_n$.

Upon execution of a joint action $u_t \in U$, the environment transitions to a new state according to the transition function $P(s_{t+1}|s_t, u_t) : S^2 \times U \rightarrow \mathbb{R}^+$, which determines the probability of moving to state s_{t+1} from state s_t given the action u_t. The reward function $R(s_{t+1}, s_t, u_t) : S^2 \times U \rightarrow \mathbb{R}$ specifies the reward obtained by all agents based on the state transition and actions taken.

Each agent's policy, $\pi_a(u_t^a|\tau_t^a, o_t^a) : (Z \times U_a)^t \rightarrow \mathbb{R}^+$, maps the agent's observation and action history to the probability of selecting action u_t^a. The collective goal of the agents is represented by the joint policy $\pi = (\pi_1, ..., \pi_n)$, aiming to maximize the cumulative discounted reward from time t over the next T steps, defined as $\sum_{k=0}^{T-1} \gamma^k r_{t+k}$, where $\gamma \in [0,1)$ is the discount factor. The ultimate objective for the agents is to derive the optimal joint policy π^* that maximizes the expected cumulative reward $E[R_0|\pi]$ over the entire episode. The expected sum of discounted reward can be defined by $\mathbb{E}[R_0] = \mathbb{E}[\sum_{t=0}^{T-1} \gamma^t \, [R_{t,f} + \sum_{a=1}^{n} \, (R_{t,ins}^a + R_{t,rep}^a) + \, R_{t,camp}]]$.

IMP-MARL

The IMP-MARL framework is an open-source suite extending the capabilities of traditional MARL frameworks designed for large-scale Infrastructure Management Planning (IMP). The framework is tailored for assessing the scalability and effectiveness of cooperative MARL methods in real-world engineering applications. It involves central training with decentralized execution, allowing agents to benefit from shared knowledge during the training phase while operating independently in execution. This methodology has shown considerable success in environments modeled after real-world engineering systems, such as offshore wind farms, where it manages up to 100 agents. IMP-MARL enhances scalability and efficiency, outperforming expert-based heuristic policies, especially in complex multi-agent settings (Leroy et al., 2023).

Among the various environments that IMP-MARL offers, the k-out-of-n system environment is well-suited for this research. This environment is designed to simulate scenarios where the failure of a certain number (k) out of a total number (n) of components leads to system failure. The environment models each component's damage condition over time, influenced by natural deterioration and external interventions such as inspections and repairs. The damage condition of components is probabilistically updated based on actions taken, and the system's overall integrity is contingent upon the collective state of all components. This modeling is particularly relevant for infrastructure like bridges or industrial machinery where safety and functionality are directly dependent on the reliability of multiple components. It can be defined as $s_t = (p(d_t^1), ..., p(d_t^n), t/T)$ and $o_t^a = (p(d_t^a), t/T)$.

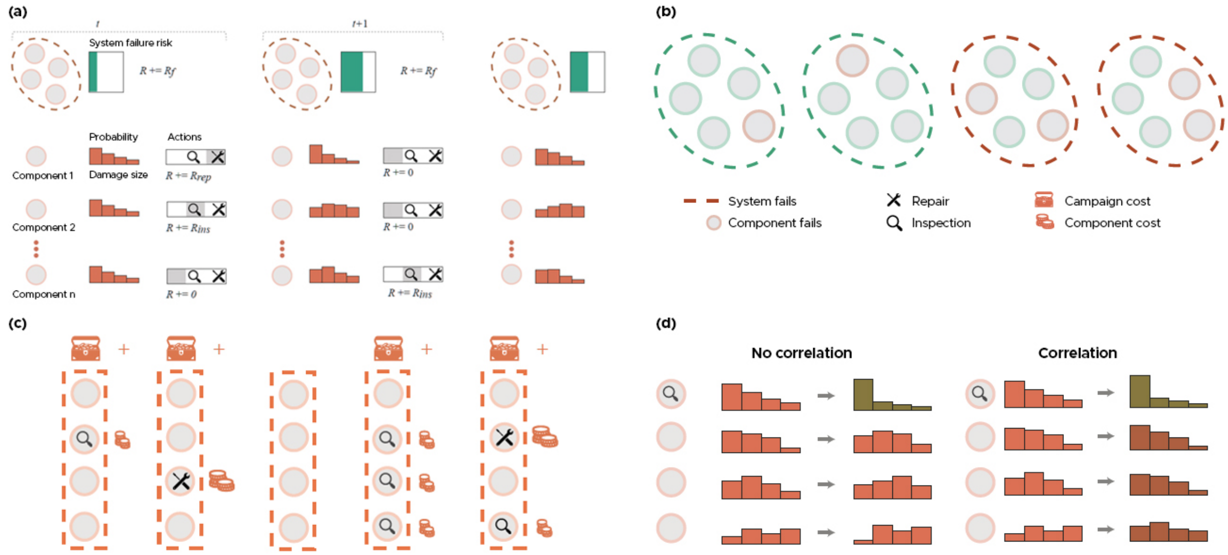

Figure 2.19: Visual representation of (a) IMP problem (b) A k-out-of-n system environment: system failure occurs if $n-k+1$ components fail (c) A campaign cost environment (d) Uncorrelated and correlated initial damage distribution: the information received from inspecting one element will or will not affect the other uninspected elements (Leroy et al., 2023)

The IMP-MARL utilizes a Decentralized Partially Observable Markov Decision Process (Dec-POMDP) approach to handle the decentralized nature of information and decision-making in the system. Each agent only has partial information about the state of the entire system but must cooperate with others to achieve the best overall outcome. The framework employs state-of-the-art cooperative MARL methods, with a focus on five centralized training with decentralized execution (CTDE) approaches, namely, QMIX, QVMix, QPLEX, COMA, and FACMAC allowing agents to learn from a global perspective while operating independently based on local observations.

According to the research results conducted by Leroy et al. (2023), all selected methods outperform the expert-based heuristic method. However, QMIX: Monotonic Value Function Factorization for Deep Multi-Agent Reinforcement Learning, highlights the efficient outcome policies with the low variance overrun as shown in the diagram below.

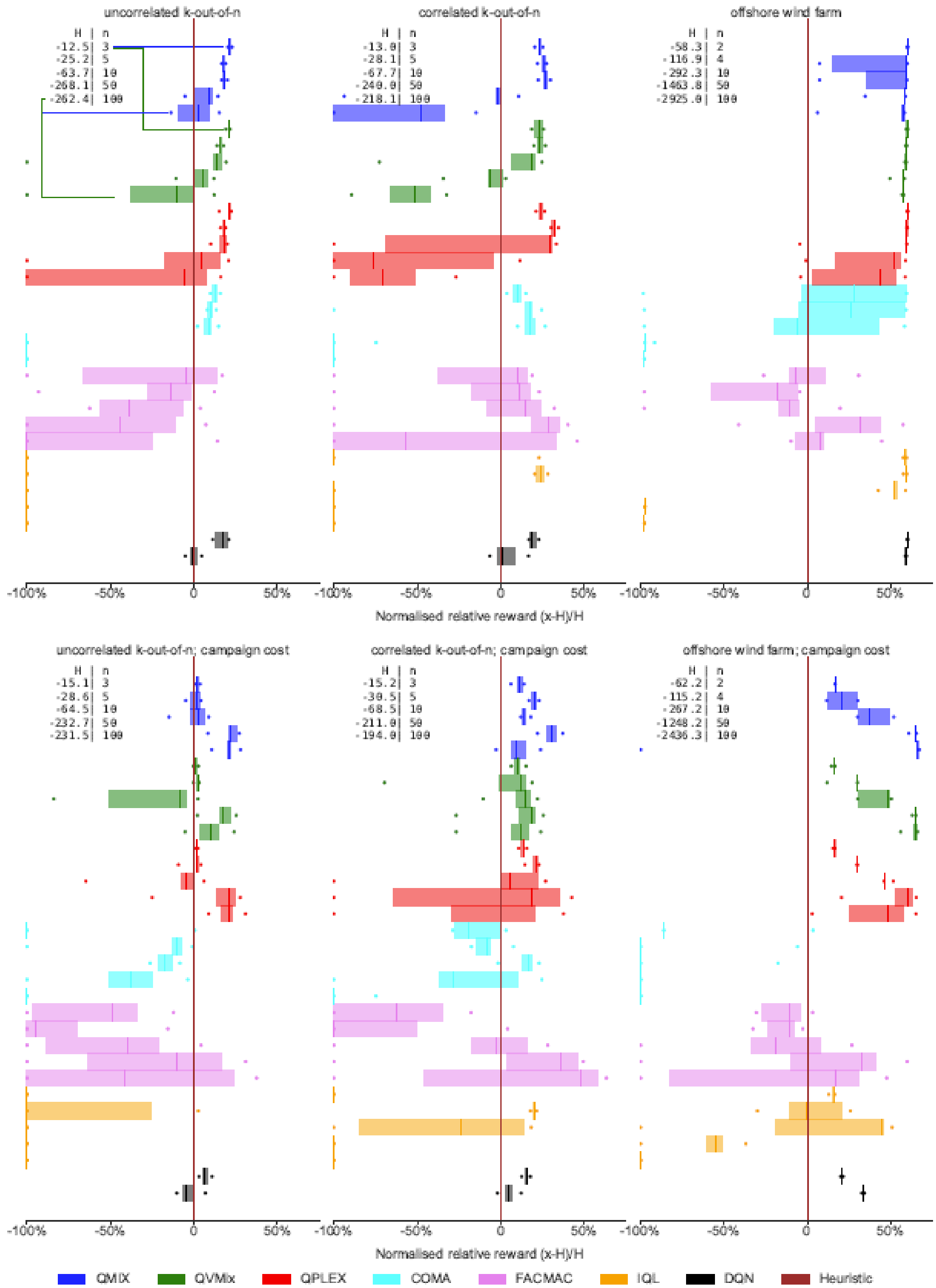

Figure 2.20: Performance achieved by MARL methods concerning normalized discounted rewards compared to expert-based heuristic policies across all IMP environments (Leroy et al., 2023)

QMIX uses a mixing network to combine individual value functions in a way that maintains consistency with the global value function, ensuring that the joint policy is optimal. This feature makes QMIX suitable for the k-out-of-n system, where the interdependencies between different components' states are critical to the system's overall performance and reliability.

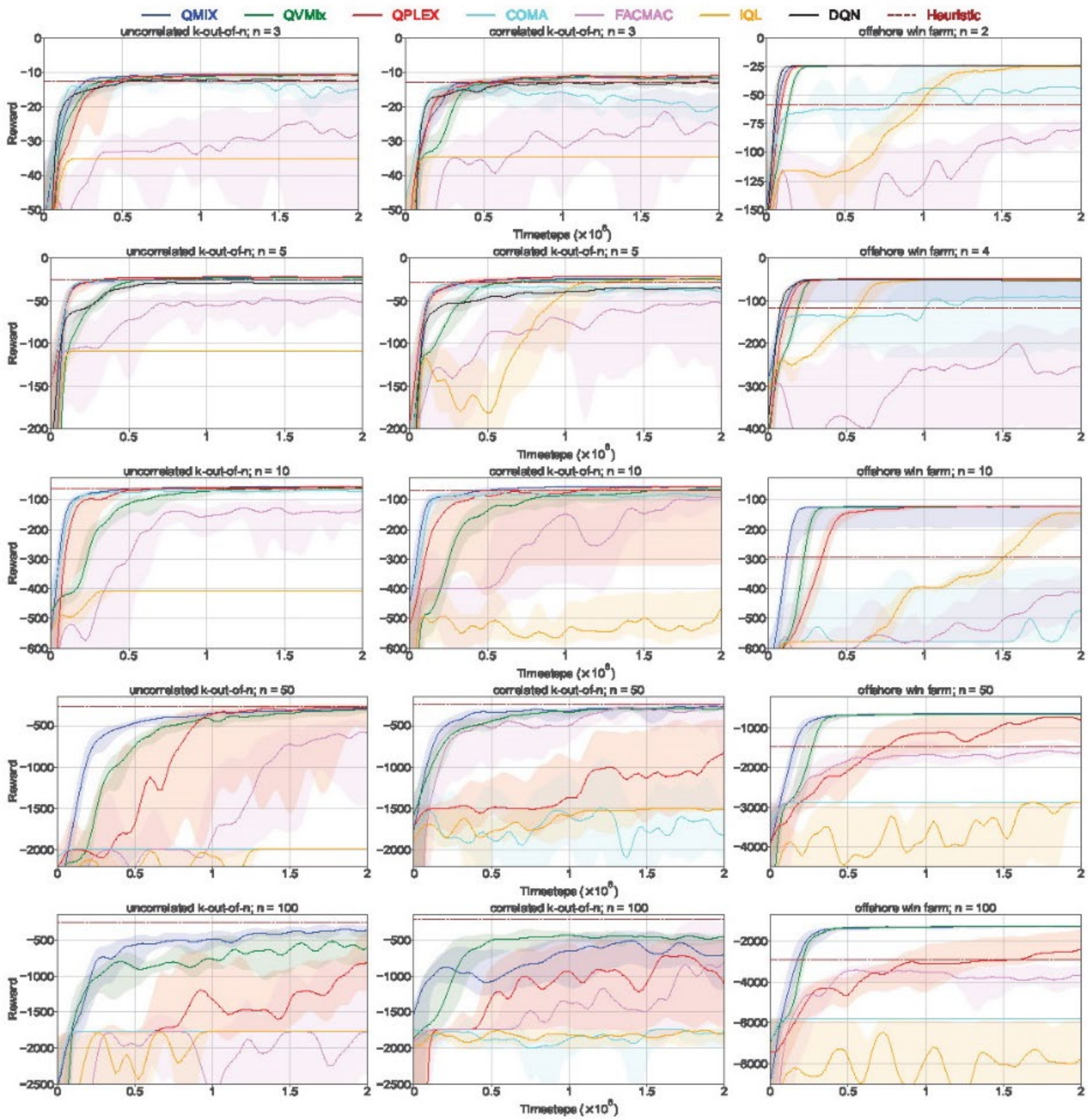

Figure 2.21: Graphs showing the learning curves of selected methods in all environments without the campaign cost (Leroy et al., 2023)

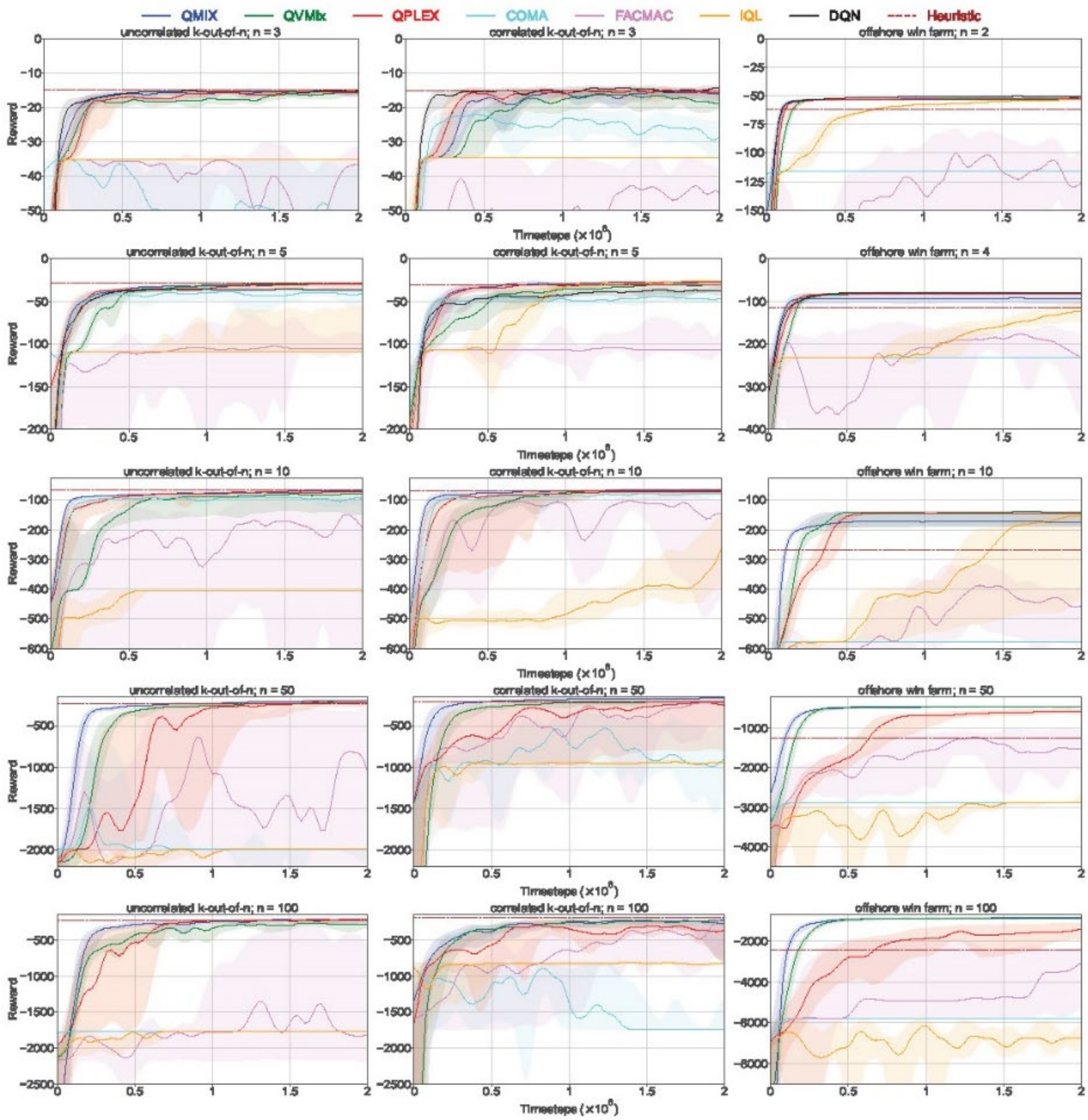

Figure 2.22: Graphs showing the learning curves of selected methods in all environments with the campaign cost (Leroy et al., 2023)

Bridging the Gap

Existing literature provides a foundation for understanding how environmental factors influence timber deterioration, yet fails to integrate these insights with structured inspection and maintenance strategies. While there is substantial research focusing on the application of reinforcement learning to develop inspection and maintenance policies for concrete infrastructures—which take deterioration into account—such methodologies have not been extended to timber structures, particularly in the context of climate change.

This study aims to bridge this gap by synthesizing three distinct but interrelated theoretical domains: climate change, timber structure integrity, and reinforcement learning. Timber, as a hygroscopic material, exhibits high sensitivity to environmental conditions, making it vulnerable to the impacts of climate change. This susceptibility necessitates adaptive inspection and maintenance (I&M) planning to effectively manage the risks associated with ongoing environmental shifts.

Traditional heuristic-based approaches to I&M are not only time-intensive but also demand a high level of skill from workers, which can be a limiting factor in timely and effective maintenance. In contrast, reinforcement learning offers a promising alternative by leveraging the ability to handle stochastic uncertainty and dynamically optimizing I&M policies. This approach utilizes a probabilistic belief about the environment's state, incorporating variables such as the current climate conditions, the physical state of the timber structure, and the outcomes of previous I&M actions.

The proposed study will develop a framework for dynamic inspection and maintenance planning that continuously updates in response to evolving information about climate change impacts, structural conditions, and the efficacy of implemented I&M actions. This innovative approach aims to enhance the resilience of timber structures to environmental changes, ensuring their longevity and structural integrity in the face of uncertain future conditions.

3

Framework

Framework Strategies

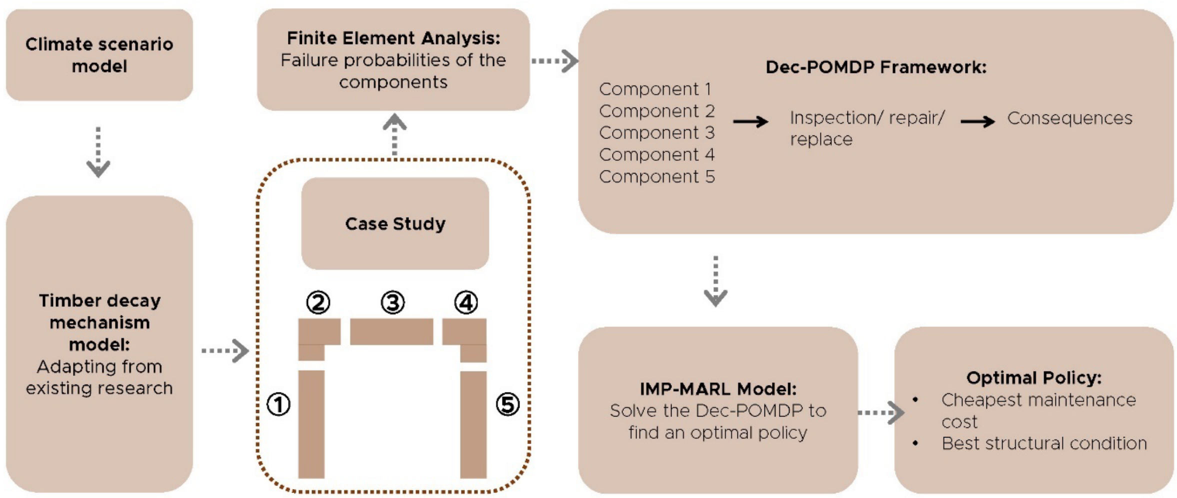

Figure 3.1: Machine Learning framework setting workflow (Own work)

To establish an optimal inspection and maintenance policy for timber structures, a comprehensive machine-learning framework has been devised. Initially, a timber deterioration mechanism model is configured based on existing models identified through a literature review. This model incorporates four illustrative climate scenarios, each modifying the input climate parameters to produce distinct trends in the decay rate, quantified as decay depth per time. This increase in decay depth is interpreted as a proportional reduction in the cross-sectional area of the structural components.

A specific case study is selected to illustrate the practical application of this framework. Detailed information relevant to the case study and its environmental conditions are collected, allowing for precise adjustments to the decay model to reflect the unique conditions and details of the selected case study. Structural analysis is then conducted using the Finite Element Analysis (FEA) method based on the load cases applied to the structure of the case study. This analysis assesses how the structural components respond to these loads in conjunction with the reduced cross-sectional area. Subsequently, the probability of structural failure is calculated using the Gamma process. This calculation informs the belief space and transitional state necessary for the Decentralized Partially Observable Markov Decision Process (Dec-POMDP) model.

Within this model, specific inspection and maintenance actions are defined, along with the consequences and costs associated with each action, the maintenance periods, and the time steps. These elements are crucial for the Dec-POMDP model. Ultimately, the Interactive Multi-Agent Reinforcement Learning (IMP-MARL) method is employed to solve this model and determine the optimal inspection and maintenance policy. This policy is optimized based on the balance of maintenance costs and the condition of the structure, ensuring sustained structural integrity and cost-effectiveness.

Case study

To demonstrate the practical application of the proposed framework, a case study of Toshodaiji Temple will be examined. This temple, established in 780 AD, features a hall that has stood for 1244 years, located in Nara, Japan. The hall primarily serves to shelter the main Buddhist statues, allowing devotees to pay their respects from outside. Notably, the structure is elevated on stone bases, strategically designed to avoid direct ground contact. This design choice serves dual purposes: firstly, to shield the timber columns from ground moisture, and secondly, to enhance earthquake resilience.

Constructed entirely from Japanese Cypress (Chamaecyparis obtusa), known in Japanese as Hinoki, the temple exhibits exceptional durability and aesthetic qualities characteristic of this wood. Details on the specific mechanical properties and mathematical values pertinent to the temple's structure will be further explored in the subsequent section.

The selection of Toshodaiji Temple for this case study is based on its moderate scale and symmetrical layout, which simplifies the analysis to a single span—findings from which can be extrapolated to other spans of the structure. Moreover, the temple's exposure to varied weather conditions offers a unique opportunity to assess the impact of environmental factors on the decay model and its application. Historical records provide comprehensive data regarding inspections and maintenance carried out over the centuries, alongside evidence of preservation efforts visible on the structure itself. This wealth of information not only enhances the reliability of the study but also enriches our understanding of historical preservation techniques.

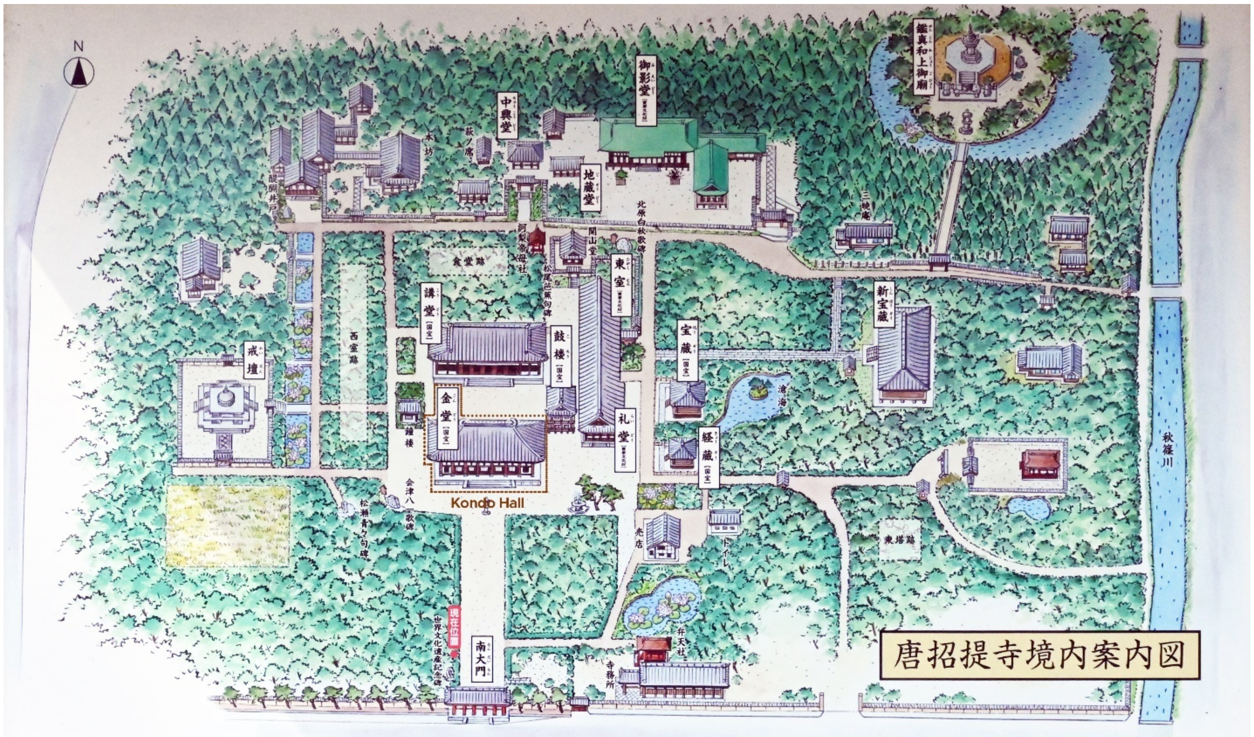

Figure 3.2: Toshodaiji Temple Map showing the location of Kondo Hall (Taken onsite)

Figure 3.3: Toshodaiji Temple Kondo (Golden Hall), Nara, Japan (Taken onsite)

Details

The hall features a rectangular layout, encompassing roughly 410 square meters of functional space. It is supported by 36 main cylindrical columns, each with a diameter of 600 mm, which bear the weight of the hipped roof structure and its extended eaves. Inside, the Buddha statues are enclosed and safeguarded by walls, while access for visitors is restricted to the exterior only. However, these static loads from the statues and the live loads from the visitor happen on the stone bases, they will not be taken into account in the structural analysis, merely roof load and wind load will be considered in this study.

Detailed architectural drawings, including the floor plan, roof plan, elevations, sections, and detailed sections with dimensions, are provided below for further reference.

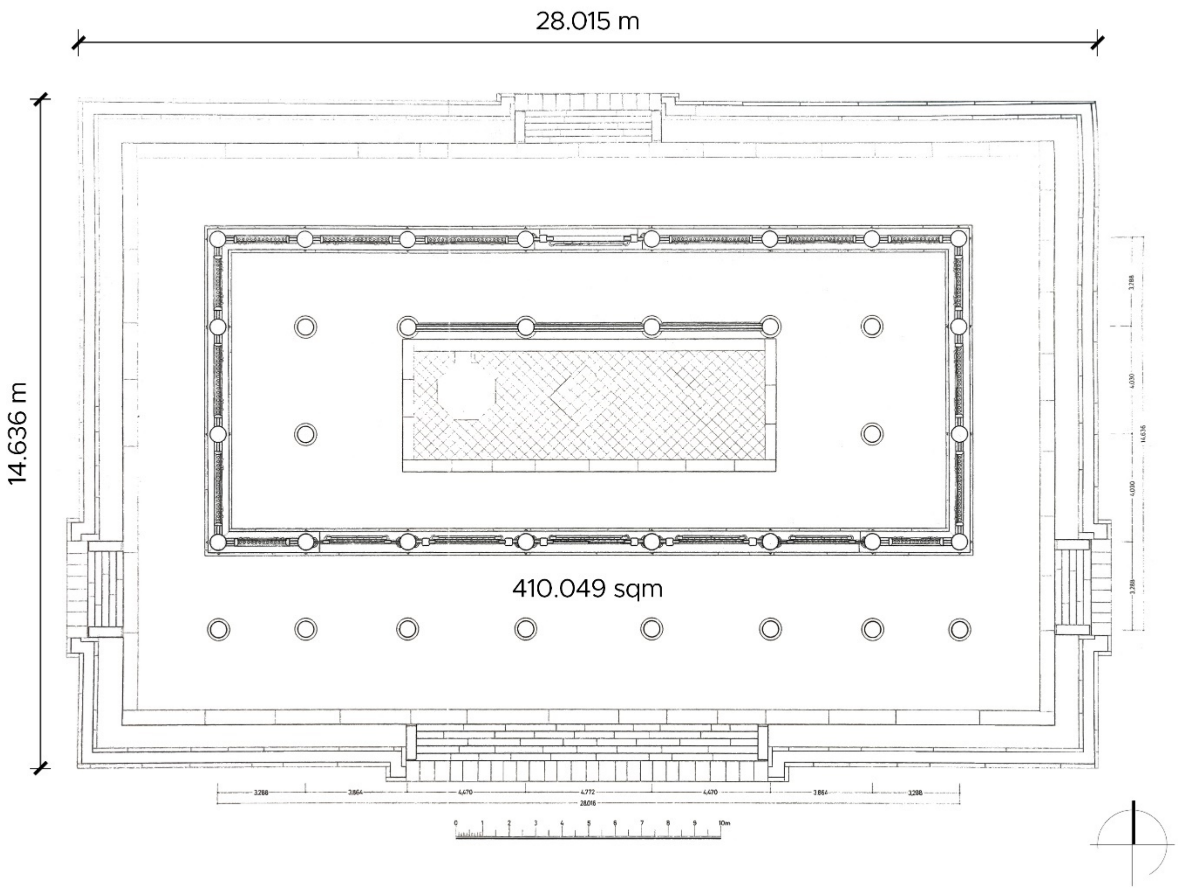

Figure 3.4: Floor Plan (Office of Cultural Assets Preservation, 2009)

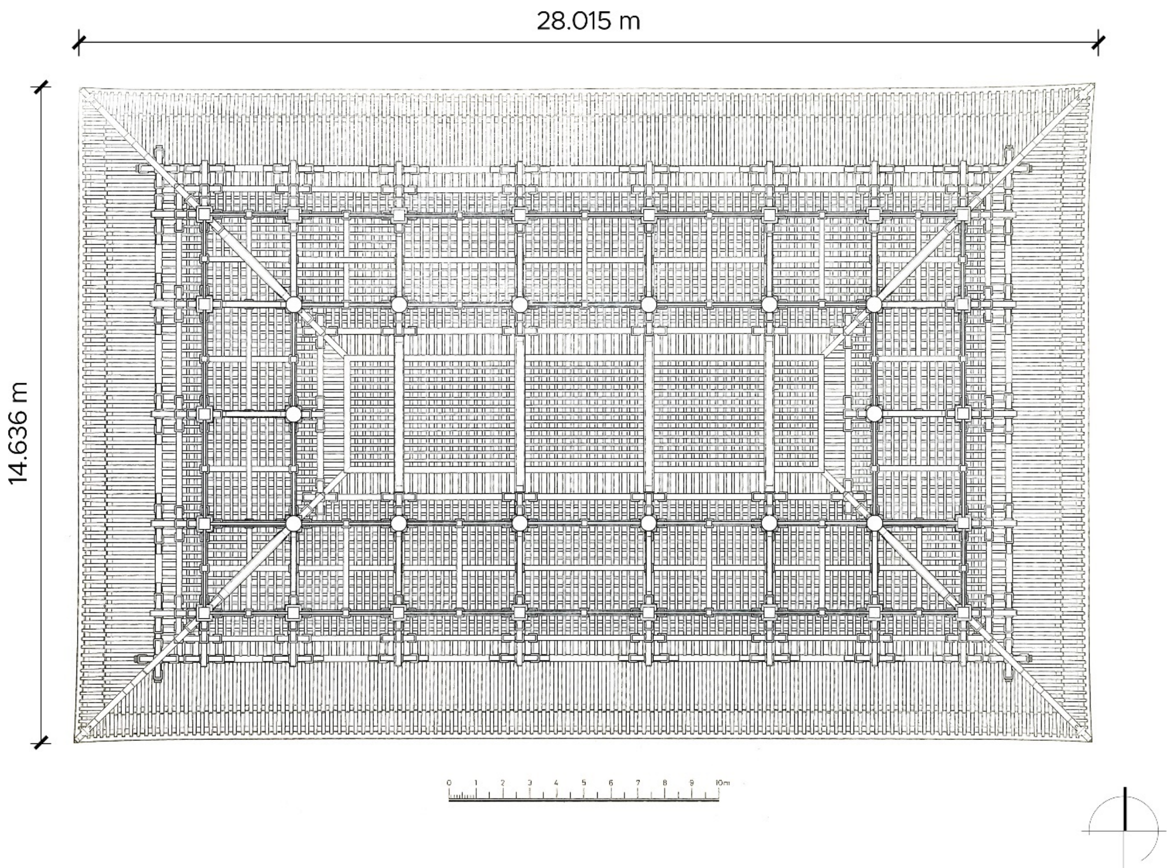

Figure 3.5: Roof Plan (Office of Cultural Assets Preservation, 2009)

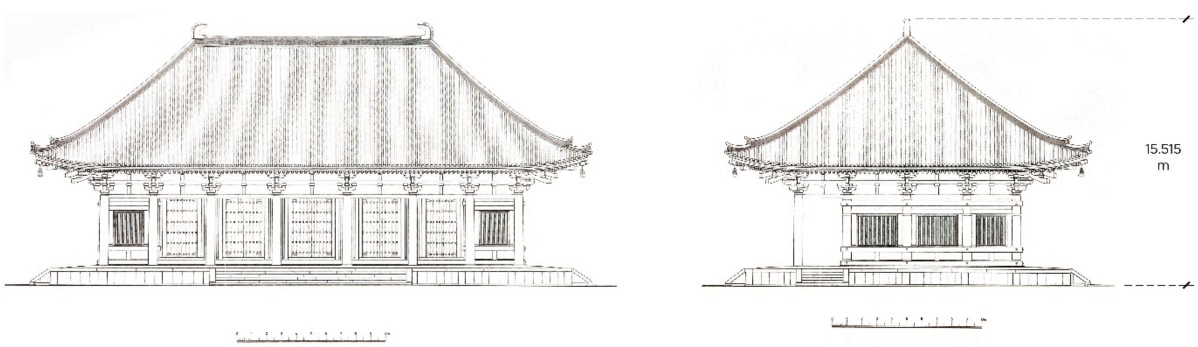

Figure 3.6: South Elevation and East Elevation (Office of Cultural Assets Preservation, 2009)

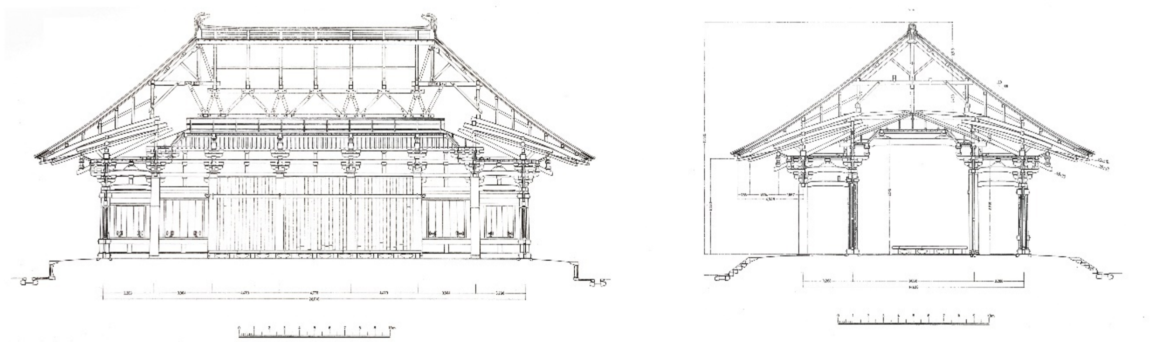

Figure 3.7: Long Section and Cross Section (Office of Cultural Assets Preservation, 2009)

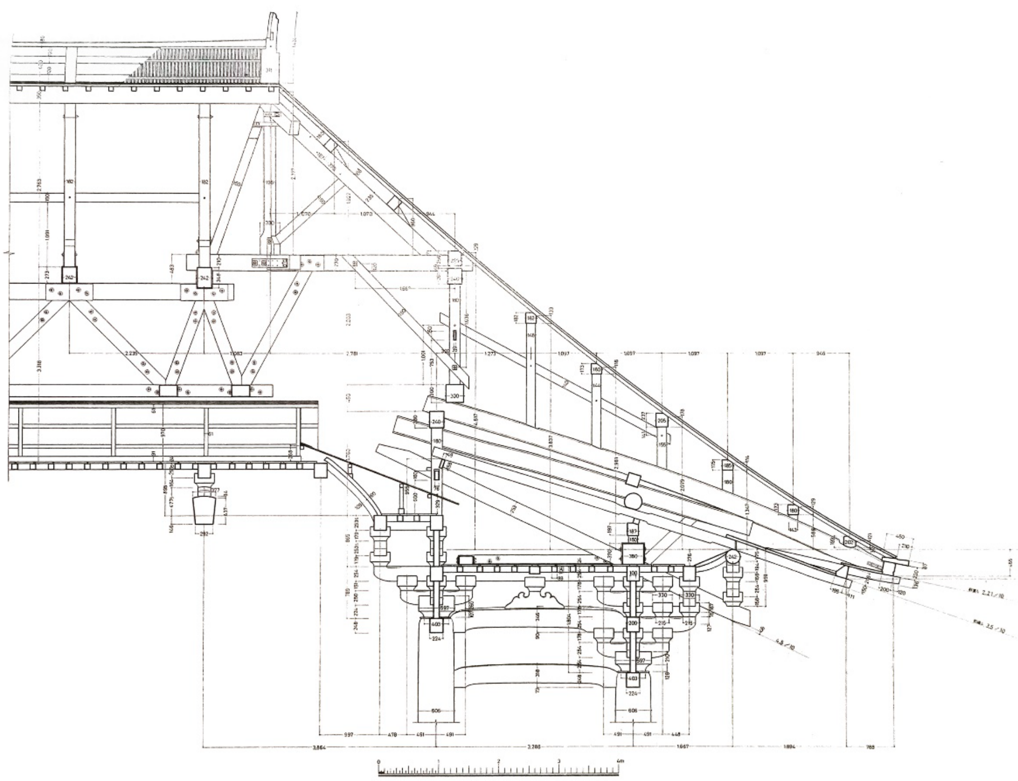

Figure 3.8: Detailed Long Section (Office of Cultural Assets Preservation, 2009)

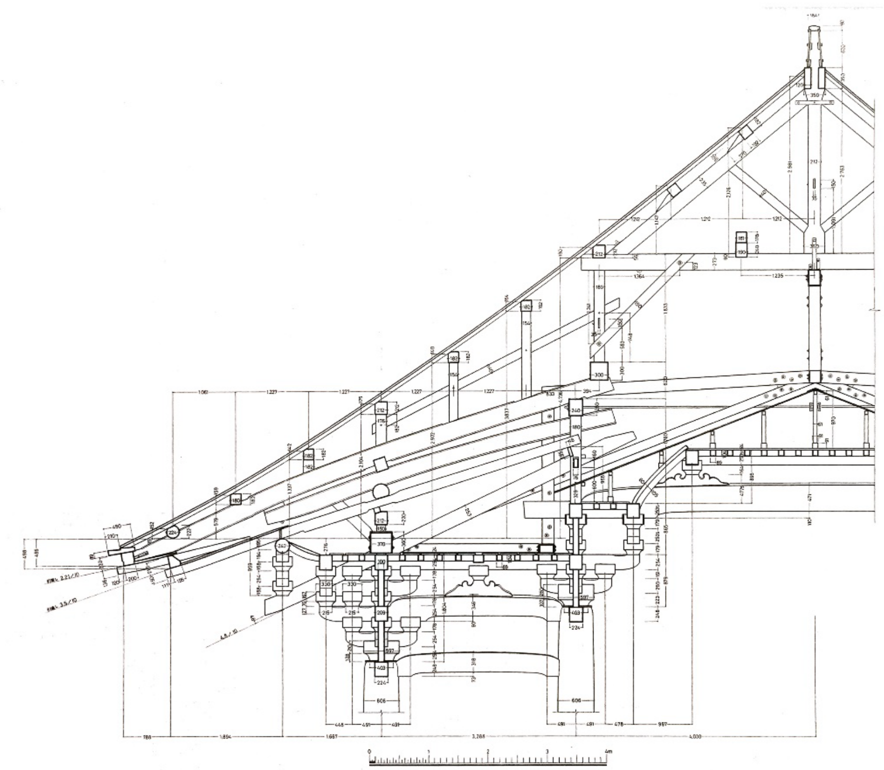

Figure 3.9: Detailed Cross Section (Office of Cultural Assets Preservation, 2009)

Maintenance records: Historical Timeline and methods

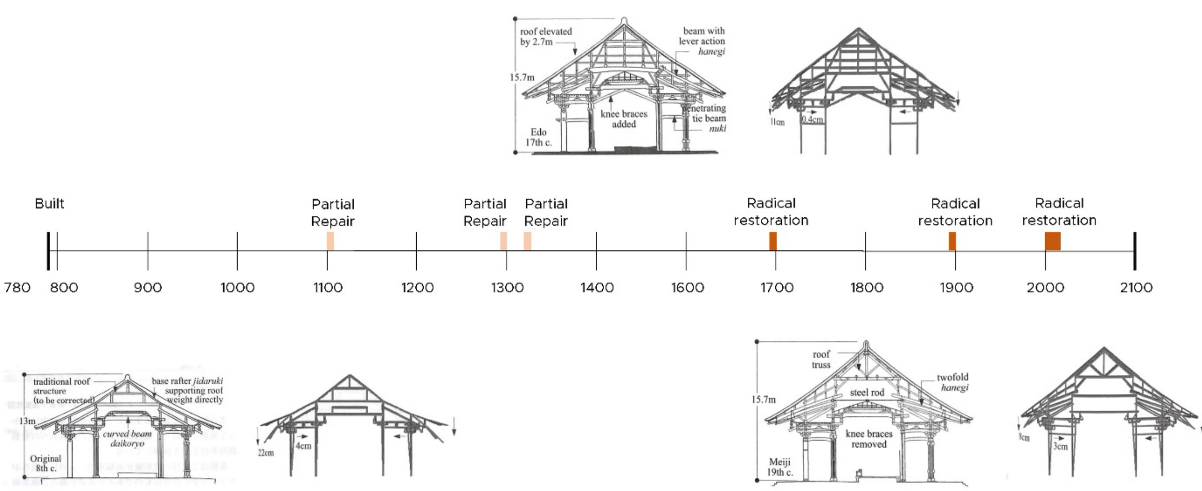

Figure 3.10: Historical maintenance timeline (Office of Cultural Assets Preservation, 2009 & Own work)

According to the historical records, the hall has undergone at least three partial repairs and three major restorations, the latter involving complete dismantlement and overhaul. In an interview with Mr. Akira Nishimura, a senior advisor at the Takenaka Carpentry Tools Museum—which is affiliated with the corporation responsible for the hall's most recent restoration—it was noted that such major restorations typically occur every 100 years and can span up to a decade. The most recent comprehensive restoration takes place from January 2000 to December 2009, with a total expenditure of 3,023,609,004 JPY (approximately 18,520,873.73 Euro). This budget covered the costs of dismantling, scaffolding, new materials, reinforcing structural elements, and other associated expenses.

Most of the major maintenance efforts are prompted by visibly apparent structural deteriorations, such as the tilting of additional eaves and the columns that support them, this shows the potential that the structure can eventually fail.

Minor repairs, which may involve replacing parts of the structure or installing metal fasteners, are carried out as needed and are not always systematically recorded.

Japanese Heritage Building Inspecting and Maintenance

In Japan, visual inspection has historically been the primary method for assessing building components. This visual inspection is normally performed for the approximate timeframe. If any parts are found to be deteriorated, they are either partially or fully replaced. After the Meiji period in the 19th century, the use of steel fasteners was introduced. In cases where critical damage is observed that could lead to structural failure, the entire structure is dismantled for a thorough examination of each element. Any components that are no longer functional are replaced with new ones matching the original dimensions. This method is considered to be time-consuming as it can take up to ten years to execute the whole process and it also requires a high level of accuracy of work that calls for the high skilled workers. More recently, a method has been implemented for reinforcing redundant structures to strengthen aging ones. However, this technique is only applied in areas not visible to occupants, such as above the ceiling. (Interviewing with Mr. Akira Nishimura, the senior advisor at Takenaka Carpentry Tools Museum, 2024).

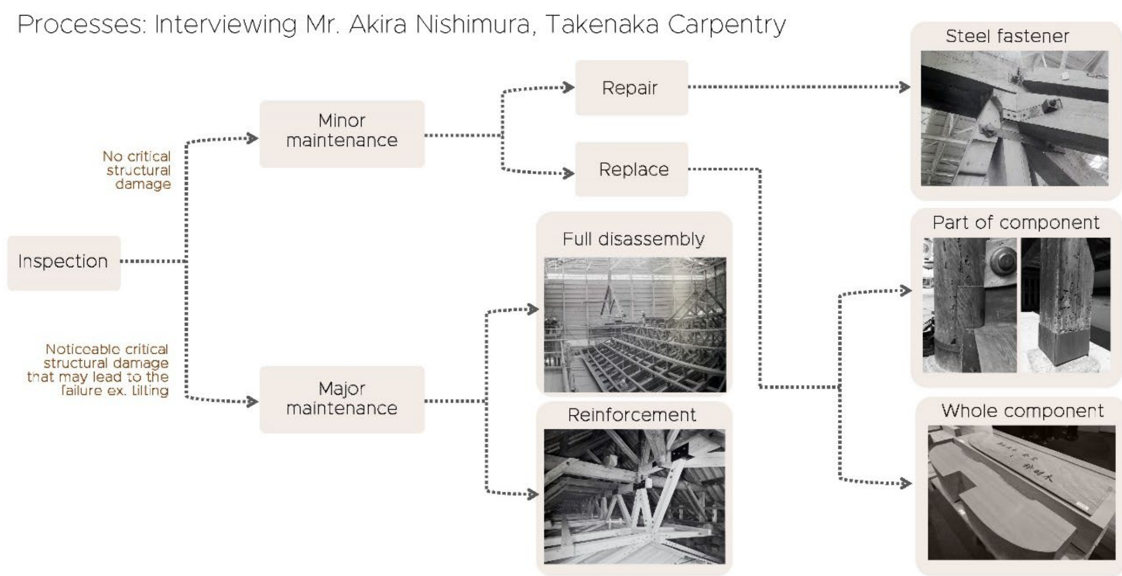

Figure 3.11: Diagram of Maintenance and Inspection Process of Japanese Timber Temples (Own work)

Figure 3.12: Minor maintenance: Metal fasteners (Taken onsite)

Figure 3.13: Minor maintenance: Components partly replace (Taken onsite)

Figure 3.14: Minor maintenance: Components fully replace (Taken at Takenaka Carpentry Tools Museum)

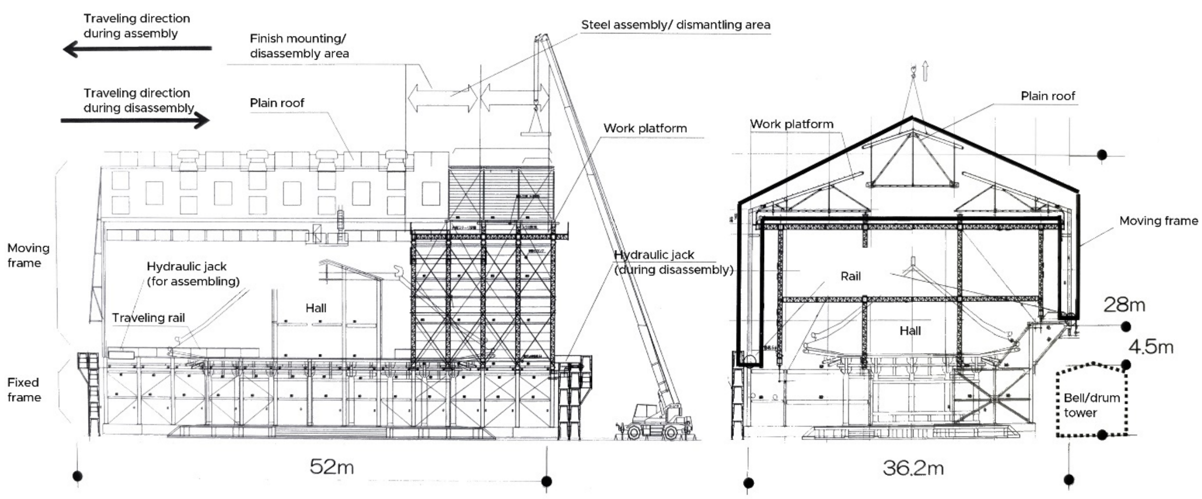

Figure 3.15: Major maintenance: Fully dismantle (Office of Cultural Assets Preservation, 2009)

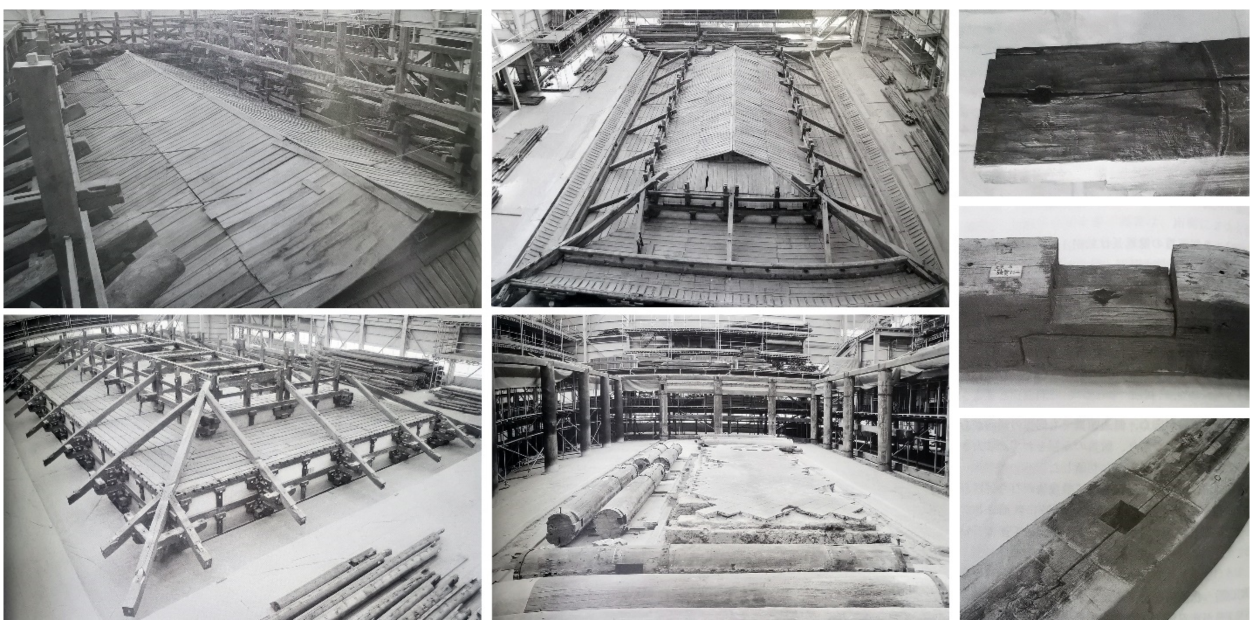

Figure 3.16: Major maintenance: Fully dismantle (Office of Cultural Assets Preservation, 2009)

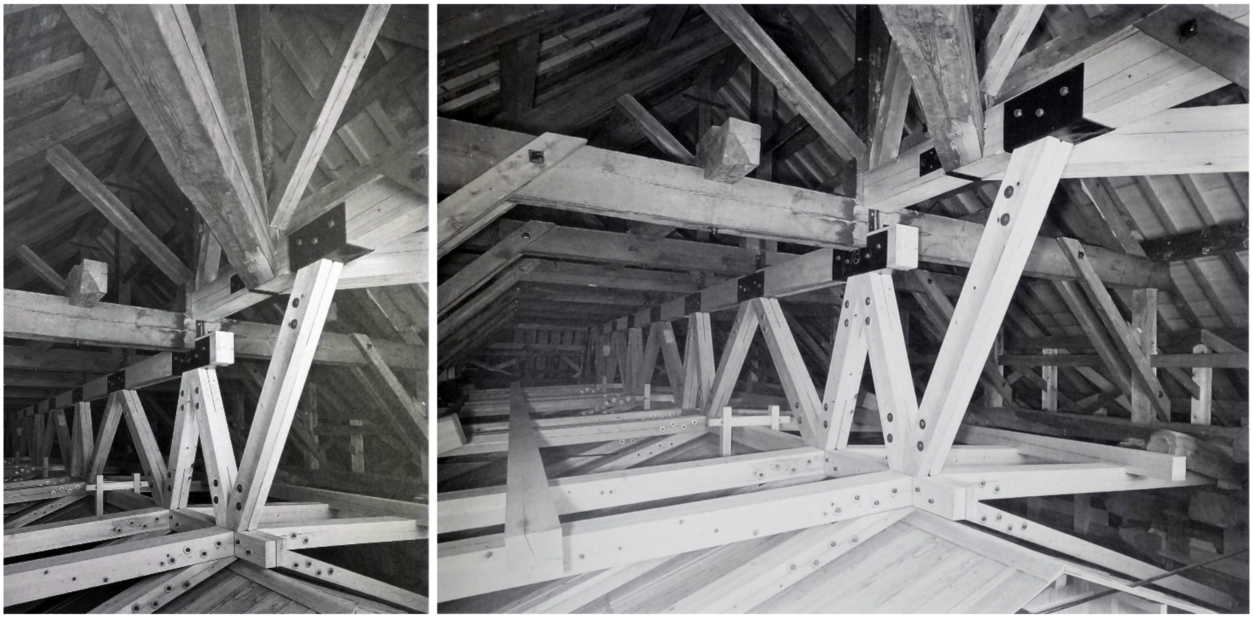

Figure 3.17: Major maintenance: Reinforcement with redundant structures (Office of Cultural Assets Preservation, 2009)

This visual inspection method is based on the heuristic decision rules, namely, it relies on either time-based or condition-based metrics to guide the maintenance actions. Time-based maintenance, a form of preventive maintenance, operates on predetermined intervals, scheduling activities like component replacement or repair strictly according to the passage of time. This approach assumes that the deterioration or failure likelihood of a component increases with time, regardless of its actual condition. On the other hand, condition-based maintenance tailors maintenance actions to the actual state of the structure, with decisions driven by direct performance metrics, such as the depth of decay observed during inspections.

While both methods aim to preempt failure and extend the lifespan of structural components, their effectiveness heavily depends on the knowledge and experience of the maintenance planner. These heuristic-based policies often utilize exhaustive policy searches to address life-cycle management challenges, however, this approach can become computationally burdensome, particularly in systems with multiple components or those requiring long-term planning. The limitations in scalability and potential sub-optimality in complex scenarios highlight the need for more sophisticated decision-making frameworks in maintenance management (Pablo G. Morato, 2022).

The Climate of the Location

The climate data and illustrative scenarios utilized in this study are derived from the data previously specified for Japan, as mentioned in the preceding section.

Japanese Cypress (Hinoki) mechanical properties

Hinoki cypress (*Chamaecyparis obtusa*) is a coniferous tree commonly utilized as a building material in Japan highlighting remarkable durability and lightness. Renowned for its ability to endure harsh weather conditions such as wind and snow over millennia, it stands as a testament to its resilience.

Figure 3.18: Hinoki leaf and texture (Museum, 2014)

Pierre et al. (2011) conduct a series of experiments employing various methodologies including the method of the single cube, four-point bending, compression, and off-axis tensile test, to investigate the mechanical characteristics of Hinoki cypress sourced from three different prefectures in Japan. The results are as follows:

Properties	**Value**	**Unit**	**SD**
Density	446	kg/m3	5.36%
MOE	11.72	GPa	3.10%
MOR	70.12	MPa	14.91%
Elastic properties			
Young's moduli			
E_R	0.93	GPa	13.10%
E_T	0.62	GPa	8.01%
E_L	11.89	GPa	6.41%
Shear moduli			
G_{TL}	0.82	GPa	8.59%
G_{LR}	0.86	GPa	13.12%
G_{RT}	0.027	GPa	19.78%
Poisson ratios			
$v_{LT/RT}$	0.416	GPa	23.04%
$v_{LR/TR}$	0.424	GPa	45.09%
Strength properties			
Compression			
R	6.3	MPa	8.57%

T	6.7	MPa	11.93%
L	37.1	MPa	3.59%
Shear			
LT	19.31	MPa	3.09%
LR	21.31	MPa	2.67%
RT	4.97	MPa	
Tensile strength			
R	3	MPa	
T	3	MPa	
L	110.8	MPa	

Table 3.1: Hinoki cypress mechanical properties (Pierre Berard, 2011)

The findings from these experiments contain the crucial data points that will be used to develop the finite element analysis (FEA) model to enhance the understanding of the performance and condition of Hinoki cypress-based structures that will change over time per the deterioration. Ultimately, this information will be used in the transitional model setup of the machine learning framework.

Framework setup

To establish the mathematical framework for the Dec-POMDP, it is essential to systematically process the information obtained from the case study. This initial step is simplifying the structures and components. Then incorporating advanced modeling techniques such as Finite Element Analysis (FEA) and the gamma process is involved to accurately simulate and predict structural deterioration. Finite Element Analysis provides a detailed simulation of the physical behavior of the structure under various loads and conditions, while the gamma process models the statistical distribution of damage increments over time. Together, these methodologies form a comprehensive basis for understanding and quantifying the structural changes that inform the Dec-POMDP framework. This processed data is then allocated to different elements of the decision-making model, including state spaces, observation and action spaces, and the functions governing observations, transitions, rewards, and the discount factor. Each component of this setup will be thoroughly explained to provide a clear understanding of how each contributes to the overall decision-making process in structural maintenance and management.

Structural deterioration model setup

Simplified case study structure and components

Once the case study has been selected, the complex structure is simplified to facilitate the setup of the model. Each component of the structure is assigned a number, and details such as dimensions, cross-sectional area, and conditions of exposure to weather are cataloged in the table provided below.

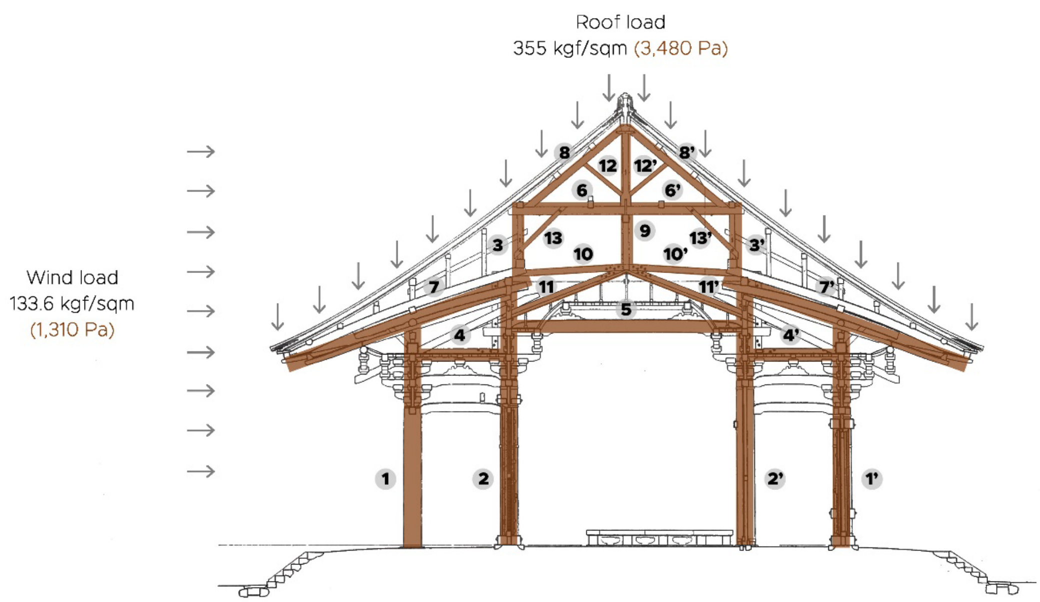

Figure 3.19: Simplified component numbers with load cases (Own work)

Component	Structural Type	width, b (mm)	height, h (mm)	cross-sectional area (mm^2)	Condition
1	Column	d = 600		282600	Exposed to climate: above-ground
1'	Column	d = 600		282600	Exposed to climate: above-ground
2	Column	d = 600		282600	Exposed to climate: above-ground
2'	Column	d = 600		282600	Exposed to climate: above-ground
3	Roof beam (vertical)	210	180	37800	In building envelope
3'	Roof beam (vertical)	210	180	37800	In building envelope
4	Beam	240	325	78000	Exposed to climate: above-ground
4'	Beam	240	325	78000	Exposed to climate: above-ground
5	Beam	330	440	145200	In building envelope
6	Beam	240	270	64800	In building envelope
6'	Beam	240	270	64800	In building envelope
7	Roof beam	240	325	78000	Exposed to climate: above-ground
7'	Roof beam	240	325	78000	Exposed to climate: above-ground
8	Roof beam	180	235	42300	In building envelope
8'	Roof beam	180	235	42300	In building envelope
9	Roof beam (vertical)	180	210	55800	In building envelope
10	Roof beam	300	200	60000	In building envelope
10'	Roof beam	300	200	60000	In building envelope
11	Roof beam	150	200	30000	In building envelope

11'	Roof beam	150	200	30000	In building envelope
12	Roof beam	140	150	21000	In building envelope
12'	Roof beam	140	150	21000	In building envelope
13	Roof beam	150	150	22500	In building envelope
13'	Roof beam	150	150	22500	In building envelope

Table 3.2: Component list with dimensions and condition

In traditional Japanese timber structures, the joints between components are critical structural elements that can significantly influence overall stability and durability. These structures typically employ dry joint connections, which do not rely on glue, bolts, nails, or screws. Such joints are meticulously crafted to fit together through precise and complex carpentry techniques, allowing for both aesthetic appeal and structural integrity without the use of metal fasteners. This method of construction requires specialized structural and failure analysis to understand the behavior of the joints under various loads.

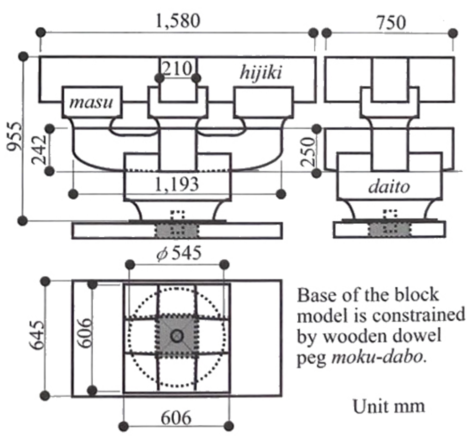

Figure 3.20: One example of the dry joints of Toshodaiji Temple (Office of Cultural Assets Preservation, 2009)

However, despite their importance, the specific analysis of these discrete joints, which vary depending on their position within the structure, will not be included in this study due to time constraints. Consequently, while the joints are acknowledged as crucial components, this research will focus on other aspects of the structure's integrity and decay, leaving the detailed examination of dry joints for future investigation.

Structural Analysis

The Finite Element Analysis (FEA) model is conducted using two distinct methodologies. The initial method employs the Karamba3D plugin within the Grasshopper platform. However, this approach identifies errors in certain sections of the structure. Furthermore, the numerical results produced by this method do not seem to be entirely precise.

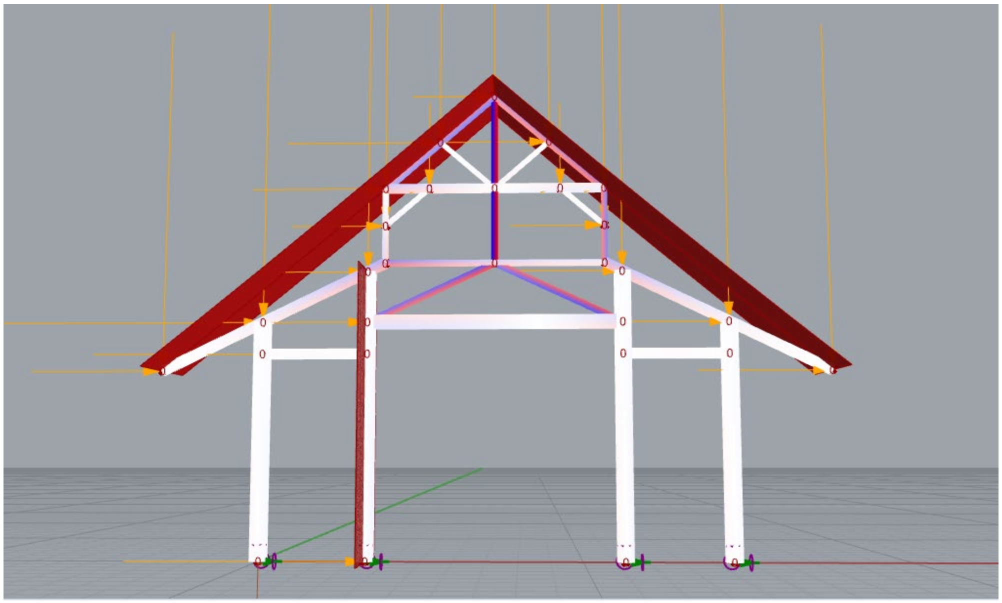

Figure 3.21: Axial stress results from the Karamba3D plugin (Own work)

Consequently, an alternative method is employed. A supplementary 2D model is developed using the platform available at https://structural-analyser.com. Within this model, various parameters are meticulously defined, including load cases, component dimensions, types of supports, hinge types, and material properties, with specific attention to Young's Modulus for each axis. Following these specifications, the structural analysis is executed. The outcomes of this analysis are comprehensively illustrated through Free Body Diagrams, which display the axial forces, bending moments, shear forces, and deflections observed in the model. The results are shown as follows:

Axial Loads

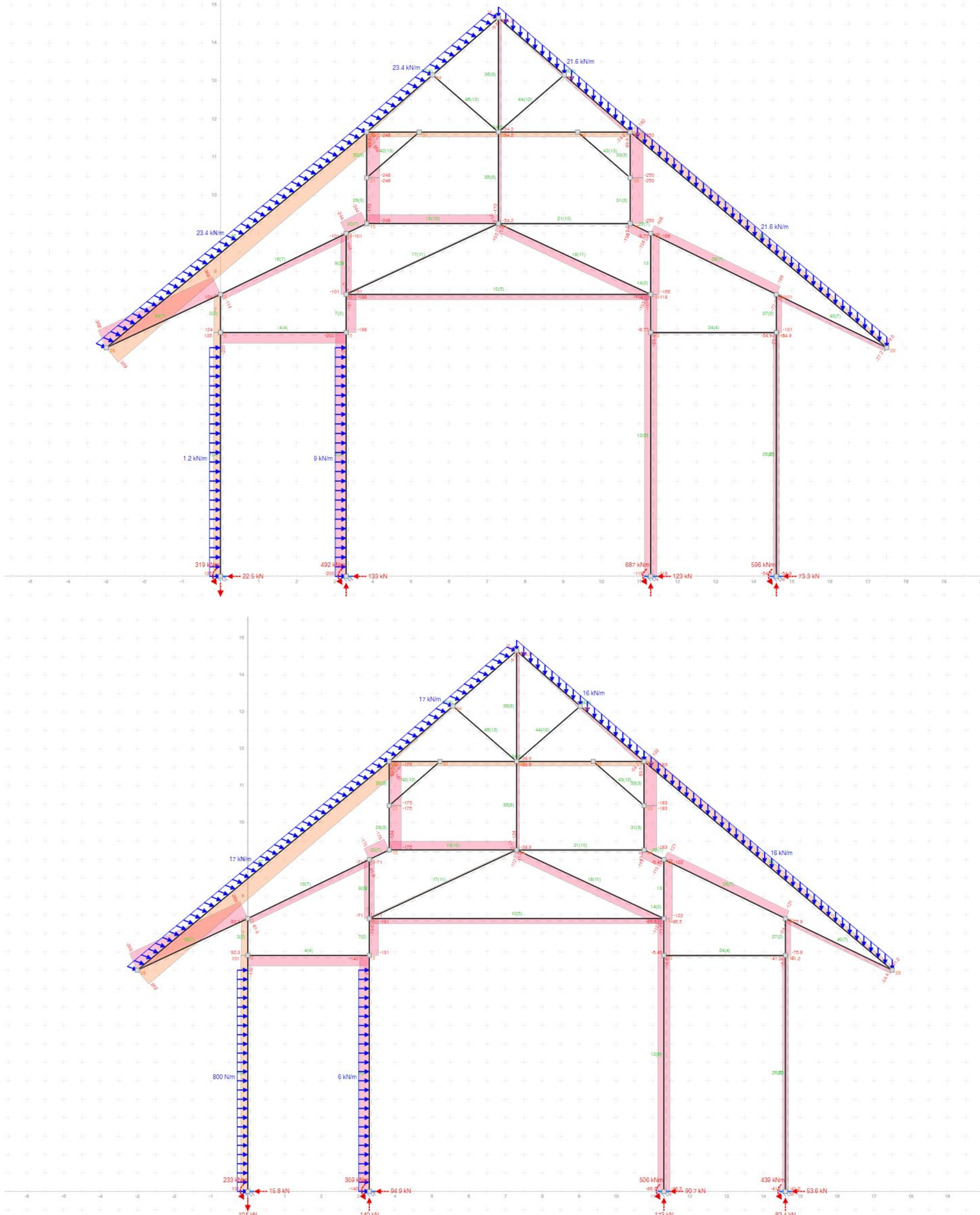

Figure 3.22: Free Body Diagram (FBD) showing axial loads with (upper) and without (lower) safety factors (Own work)

Bending Moments

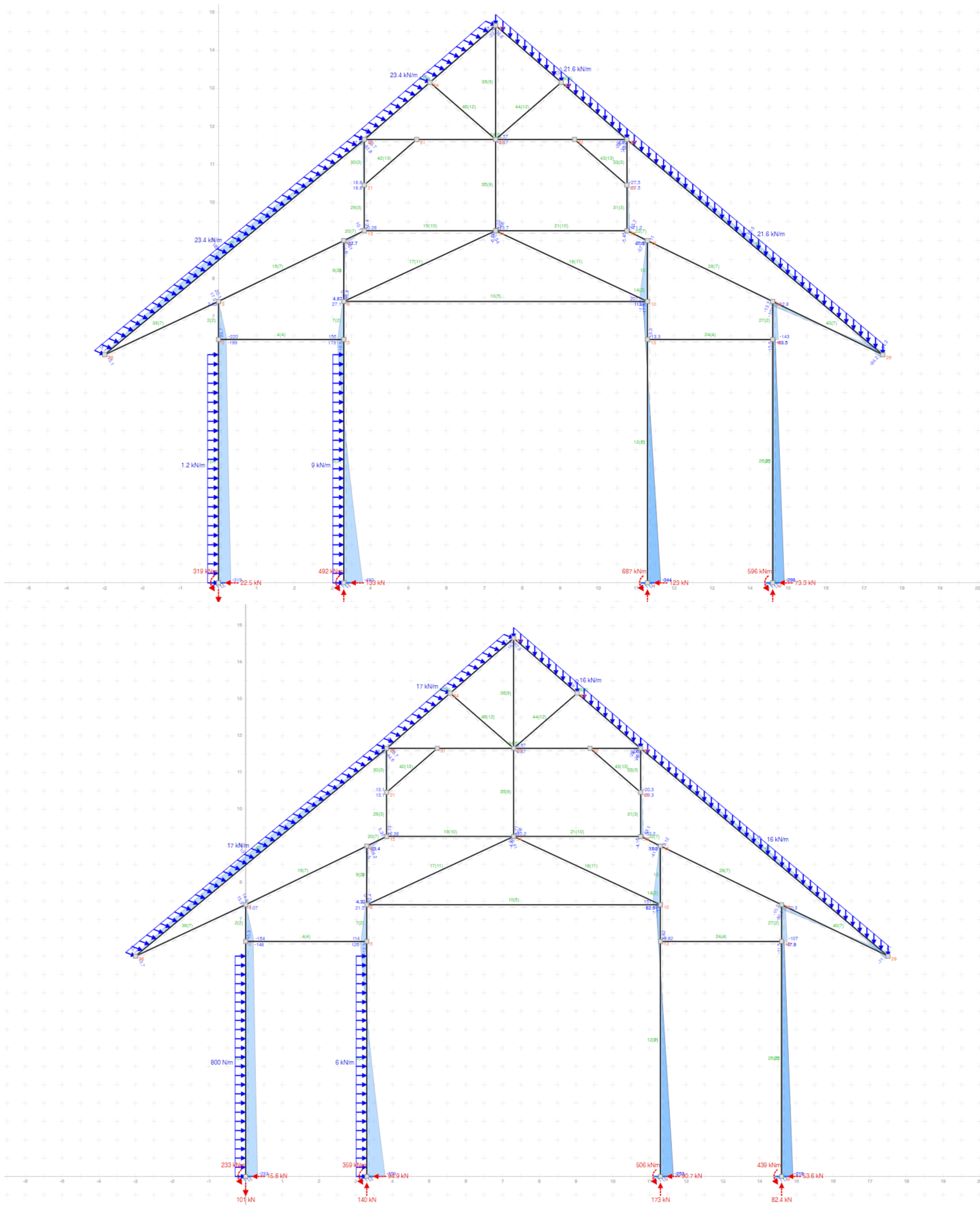

Figure 3.23: Free Body Diagram (FBD) showing bending moments with (upper) and without (lower) safety factors (Own work)

Deflections

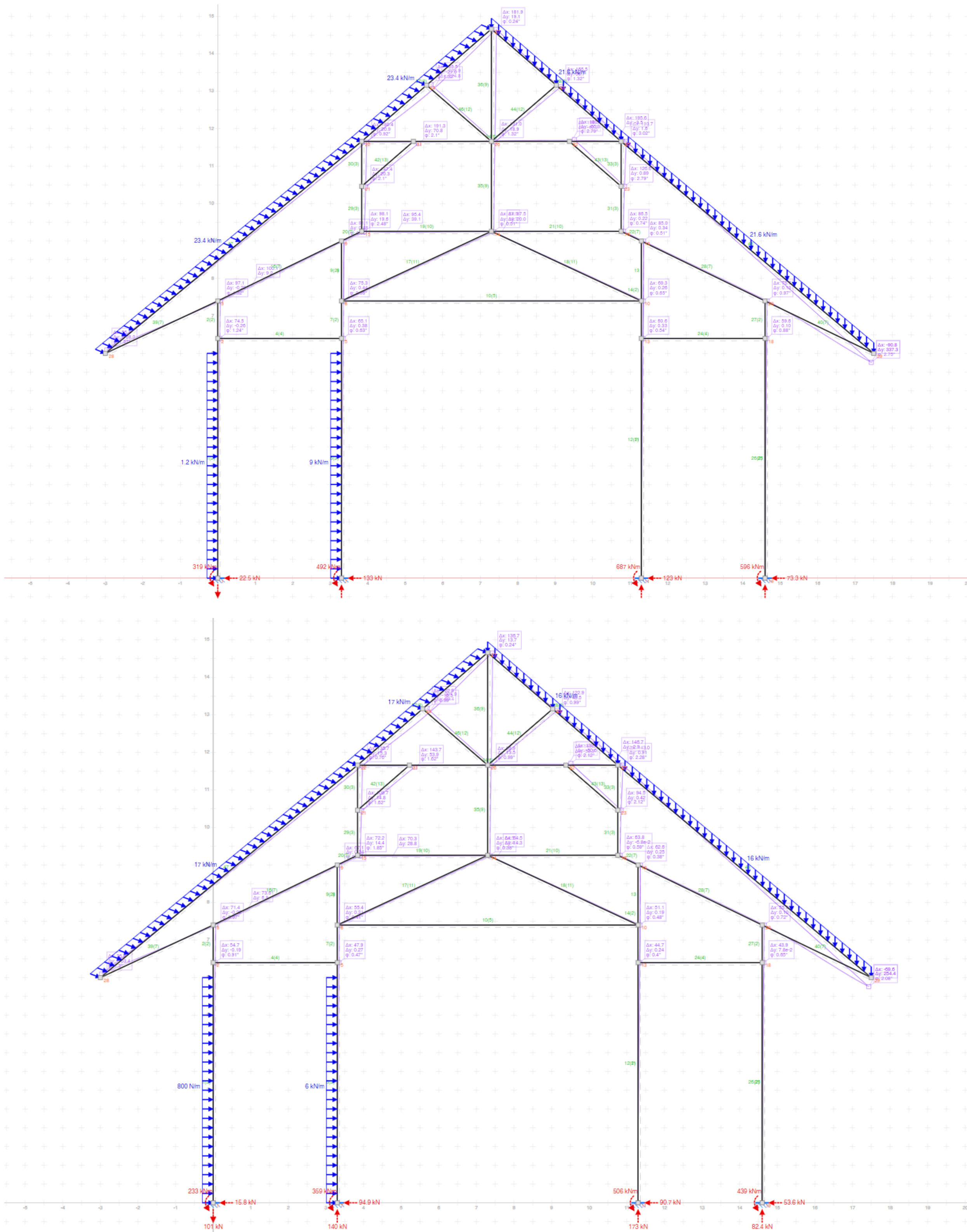

Figure 3.24: Free Body Diagram (FBD) showing deflections with (upper) and without (lower) safety factors (Own work)

After the structural analysis is completed, the results were systematically compiled. The maximum axial loads, encompassing both compression and tension, along with the maximum bending moments for each component, are tabulated. These were presented alongside the cross-sectional area, moment of inertia, and specific strength of the timber along each axis for each component. These critical parameters will be utilized to determine the critical decay depth necessary to predict the failure of the components.

Component	Structural Type	width, b (mm)	height, h (mm)	y (mm)	cross-sectional area (mm^2)	Moment of Inertia, I (mm^4)	Hinoki: Axial strength (MPa)	Maximum axial force: with safety factors (kN)	Maximum axial force: without safety factors (kN)	Hinoki: MOR (MPa)	Maximum bending moment with safety factors (kNm)	Maximum bending moment without safety factors (kNm)
1	Column		600	300	282600	6358500000	110.8	135	101	70.12	319	233
1'	Column		600	300	282600	6358500000	37.1	101	75.9	70.12	298	219
2	Column		600	300	282600	6358500000	37.1	200	140	70.12	492	359
2'	Column		600	300	282600	6358500000	37.1	166	122	70.12	344	253
3	Roof beam (vertical)	210	180	90	37800	138915000	37.1	248	175	70.12	37.9	28.6
3'	Roof beam (vertical)	210	180	90	37800	138915000	37.1	250	183	70.12	71.2	53.2
4	Beam	240	325	162.5	78000	686562500	6.3	207	152	70.12	20.7	15.3
4'	Beam	240	325	162.5	78000	686562500	6.3	23.4	16.6	70.12	15.6	11.5
5	Beam	330	440	220	145200	2342560000	6.3	101	73.6	70.12	17.6	13
6	Beam	240	270	135	64800	393660000	6.3	170	124	70.12	13.7	10.5
6'	Beam	240	270	135	64800	393660000	6.3	17.2	11.2	70.12	13.7	10.5
7	Roof beam	240	325	162.5	78000	686562500	6.3	368	268	70.12	81	58.2
7'	Roof beam	240	325	162.5	78000	686562500	6.3	166	121	70.12	107	80.5
8	Roof beam	180	235	117.5	42300	194668125	3	44.1	33.8	70.12	38.6	27.9
8'	Roof beam	180	235	117.5	42300	194668125	6.3	74.2	54.7	70.12	38.2	28.5
9	Roof beam (vertical)	180	210	105	55800	102060000	37.1	54.2	38.9	70.12	13.7	11.3
10	Roof beam	300	200	100	60000	200000000	6.3	170	124	70.12	10.4	7.73
10'	Roof beam	300	200	100	60000	200000000	6.3	17.2	11.2	70.12	5.45	4.16
11	Roof beam	150	200	100	30000	100000000	3	21.4	17.2	70.12	0.58	0.44
11'	Roof beam	150	200	100	30000	100000000	6.3	153	112	70.12	1.59	1.16
12	Roof beam	140	150	75	21000	39375000	0	0	0	70.12	0	0
12'	Roof beam	140	150	75	21000	39375000	0	0	0	70.12	0	0
13	Roof beam	150	150	75	22500	42187500	0	0	0	70.12	0	0
13'	Roof beam	150	150	75	22500	42187500	0	0	0	70.12	0	0
							(-) compression					
							(+) tensile					

Table 3.3: Component list with the details needed for defining the failure conditions

The table above indicates that components 12, 12′, 13, and 13′ exhibit neither axial force nor bending moment. Consequently, these specified components will be excluded from the model.

Decay Models with Climate Scenarios

The decay models are established according to the research conducted by Wang et al. (2008), as referenced in the previous section. These models are configured based on the specific conditions of each component, with separate models for 1) components within the building envelope and 2) components that are located above ground and exposed to climatic conditions. Furthermore, various climate scenarios are integrated into these models through the application of climate parameters.

Model for components in the building envelope

In this model, the decay rate *(r)* is determined by three specific parameters: material, geometry, and climate. These parameters are tailored based on the information from the case study.

Material parameter (k_{wood}): This parameter is defined by the durability class of the structural material. For this case study, the focus is on Hinoki Cypress, which is renowned for its durability. Given its proven longevity of over 400 years, it is classified as class 1, indicating the highest level of durability.

Geometry parameter ($k_{geometry}$): This parameter assesses the contact surface factor, determining whether the structural member is in contact with other structural elements.

Climate parameter ($k_{climate}$): For components located in the roof space, the climate parameter is gauged by the annual duration of timber wetness, measured in hours per year. The relationship between the $k_{climate}$ value and the frequency of rainfall events is illustrated as follows:

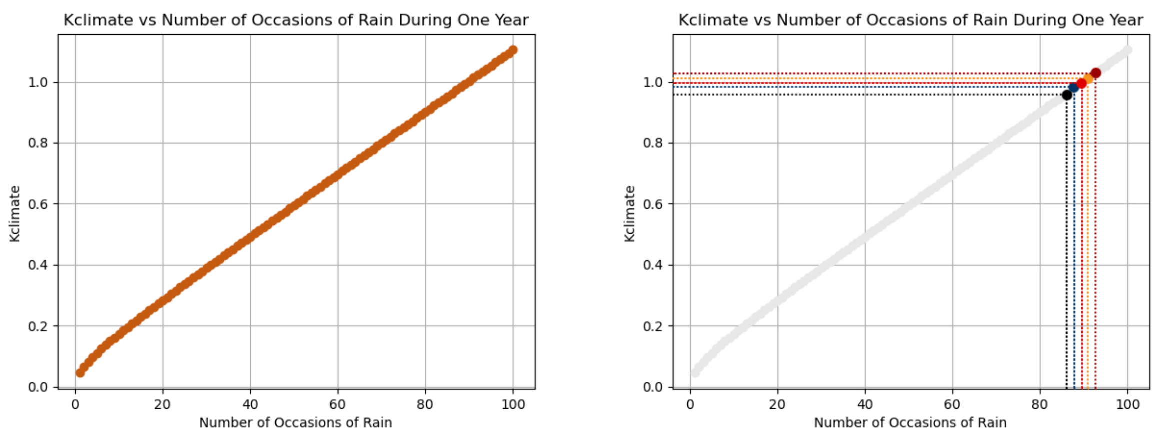

Figure 3.25: Relationship between the rain occasion and $k_{climate}$ value (Own work)

The graph illustrates that as rain occurrences vary due to climate change, the $k_{climate}$ value also adjusts. Consequently, this alteration affects the decay rate (r). Ultimately, this impact is depicted through the relationship between decay depth (measured in millimeters) and time (expressed in years), as demonstrated in the following representation:

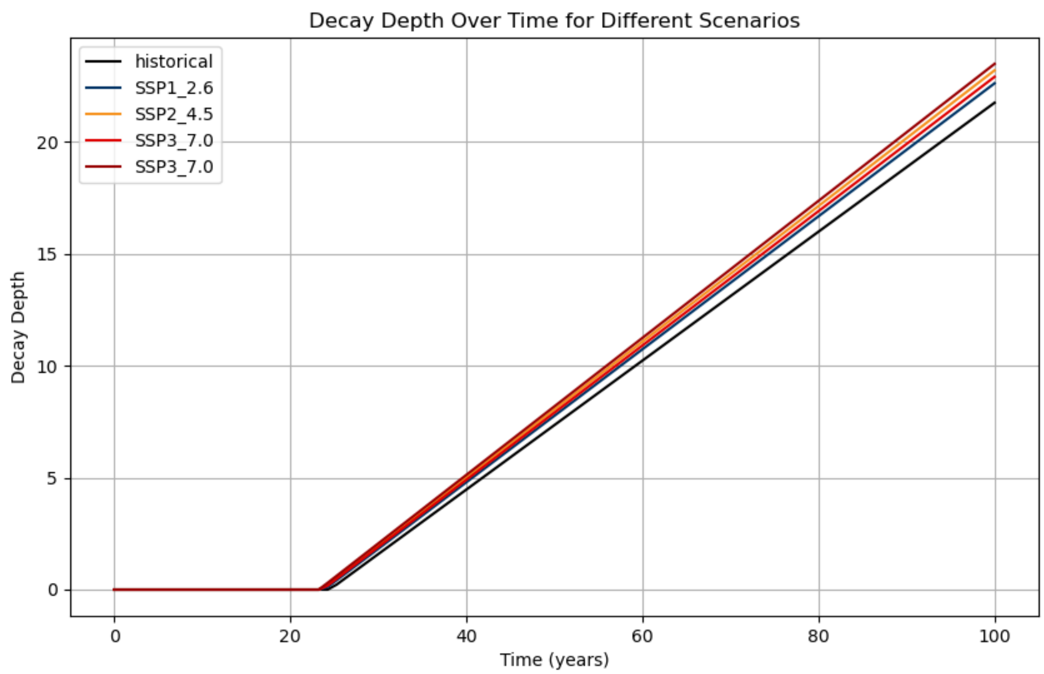

Figure 3.26: Decay depth (mean) over time of components within building envelope for different climate scenarios (Own work)

Model for components exposed to climate

The decay rate *(r)* in this model is defined by the wood durability parameter (k_{wood}), climate parameter ($k_{climate}$), paint parameter (k_p), thickness parameter (k_t), width parameter (k_w), fastener parameter (k_n), and geometry parameter ($k_{geometry}$).

While each component shares identical values for the wood durability parameter, paint parameter, and fastener parameter, the decay rate will differ due to the varying dimensions (specifically thickness and width) of each component. Additionally, the decay rate is influenced by different climate scenarios.

In this model, the climate parameter is characterized by the Climate Scheffer Index, which is determined based on temperature and precipitation days, as outlined in the literature review. With varying scenarios of climate change, the $k_{climate}$ will adapt accordingly. The methodology for determining the $k_{climate}$, as described in the referenced paper concerning climate conditions in Australia, is utilized to establish the relationship between the k value and the Scheffer Index Value. Ultimately, the $k_{climate}$ for each climate scenario will be defined based on this approach.

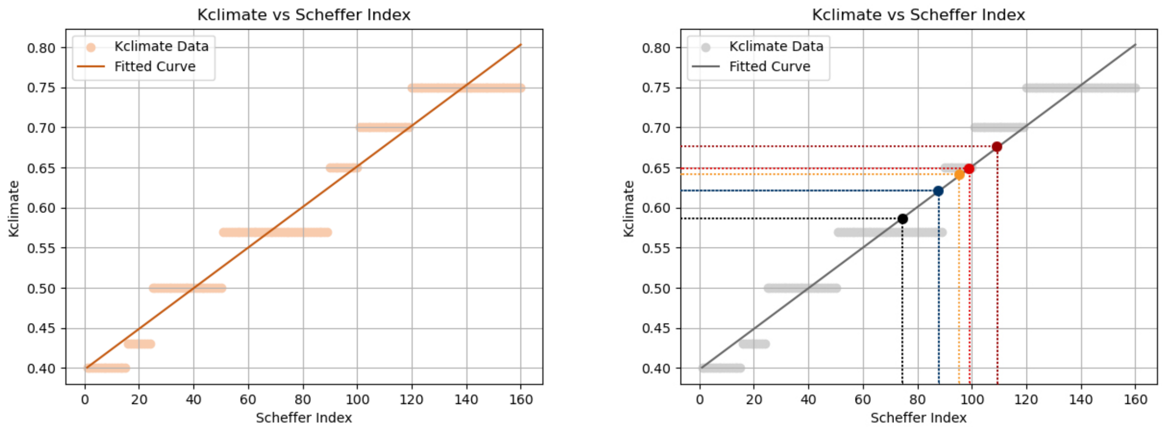

Figure 3.27: Relationship between the Climate Scheffer Index and $k_{climate}$ value (Own work)

The impact of varying $k_{climate}$ and dimension parameters on the decay rate *(r)* are illustrated through the differences in the increase of decay depth (in millimeters) over time across each climate scenario for the different components:

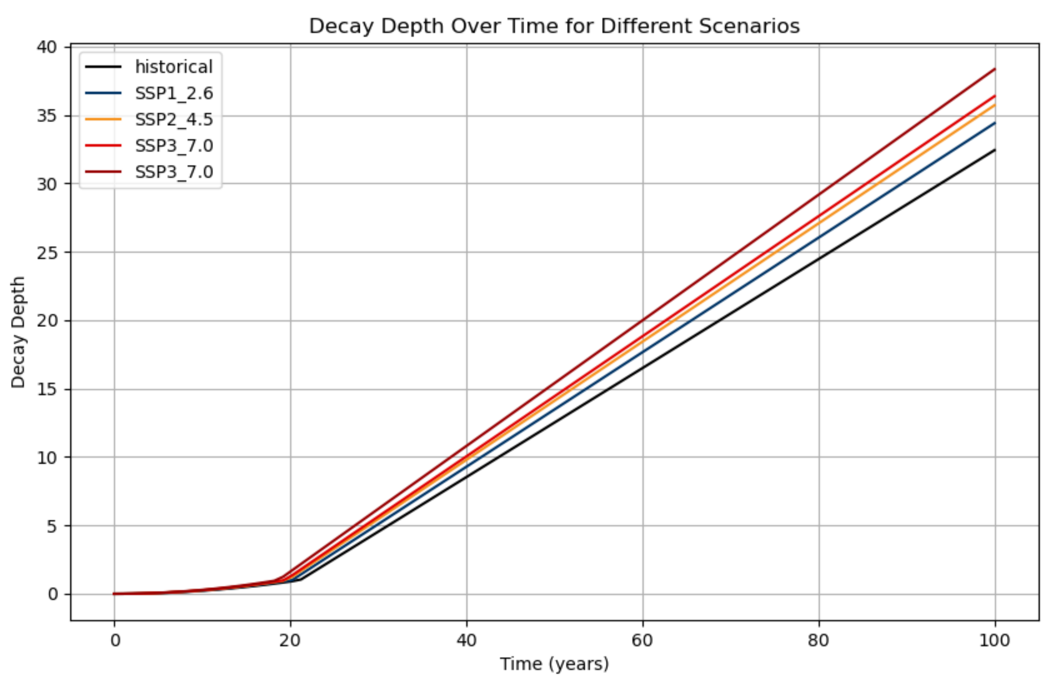

Figure 3.28: Decay depth (mean) over time of components 1 and 1' above exposed to the weather for different climate scenarios (Own work)

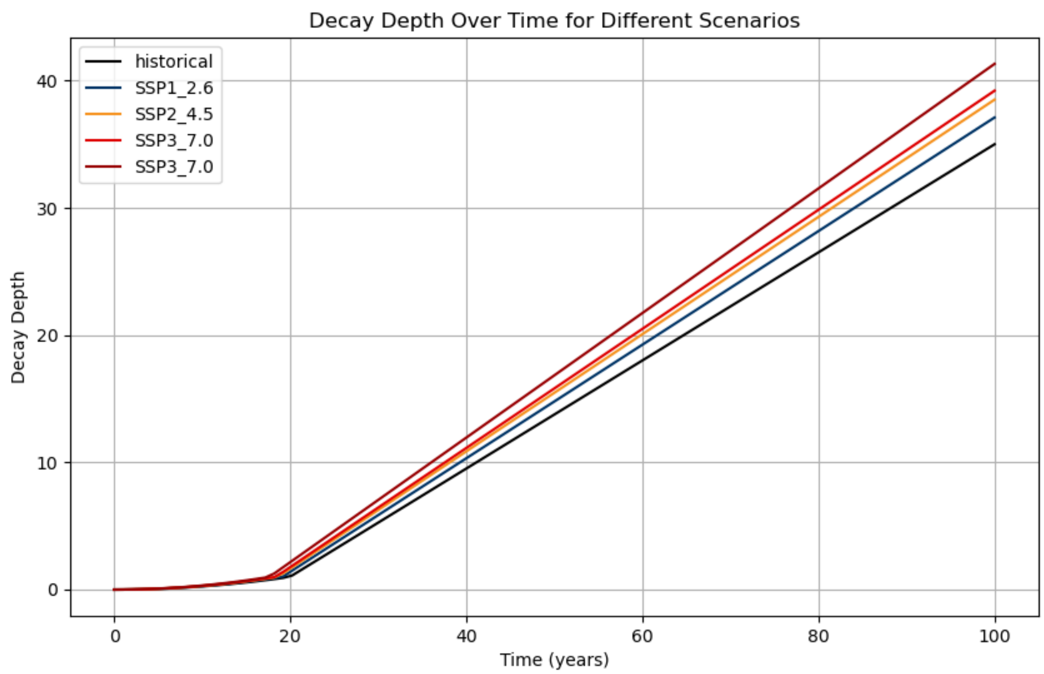

Figure 3.29: Decay depth (mean) over time of components 2 and 2′ above exposed to the weather for different climate scenarios (Own work)

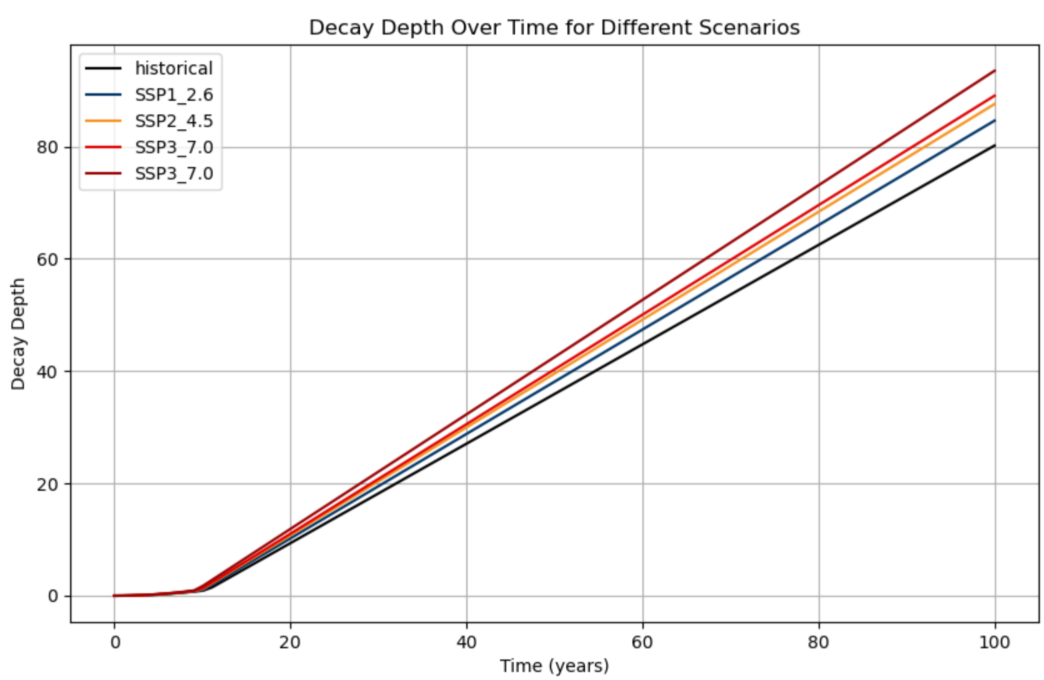

Figure 3.30: Decay depth (mean) over time of components 4, 4′, 7, and 7′ above exposed to the weather for different climate scenarios (Own work)

Damaged cross-sectional area

In this research, the decay depth (in mm) is assumed as the mass loss in the cross-sectional area of timber elements.

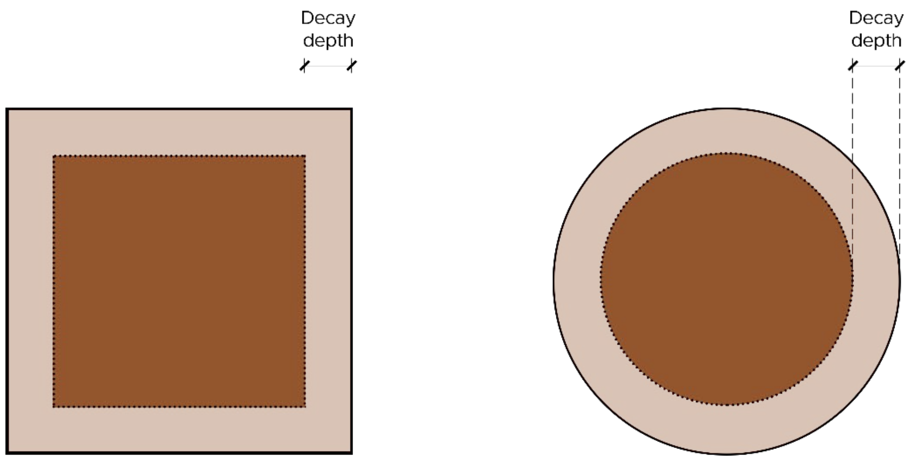

Figure 3.31: Decay depth and the loss of cross-sectional area of timber components (Own work)

The damaged cross-sectional area is represented by: $\frac{A(0)-A(\tau)}{A(0)}$

When $A(0)$ is an initial cross-sectional area and $A(\tau)$ is a cross-sectional area at the exposure time τ.

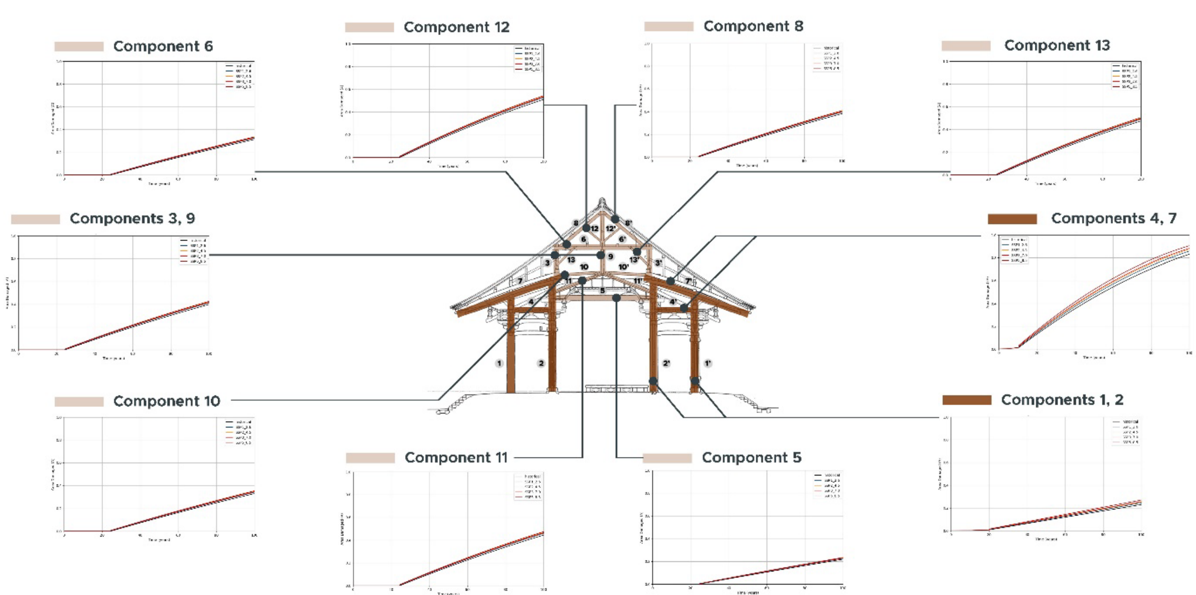

Figure 3.32: Damaged cross-sectional area changes over time for every component (Own work)

Stochastic deterioration process

Gamma Process

The gamma process is essential for simulating random positive damage increments for each component and updating the belief state based on a transition model. It effectively captures continuous Markovian transitions in discrete time steps. Specifically, for two-time steps, deterioration τ_1 and τ_2 where $\tau_1 < \tau_2$, the damage increment also adheres to a gamma distribution. Employing the gamma process is a practical modeling approach in many stochastic deterioration engineering scenarios, such as structural maintenance. It is particularly effective for modeling gradual damage accumulation, such as decay (van Noortwijk, 2009).

Assumptions include that each component's damage process is independent and that no decay occurs in any component (maintaining intact condition) at the beginning of the inspection and maintenance schedule at $\tau = 0$. Only temperature and precipitation are considered to influence the decay rate due to fungi, with other climate effects disregarded. Given a time constraint, component 7 is chosen to exemplify the decay pattern for all components.

The gamma process results in random positive damage increments at each decision step for each component. As resistance is influenced by potential climate scenarios, a stochastic deterioration process is established for each. This process is used to set up the environmental transition model, $T \leftarrow P(s'|s, a)$.

The mean uniform section loss percentage, d_m, is approximated as proportional to τ^{β},

$$d_m = \frac{A(\tau)}{A(0)} \propto \tau^{\beta}$$

Where β is a constant typically ranging between $0 < \beta \leq 2.0$ depending on environmental conditions, causes of deterioration, material properties, etc. β controls the shape parameter of the gamma distribution; when $\beta = 1$, the relationship is linear, in other words, stationary. To model the stochastic nature of deterioration, the section loss percentage, d, is treated as a gamma process with a mean value of d_m. The rate of deterioration is assumed to correlate directly with exposure time.

The input for the gamma process is based on the relationship between the loss of cross-sectional area and time, as described by the earlier-mentioned equation. The average damage to the area after 100 years varies according to different climate scenarios, as outlined in the table below. It is assumed that the standard deviation is 10% over a 100-year period. The deterioration process corresponding to these parameters is illustrated in the figure below.

Climate scenarios	Variable	Average	Unit
historical	Decay depth	80.15	mm
	Damaged Area	13260	mm^2
	Damage	0.83	n/a
SSP1-2.6	Decay depth	84.59	mm
	Damaged Area	11700	mm^2
	Damage	0.85	n/a
SSP2-4.5	Decay depth	87.55	mm
	Damaged Area	10140	mm^2
	Damage	0.87	n/a
SSP3-7.0	Decay depth	89.03	mm
	Damaged Area	9360	mm^2
	Damage	0.88	n/a
SSP5-8.5	Decay depth	93.47	mm
	Damaged Area	7800	mm^2
	Damage	0.9	n/a

Table 3.4: Average decay depth and damaged cross-sectional area at the time of 100 years per different climate scenarios

(a)

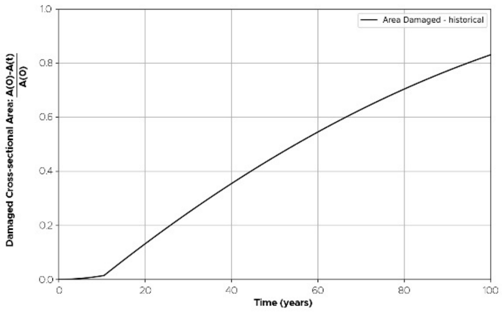
Area Damaged - historical
Damaged Cross-sectional Area: $\frac{A(O)-A(t)}{A(O)}$
Time (years)

(a)

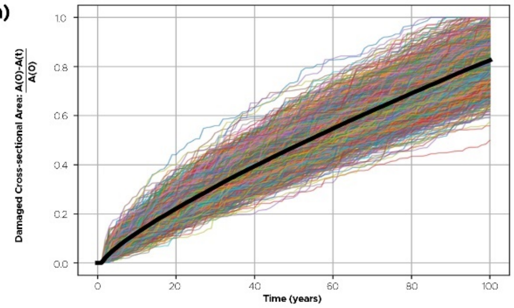
Damaged Cross-sectional Area: $\frac{A(O)-A(t)}{A(O)}$
Time (years)

(b)

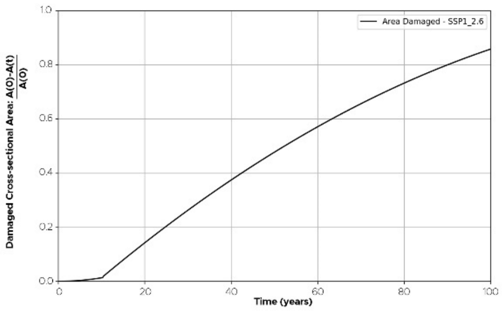
Area Damaged - SSP1_2.6
Damaged Cross-sectional Area: $\frac{A(O)-A(t)}{A(O)}$
Time (years)

(b)

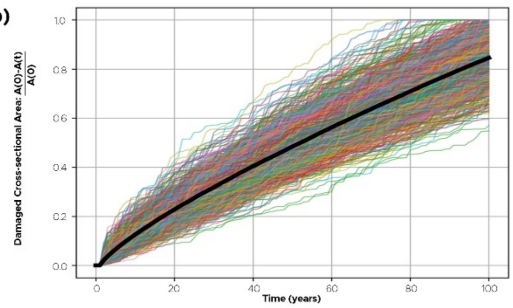
Damaged Cross-sectional Area: $\frac{A(O)-A(t)}{A(O)}$
Time (years)

(c)

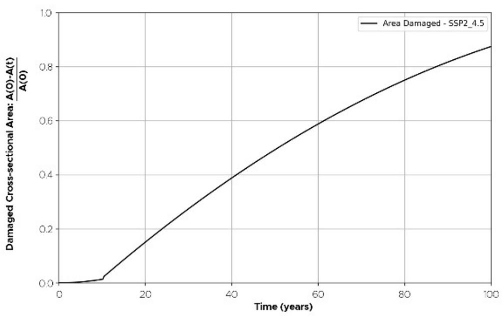
Area Damaged - SSP2_4.5
Damaged Cross-sectional Area: $\frac{A(O)-A(t)}{A(O)}$
Time (years)

(c)

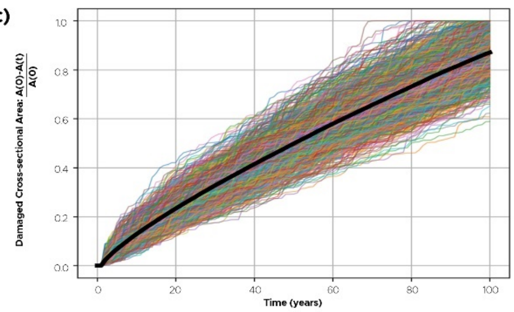
Damaged Cross-sectional Area: $\frac{A(O)-A(t)}{A(O)}$
Time (years)

(d)

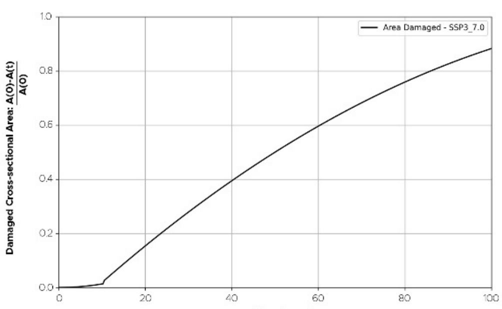
Area Damaged - SSP3_7.0
Damaged Cross-sectional Area: $\frac{A(O)-A(t)}{A(O)}$
Time (years)

(d)

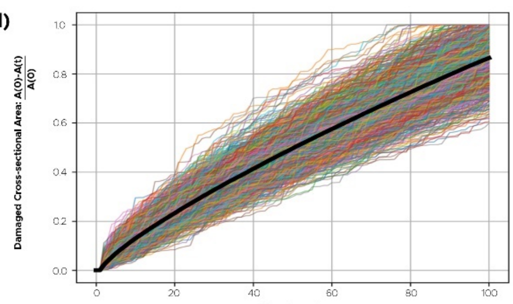
Damaged Cross-sectional Area: $\frac{A(O)-A(t)}{A(O)}$
Time (years)

(e)

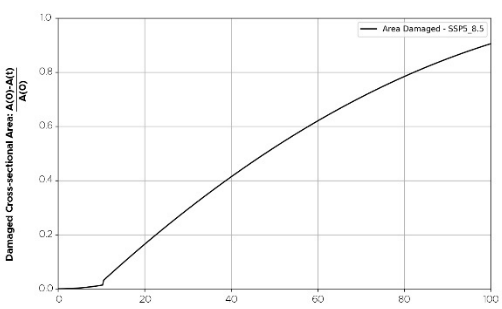
Area Damaged - SSP5_8.5
Damaged Cross-sectional Area: $\frac{A(O)-A(t)}{A(O)}$
Time (years)

(e)

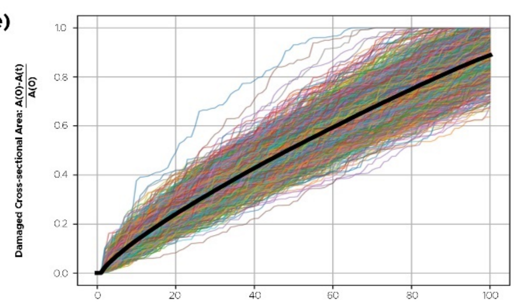
Damaged Cross-sectional Area: $\frac{A(O)-A(t)}{A(O)}$
Time (years)

Figure 3.32: Relationship between damaged cross-sectional area and time from fungi deterioration model (left) and Random trajectories of a Gamma Process describing cross-sectional damage over time (right) per climate scenarios (a) historical (b) SSP1-2.6 (c) SSP2-4.5 (d) SSP3-7.0 (e) SSP5-8.5 of component 4 and 7 (Own work)

Dec-POMDP framework setup

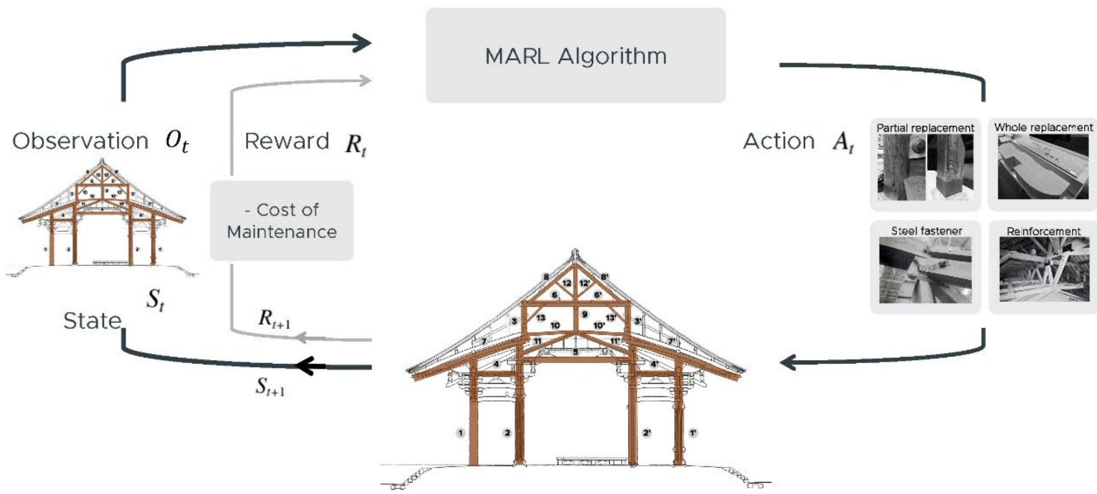

Figure 3.33: Dec-POMDP framework (Own work)

Following the setup of the Structural Deterioration Model, the gathered data is integrated into the Dec-POMDP, which is the mathematical framework used for sequential decision-making. This integration involves distributing the data across various components of the framework, including the number of structural elements, state space (S), observation space (Z), action space (U), observation function (O), reward function (R), transition function (P), and discount factor (γ). Each aspect of this process will be elaborately detailed in the subsequent sections.

Belief State

In the Decentralized Partially Observable Markov Decision Process (Dec-POMDP) framework, the belief state plays a crucial role in managing the uncertainty inherent in the monitoring and maintenance of structural health. The belief state encapsulates the agent's uncertainty regarding the actual state of the environment by representing all possible probability distributions over the states. For the scenario described, the belief space is modeled as a 20-dimensional discrete space, with each dimension corresponding to the belief about the condition of one of the structural elements in a timber structure.

The belief values are determined by several factors, including the Ultimate Limit States (ULS) and Serviceability Limit States (SLS), which define acceptable limits for structural integrity and functionality, respectively. Additionally, operational guidelines dictate maintaining decay depth over 10mm, guiding the updates to the belief state.

This environment assumes that during extreme load events, the resistance of the structure does not degrade, and failure is only triggered when loads exceed the established thresholds. At the onset of the maintenance life cycle, it is assumed that all components are in an intact state. However, varying loads and exposure to different weather conditions introduce stochasticity, causing each component to potentially deteriorate uniquely. As such, at each time step, the belief regarding the cross-sectional area damage of each structural component may change.

For this study, we focus solely on the belief space related to component 7, simplifying the analysis within a belief space that totals 4^{20} discrete states. This approach allows for a detailed examination of the deterioration processes under specific environmental and load conditions, providing a nuanced understanding of structural health progression within the Dec-POMDP framework.

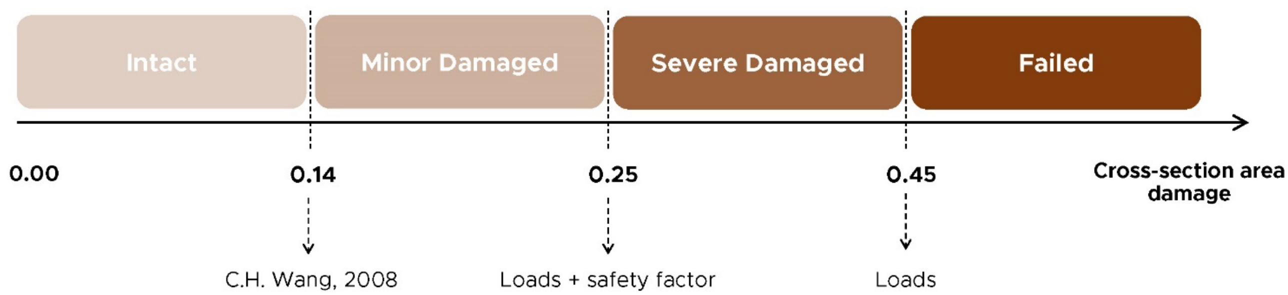

Figure 3.34: Four discrete states of the cross-sectional area of component 7 defining from ULS, SLS, and research suggestion (Own work)

Action space

The action space plays a role in guiding the management strategies to maintain structural integrity. The ultimate objective is to implement maintenance and inspection actions that ensure the structures remain in a condition deemed acceptable, balancing effectiveness and economic considerations.

After considering the current inspection and maintenance methods, in this study, the action space is scoped and categorized into four distinct actions for each structural component, designed to address different levels of deterioration and information requirements:

Do Nothing: This action is chosen when the belief state indicates that the structural component is in good condition or when intervening may not be cost-effective at that time.

Inspection: This is a cost-effective action aimed at updating the belief state about the condition of a component. Inspections provide valuable data that help in assessing the current state of the structure, although they do not directly improve the condition of the component.

Repair: This action is used to address early signs of deterioration or damage. Minor repairs are less costly than full replacements and are crucial for extending the lifespan of a component and preventing further degradation. This case study considers repairing using metal fasteners and adding extra elements to reinforce the existing structure.

Replace: This action involves replacing the entire component. It is the costliest option and is typically reserved for cases where the component's condition has severely deteriorated or is no longer feasible to repair.

Different maintenance actions impact building structural components in discrete key ways. As detailed by Neves and Frangopol (2005), the influence of these actions on building components can be represented through one or a combination of the following effects:

1. Improvement of Degradation Condition: Maintenance actions such as replacement can immediately improve a building component's condition. When components are replaced, the degradation condition reverts to an intact or better state as shown in Figure 3.35. This improvement is crucial for ensuring that parts of the structure meet safety and functionality standards without compromising the building's integrity.

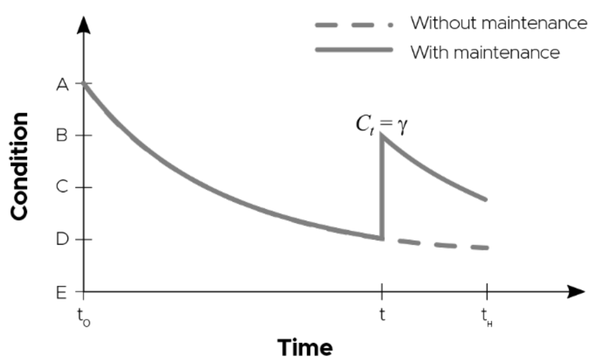

Figure 3.35: Improvement of the degradation condition (Neves & Frangopol, 2005)

2. Suppression of the Degradation Process: Certain maintenance actions can halt the degradation process for a specified period. For example, the use of metal fasteners not only stabilizes the structure but also helps to maintain its form, preventing further deterioration. This is particularly effective in controlling the shape of the structure, thereby mitigating factors like moisture penetration that can accelerate degradation. During the period of suppression, the component does not deteriorate, which is beneficial for extending the life span of vulnerable elements within the structure. The effect can be depicted in the figure below.

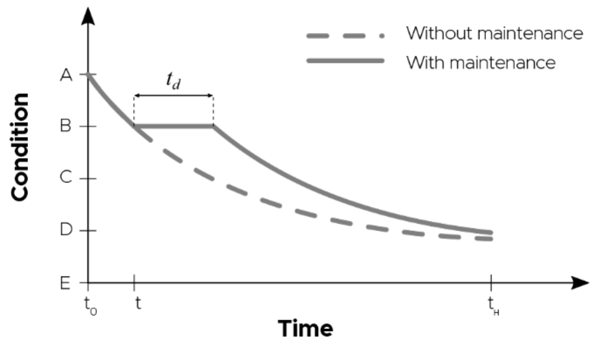

Figure 3.36: Suppression of the degradation process during a given period (Neves & Frangopol, 2005)

3. Reduction of the Degradation Rate: Other maintenance interventions are designed to reduce the rate of degradation. This approach involves adjusting how quickly a component deteriorates over time by introducing supportive measures like additional structural reinforcements. These reinforcements help to distribute loads more evenly, thereby reducing the stress on aging components. By doing so, the overall degradation rate is slowed, extending the functional life of the building components and delaying the need for more invasive repairs.

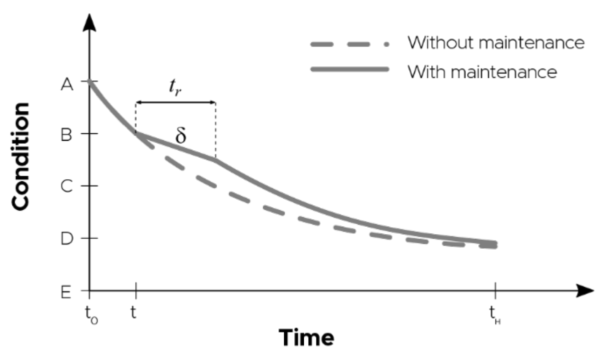

Figure 3.37: Reduction of the degradation rate during a given period (Neves & Frangopol, 2005)

The table below provides a summary of the actions available, along with their respective consequences and costs for the environment setup.

Index	Actions	Consequences	Costs	Ratio
a_0	No inspection, no action	Transition according to the transition model	0	0
a_1	Inspection, no action	Transition according to the transition model and update belief according to the observation model	C_i	0.01 * C_r
a_2	Minor maintenance: Repair: Fixing damaged components with steel fasteners	The state of the component remains unchanged for a determined period, then resume at the original rate	C_{m1}	0.70 * C_r
a_3	Major maintenance: Adding reinforcement elements	Reduce and delay deterioration rate	C_{m2}	Cannot define
a_4	Major maintenance: Replace: Whole replacement of damaged components	Reset the deterioration rate and the damage of the component to the intact state	C_r	1 * C_r

Table 3.5: Four Actions with their consequences and costs

By selecting from these actions, agents can strategically manage each component of the structure based on its current state, predicted deterioration, and the costs associated with each action. This action space thus enables a dynamic and responsive maintenance strategy, tailored to maximize the longevity and safety of the structure while optimizing resource allocation.

Transition Probabilities

Transition probabilities model how the state of a system evolves over time, particularly in response to various actions taken by the agent. For the purposes of this thesis project, these probabilities are used to describe the likelihood of transitioning from one structure's condition state to another, within the context of managing structural integrity.

The transition model is constructed by generating a large number of random samples using the gamma process tailored to a specific climate scenario. This data is used to calculate how frequently state transitions occur, thereby defining the probabilities of moving between different states of deterioration.

This model not only predicts state transitions but also updates the belief state with each decision step. This updated belief state is then used to estimate the probability of structural failure in subsequent steps. The structure of the transition probabilities matrix is denoted as (A, S, S), where A represents the number of possible actions, and S denotes the number of discrete belief states.

The transition probabilities are specifically arranged in a matrix form:

$$P(s_{t+1}|s_t,\ a_t) = \begin{bmatrix} p(s_0|s_0) & p(s_1|s_0) & p(s_2|s_0) & p(s_3|s_0) \\ 0 & p(s_1|s_1) & p(s_2|s_1) & p(s_3|s_1) \\ 0 & 0 & p(s_2|s_2) & p(s_3|s_2) \\ 0 & 0 & 0 & p(s_3|s_3) \end{bmatrix}$$

$$\sum_{i=0}^{n} P(s'|s_n) = 1$$

Here, $P(s_{t+1}|s_t)$ is the transition model for an environment undergoing deterioration, where $p(s_i|s_j)$ indicates the likelihood of transitioning to a state s_i from state s_j. This matrix explicitly shows that states do not revert to a better condition once they have deteriorated, as evidenced by the zeros below the diagonal—reflecting the irreversible nature of damage once it has occurred. The sum of the probabilities for any given state transition scenario equals one, ensuring a complete and normalized model. This meticulous construction of transition probabilities provides a robust framework for predicting and managing the evolution of structural states under varying operational and environmental conditions.

$$P(s'|s, \{"Do\ nothing", "Inspect"\}) = \begin{bmatrix} 0.928 & 0.072 & 0. & 0. \\ 0. & 0.914 & 0.086 & 0. \\ 0. & 0. & 0.959 & 0.041 \\ 0. & 0. & 0. & 1. \end{bmatrix}$$

$$P(s'|s, \{"Repair"\}) = \begin{bmatrix} 1. & 0. & 0. & 0. \\ 1. & 0. & 0. & 0. \\ 0. & 1. & 0. & 0. \\ 0. & 0. & 1. & 0. \end{bmatrix}$$

$$P(s'|s, \{"Replace"\}) = \begin{bmatrix} 1. & 0. & 0. & 0. \\ 1. & 0. & 0. & 0. \\ 1. & 0. & 0. & 0. \\ 1. & 0. & 0. & 0. \end{bmatrix}$$

Observation Probabilities

In the Dec-POMDP framework, observation probabilities are essential for accurately inferring the current state of a structure based on the actions and observations of an inspector. These probabilities quantify the likelihood of observing a particular outcome given the actual state of the environment and an action taken by the agent. Specifically, they help in reducing the uncertainty associated with the belief state, particularly through visual inspections which, despite their utility, do not always guarantee perfect observations due to the potential misinterpretation of the structural condition.

The observation model for this framework is captured by a matrix O, where the element $O = [p\left(o_{t+1}^{(l)} = j \,\middle|\, x_{t+1}^{(l)} = i, a_t\right)]_{i,j \in X}$ defines the probability of observing the state j given the true state i of component l after action a_t has been taken. In this study, it is assumed that inspectors correctly infer the state of the structure with a probability of $p = 0.8$. This leads to an observation matrix for each component l of size $S \times S$, where S is the number of possible states (or beliefs).

$$O(o_{i+1} = j | s_{t+1} = i, a_t) = \begin{bmatrix} p & 1-p & 0 & 0 \\ (1-p)/2 & p & (1-p)/2 & 0 \\ 0 & (1-p)/2 & p & (1-p)/2 \\ 0 & 0 & 1-p & p \end{bmatrix}$$

This matrix configuration suggests that while the agent observes the correct component state with a high probability p, there is still a chance of observing adjacent states, indicating imperfect observations. In scenarios of perfect observation, the matrix would simply be the identity matrix, where the diagonal elements are 1, reflecting absolute certainty in observation:

$$O = \begin{bmatrix} 1 & 0 & 0 & 0 \\ 0 & 1 & 0 & 0 \\ 0 & 0 & 1 & 0 \\ 0 & 0 & 0 & 1 \end{bmatrix}$$

This observation model assigns a probability of 1 to observing the true state, highlighting the ideal but often unattainable scenario of perfect inspection accuracy. Such detailed modeling of observation probabilities in the Dec-POMDP framework allows for a more nuanced understanding and management of structural integrity assessments under uncertainty.

$$O(o|s', \{"Do\ nothing", "Repair", "Replace"\}) = \begin{bmatrix} 0.2 & 0.2 & 0.2 & 0.2 \\ 0.2 & 0.2 & 0.2 & 0.2 \\ 0.2 & 0.2 & 0.2 & 0.2 \\ 0.2 & 0.2 & 0.2 & 0.2 \end{bmatrix}$$

$$O(o|s', \{"Inspect"\}) = \begin{bmatrix} 0.9 & 0.1 & 0. & 0. \\ 0.05 & 0.9 & 0.05 & 0. \\ 0. & 0.05 & 0.9 & 0.05 \\ 0. & 0. & 0.1 & 0.9 \end{bmatrix}$$

Reward function

The reward function is designed to support the primary objective of minimizing maintenance costs in the management of timber structures. It quantitatively assesses the economic impact of various actions within the structured environment, guiding decision-making towards cost-efficiency.

The reward function incorporates all monetary costs associated with the maintenance and inspection of timber structures, ensuring a comprehensive evaluation of financial implications. These costs include:

Cost of Maintenance Actions: This includes expenses incurred from performing maintenance activities on a timber structure, as detailed in the previously mentioned table. These actions are necessary to prevent or correct deterioration and extend the lifespan of the structure.

Cost of Inspection Actions: This covers the costs associated with conducting inspections to assess the current condition of the timber structures. Inspections are critical as they provide the data needed to update the belief state of the structure's condition and to make informed decisions about subsequent maintenance actions.

Cost of Global Failure: This involves the financial implications associated with a complete failure of a timber structure, encompassing the replacement costs, potential liability, loss of service, and other associated consequences. Given the severe impact of such events, this cost is typically substantial. For instance, the cost could be estimated at 100 times the average cost of maintenance actions, reflecting the severe financial and operational repercussions of a global failure.

By integrating these cost elements, the reward function effectively prioritizes actions that yield the greatest benefit in terms of cost savings and structural health, guiding the system toward the most economical and effective maintenance strategies. This tailored reward function is essential for managing the delicate balance between maintaining safety and minimizing expenditure in timber structure maintenance.

Discount factor

The discount factor, denoted as γ, plays a role in balancing the importance of immediate versus future decisions within the decision-making process. γ is a positive scalar-valued less than 1, which quantitatively adjusts the weight given to rewards received at different times. Specifically, a lower value of γ (approaching 0) signifies that the decision-making is predominantly influenced by immediate outcomes, effectively focusing the strategy on the present moment. In this scenario, only the rewards obtained in the current decision step, t, are considered, discounting the importance of future rewards.

Conversely, when γ is set closer to 1, the model attributes nearly equal significance to decisions made across all time steps up to a designated horizon, T. This implies that every decision, from the initial to the final step within the specified time frame, contributes equally to the overall outcome, promoting a strategy that is more forward-looking and comprehensive. By adjusting γ, decision-makers can strategically shift the focus of the model between immediate and long-term objectives, allowing for a tailored approach to planning and execution in complex environments where both present actions and future outcomes are critical.

Finding the optimal policy

After each component of the Dec-POMDP is thoroughly defined, effectively completing the setup of the environment, the subsequent step involves developing an optimal inspection and maintenance policy for this environment.

This section will delve into the implementation of the IMP-MARL algorithm and the benchmarks for comparison.

Algorithm

In the previous section of this report, we explored the main categories of Multi-Agent Reinforcement Learning for Infrastructure Management Planning (IMP-MARL) algorithms. Building upon that foundational knowledge, the initial implementation of MARL in our study employed the uncorrelated k-out-of-n method, particularly focusing on a system with three components. This trial utilized the QMIX algorithm, which is known for its Monotonic Value Function Factorization approach, tailored specifically for deep multi-agent reinforcement learning scenarios. The setup was configured to handle three distinct actions for each agent: Do Nothing, Inspection, and Replace. The entire trial was facilitated using the EpyMARL wrapper, a versatile tool that provides a structured environment for running and evaluating MARL algorithms. This running was based on the GitHub repository provided by Pascal Leroy and his coworkers, leveraging their collective expertise and contributions to ensure the robustness and efficacy of the implementation. This configuration represents a strategic application of MARL techniques, aimed at optimizing decision-making processes in a controlled, yet complex, multi-agent setting.

Benchmarks

In this study, the benchmarking process is grounded in a traditional heuristic approach, which utilizes a conventional method where decisions are driven by a set of predefined, optimized rules. These rules are specifically designed to minimize inspection and maintenance costs while effectively managing the probabilities of system failure. For the initial experiment within this benchmark framework, the performance of heuristic policies is quantitatively evaluated based on their ability to optimize rewards. The specific values for these rewards are derived from a dictionary that is part of the extensive resources available on the GitHub repository maintained by Pascal Leroy and his coworkers. This approach ensures that the benchmark not only reflects realistic operational conditions but also adheres to established industry practices, providing a robust baseline against which the efficacy of more advanced Multi-Agent Reinforcement Learning (MARL) strategies can be assessed.

4

Results and analysis

This section shows the results and discussion of the outcomes derived from applying this strategy to determine the optimal policy. Each result will be briefly analyzed and discussed in the respective section.

Results

The preceding sections have detailed the algorithm selected for identifying the optimal policy and the benchmarks used to verify the results. This section presents the application of the algorithm to a specific case study, which includes a comprehensive description of the training process and the data obtained from it.

The training environment utilizes the EpyMARL wrapper, enabling a four-hour training session during which agents interact with their surroundings. As the agents engage with the environment, the distributions of observations and rewards evolve, showcasing the learning process through the data collected.

Given the time limitations, the study applies a 'k-out-of-n' framework, selecting only five components for analysis. The failure criterion is stringent, with all five components required to fail for the overall system to be considered failed. Each component is chosen based on the variation in failure modes, type of cross-sectional area, and exposure to environmental conditions.

In this framework, four different actions are implemented: do nothing, inspect, repair, and replace. These actions allow for dynamic decision-making as each component's state and the associated risks evolve. The analysis highlights the unique policies adapted for each component, which differ according to their state configurations and transition probabilities from the deterioration model.

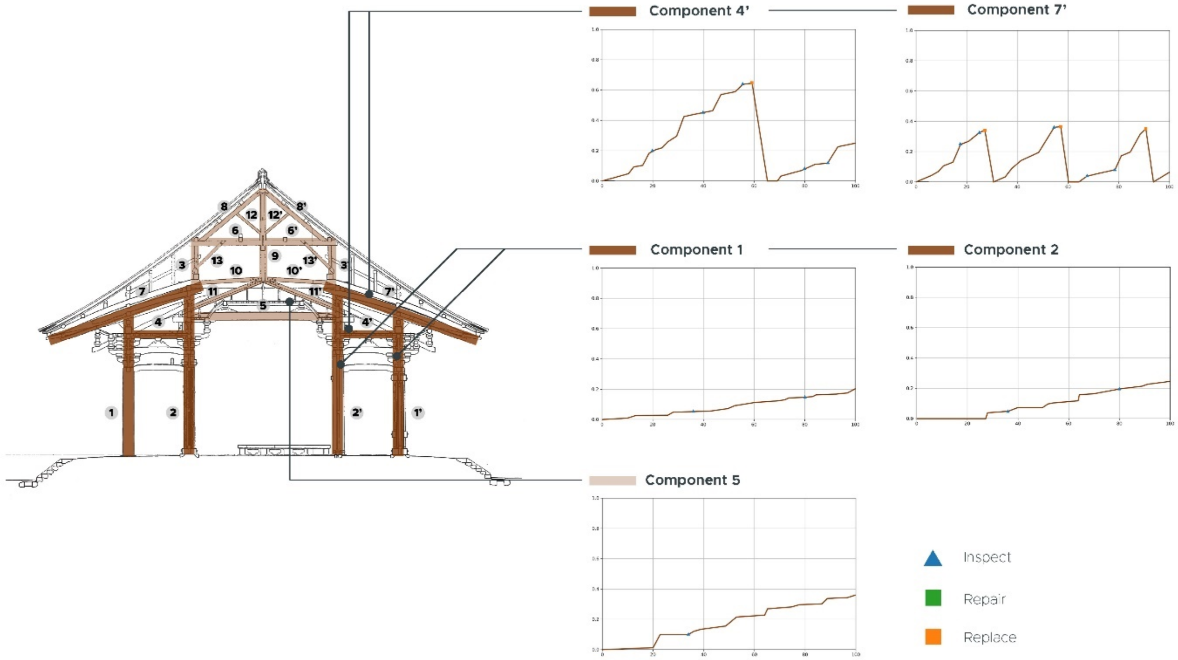

Figure 4.1: Policy realization of five components (Own work)

The initial performance analysis of the run shows that, while the outcomes are somewhat comparable to those of heuristic-based policies, significant advantages emerge when contrasted with traditional maintenance methods, particularly those employed in Japan. The conventional Japanese approach typically involves dismantling the entire building and reassembling it, a process that not only requires a large number of skilled workers but is also time-consuming.

In contrast, the component-based policy employed in this study offers a markedly more efficient solution. By focusing on individual component failures and addressing these through targeted actions such as inspection, repair, or replacement, this policy minimizes downtime and reduces the need for extensive labor. This approach not only optimizes maintenance operations but also potentially decreases overall costs and disruption, making it a compelling alternative to traditional methods. This efficiency gain underscores the value of adopting advanced maintenance strategies like MARL, which facilitate precise and adaptive decision-making in complex systems.

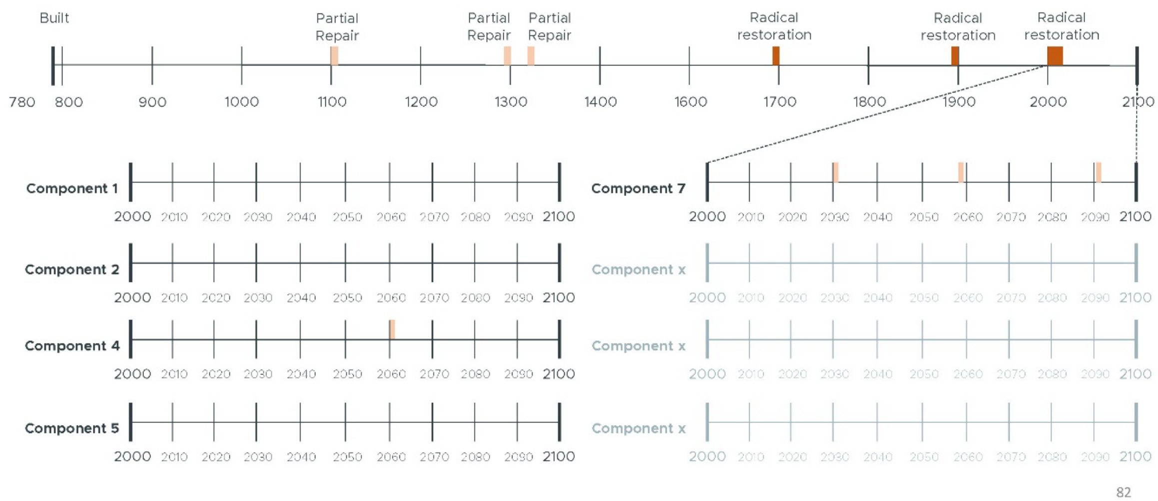

Figure 4.2: Policies for each component in the timeline (Own work)

Analysis

In the initial analysis, the study focused on five distinct components, each characterized by its unique deterioration model. The policies derived highlight the differences in policies between each component, reflecting variations in their states and transition probabilities. Components exhibiting higher rates of deterioration are identified as requiring more frequent maintenance actions. Notably, the analysis observed minimal utilization of the repair action. This outcome may be attributed to the minimal cost difference between the repair and replacement actions within the action model, suggesting a potential area for model adjustment to better distinguish between these actions.

Although the preliminary findings did not demonstrate a marked performance advantage of Multi-Agent Reinforcement Learning (MARL) methods over traditional heuristic-based policies, research by Pascal Leroy et al. (2023) supports the superiority of MARL in more complex scenarios. MARL's strength lies in its ability to manage intricate, high-dimensional decision spaces and coordinate the interdependencies among numerous agents in expansive systems. This capability becomes increasingly significant as the number of agents and the complexity of the environment grow.

There is potential for further optimization of the environment setup to improve both efficiency and accuracy in future studies. Additionally, the exclusion of climate scenarios in this initial analysis is noted as a limitation that could significantly influence the outcomes in subsequent runs. Integrating these scenarios could provide a more comprehensive understanding of the environmental impacts on component deterioration and policy effectiveness.

5

Discussion, conclusion, and reflection

Conclusion

This analysis underscores the potential of Multi-Agent Reinforcement Learning (MARL) methods in optimizing inspection and maintenance policies within large-scale infrastructure systems. Although the initial results are promising, they do not conclusively demonstrate the superiority of MARL over heuristic approaches under the tested conditions. However, the literature and prior studies indicate that MARL's advantages are likely to become more apparent in more complex scenarios involving a greater number of agents and environmental variables. Future explorations should focus on refining the environmental setup and incorporating variables such as climate scenarios, which could critically affect the outcomes. It is also essential to expand the deterioration models to include all components rather than a subset, to provide a more comprehensive assessment of MARL's capabilities.

To address the research question, "How can machine learning consider climate change effects to inform inspection and maintenance for timber structures?" the study proposes a detailed workflow requiring specific inputs:

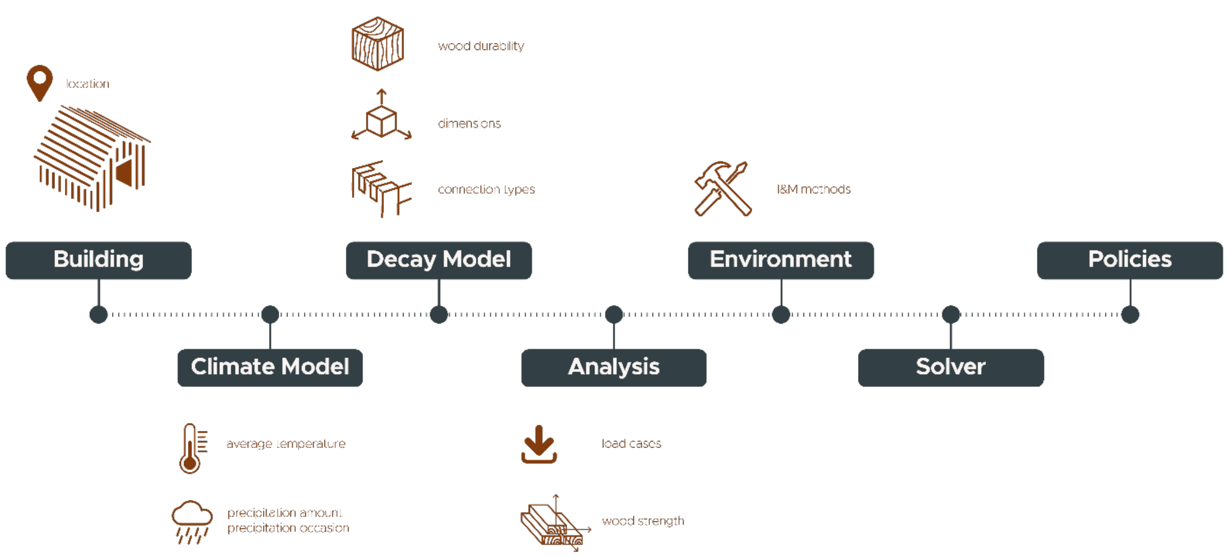

Figure 5.1: Framework's workflow with the required information (Own work)

1. Specification of the timber building and its location,
2. Climate data for the location,
3. Identification of the wood species and its properties,
4. Dimensions of each structural component,
5. Types of connections between components,
6. Load cases applicable to the building,
7. Inspection and maintenance methods applied to the building.

This framework, while simplified, highlights the foundational elements necessary for integrating climate change effects into machine learning models for timber structure maintenance. The components and considerations excluded from this study are further elaborated in the reflection section that follows.

Thus, while these findings contribute valuable insights into the application of MARL for infrastructure management, they represent only the beginning of a more extensive exploration into its potential. Further research and more detailed simulations are needed to fully leverage MARL's capabilities and refine the strategies for practical applications.

Reflection

MARL Method's Efficacy vs. Traditional Methods

The initial findings suggest that the MARL approach could potentially enhance the efficiency of inspection and maintenance plans for historical timber structures by adopting a proactive strategy. This strategy aims to identify and address potential structural failures before they reach critical stages, contrasting with traditional methods that rely heavily on visual inspections and the experience and judgment of inspectors. While the current results do not yet show a significant advantage over heuristic methods, MARL holds promise for reducing the need for detailed inspections of every component. By allowing for more targeted maintenance, MARL could save time and resources, and minimize human error in the long run. Further research and refinement of this approach are needed to fully realize these potential benefits.

Traditionally, major maintenance of the case study structure, a 1244-year-old temple in Nara, Japan, involved a complete dismantling and reassembly approximately every 100 years, a process that could extend up to a decade. The MARL-generated policies suggest a shift from this highly labor-intensive and time-consuming method to a more efficient, data-driven approach.

Limitations and Challenges

Even though the perks of this machine learning method are previously mentioned, there are some challenges and limitations that should be pointed out for this study.

1. Complexity and Accessibility:
   The complexity of setting up and operating the MARL framework is a significant barrier. This complexity limits accessibility for practitioners who are not well-versed in artificial intelligence techniques as it requires specific technical skills and resources, which may not be readily available, particularly in regions with limited technological infrastructure.

2. Exclusions in the Study:

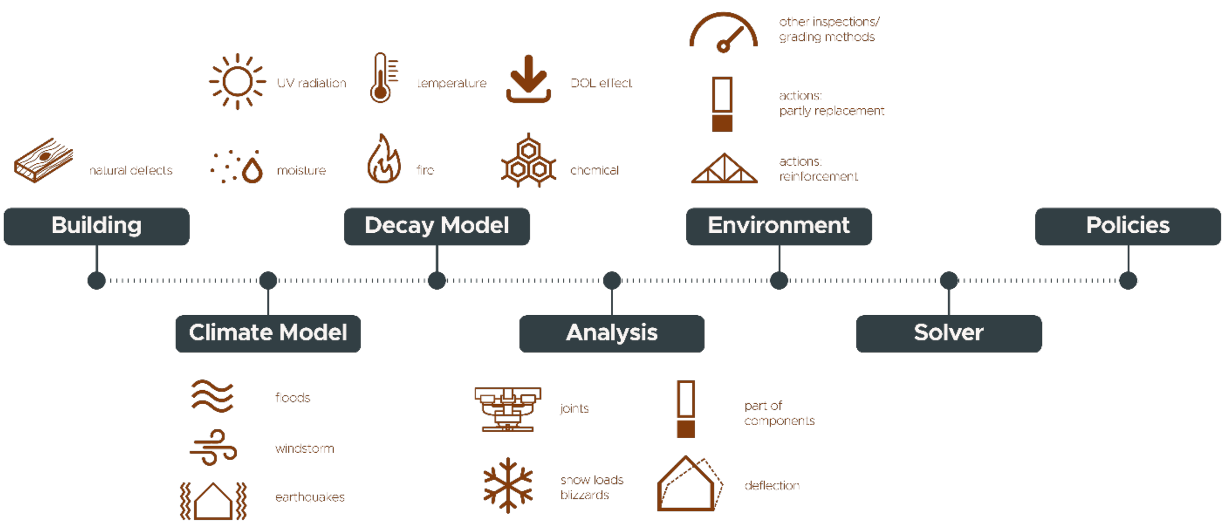

Figure 5.2: Exclusions from the study (Own work)

- Natural Defects in Timber: Timber, as an organic material, inherently possesses natural defects that arise during its growth. These defects include knots, pitch pockets, cross-grain, and other irregularities that can significantly affect the mechanical properties and strength of wood. The complexity and variability of these defects present substantial challenges in predicting their effects on timber's performance, particularly under changing climatic conditions. Due to the broad scope of this study and the difficulty in quantifying how these defects influence long-term deterioration, a detailed analysis of natural timber defects has been excluded. Future research could focus on integrating advanced imaging and analysis techniques to better understand and model how these natural variations impact the structural integrity of timber.

- Timber Deterioration Factors and other Modes of Timber Failure Criteria: The study excluded several critical factors affecting timber deterioration due to the lack of comprehensive data on their precise impacts and the complex interactions with climate change. These exclusions include:

1. **Weather-related Factors:** Direct effects from environmental conditions such as temperature fluctuations, moisture levels, ultraviolet (UV) radiation, and exposure to fire. Each of these factors can independently or synergistically influence the degradation and longevity of timber structures.

2. **Time-related Factors:** The duration of load effects and chemical changes over time in the cellular structure of timber. These aspects involve the gradual transformation in wood properties under sustained loads and the natural aging process, which can weaken timber's structural capabilities.

3. **Mechanical Integrity:** Timber failure due to cracking and other structural integrity issues that arise from internal stresses, material fatigue, or external forces. Cracking is a significant concern as it can compromise the load-bearing capacity and overall stability of timber constructions.

- **Extreme Events:** The model does not account for extreme climate-related events such as floods, windstorms, blizzards, or earthquakes. These are critical gaps, given that such events are likely to increase in frequency and intensity due to climate change.

- **Analysis of Traditional Japanese Timber Joints:** In traditional Japanese timber structures, the joints between components are critical for ensuring structural stability and durability. These structures typically utilize dry joint connections that do not involve glue, bolts, nails, or screws. Instead, they rely on precise and complex carpentry techniques that allow the components to fit together seamlessly, providing both aesthetic appeal and structural integrity without metal fasteners. Despite their crucial role, the specific analysis of these discrete joints—each varying depending on its position within the structure—will not be included in this study due to time constraints. Acknowledging their importance, this research will focus more broadly on the structural integrity and decay of the overall construction, deferring the detailed examination of dry joints to future investigations.

- **Snow load in Structural Analysis:** The study does not account for the impact of snow load in the Finite Element Analysis (FEA). This is primarily due to the uncertainty surrounding the projected increases in snowfall and the duration of snow cover as consequences of climate change. Reliable data on these variables are crucial for accurately modeling the additional stress and strain that snow can impose on timber structures, particularly in regions prone to heavy snowfall.

- Partial Decay of Structural Components: Observations from onsite visits to Japanese timber structures revealed that decay does not occur uniformly across structural components. Different parts of a single component may be exposed to varying levels of weathering, with areas experiencing higher moisture levels showing more significant decay and potential fungal growth. The study does not delve into the granularity of decay at the component level nor does it explore methods for partial replacement of components. This is a significant area for future development, as understanding and addressing partial decay can lead to more targeted and efficient maintenance strategies, reducing the need for complete component replacement.

- Structural Deflection: The deflection of the structure under specific load cases, which could indicate the transitional state of a timber structure's condition, is also excluded from this study. Monitoring and analyzing deflection can provide valuable insights into the structural health of timber and its ability to withstand external loads over time. In this study, the deflection analysis is already conducted, however, its effects on the structure's condition are not yet included in the current research framework.

- Advanced Inspection and Maintenance Techniques: The study did not incorporate various developing NDT methods that utilize supervised learning to detect flaws or deterioration in timber structures. These methods, which can include technologies like ultrasonic testing, infrared imaging, and digital radiography, represent a significant advancement in the ability to diagnose structural health without causing damage to the material.

  Including these NDT methods in the MARL framework could potentially refine maintenance policies by providing more precise data on the condition of the structure, leading to even more targeted and effective maintenance interventions.
- Innovative Maintenance Approaches: Another significant exclusion from the research was the exploration of maintenance methods that involve adding redundant structures to reinforce existing timber without the need for dismantling. This approach can offer a less invasive and potentially more cost-effective alternative to traditional methods that require extensive disassembly and reassembly of structures.
  Integrating these maintenance techniques into the MARL model could provide a broader range of solutions for preserving historical timber structures, especially in scenarios where traditional restoration methods are either too invasive or economically unfeasible.

The exclusion of these cutting-edge inspection and maintenance techniques may limit the scope of the MARL policies developed in this study. By not incorporating the full spectrum of available technologies, the model might not fully capitalize on the potential efficiencies and effectiveness these methods offer.

- Unexplored Reinforcement Learning Methods: This study focuses on the application of Multi-Agent Reinforcement Learning (MARL) for the inspection and maintenance planning of historical timber structures. However, there are several other reinforcement learning techniques and configurations that were not explored within this framework. Techniques such as Deep Reinforcement Learning (DRL), which utilizes deep neural networks to handle high-dimensional state spaces, could potentially offer more nuanced insights into complex decision-making scenarios involving historical preservation. Additionally, Single-Agent Reinforcement Learning, although less suited to scenarios requiring coordination among multiple decision-makers, could provide valuable baseline comparisons or simpler models for initial exploratory analysis.
  The potential integration of hybrid models combining elements of both MARL and DRL, or the use of alternative reward structures and state representations, also remains unexplored. These methods could further refine the accuracy of predictive maintenance schedules and adapt more dynamically to the unique challenges posed by the preservation of historical timber structures under the impact of climate change.

Recommendations for Future Research

The study of historical timber structures under the influence of climate change and their maintenance using Multi-Agent Reinforcement Learning (MARL) has opened several avenues for exploration and highlighted specific areas where current research is limited. While this thesis has laid foundational work in understanding the complexities of maintaining timber structures, several critical factors were necessarily excluded due to constraints in data, technology, and scope. These exclusions not only define the limitations of the current study but also delineate clear paths for future research.

Addressing these gaps is crucial for advancing the field and enhancing the practical application of conservation techniques. The following recommendations are designed to guide subsequent investigations, ensuring that future research builds comprehensively on the insights gained and addresses the nuanced challenges of preserving historical timber structures in a changing climate. Each recommendation corresponds directly to the exclusions identified, proposing targeted studies and methodologies that promise to refine our understanding and improve the longevity and integrity of these valuable cultural assets.

1. Integration of Natural Defects in Timber Analysis:
   Future research should incorporate detailed studies on the natural defects of timber, such as knots, pitch pockets, and cross-grain. Advanced imaging techniques, machine learning models, or stochastic models that simulate the random nature of defect impact on timber strength and durability could be used to predict how these defects affect the timber's mechanical properties and long-term durability under various environmental conditions.
2. Comprehensive Timber Deterioration and Failure Criteria:
   Expanding the study to include more exhaustive factors in timber deterioration, such as direct effects from weather-related factors (temperature, moisture, UV radiation, and fire) and time-related factors (duration of load effects and chemical changes in timber's cellular structure) can be challenging. While experiments have been conducted on certain wood species, these studies have not yet culminated in a generalized model applicable to a broad range of wood species. To address this, the following specific steps are recommended:
   - Species-Specific Analysis/Experiments: Conduct controlled experiments on various wood species to understand specific degradation patterns under different environmental conditions.
   - Predictive Model Development: Use experimental data to develop predictive models that reflect the unique responses of different wood species to environmental stressors.
   - Long-Term Observational Studies: Monitor historical timber structures over extended periods to validate laboratory findings and adjust models based on real-world data.
   - Enhanced Simulations: Improve simulation models to include detailed wood chemistry and structural responses to prolonged environmental exposure and mechanical stress.

3. Inclusion of Extreme Events in Structural Analysis:

   Integrate models that account for extreme weather events such as floods, earthquakes, and increased snow load due to climate change. This could involve developing probabilistic models that simulate the impact of these events on structural integrity over time.

4. Specialized Studies of Traditional Japanese Timber Joints:
   Conduct specialized studies focusing on the unique construction techniques of traditional Japanese timber joints. These joints are fundamental to the structural stability and aesthetic integrity of timber structures and require comprehensive analysis under various stress conditions. The steps that can enhance the understanding of these joints are as follows:
   - Detailed FEA Modeling: Utilize FEA models to simulate the behavior of the joints under various loads. This simulation should accurately reflect the intricate

carpentry techniques used in these joints, allowing for precise analysis of stress distribution and joint performance.

- Incorporation of Decay Effects: It is critical to investigate the impact of decay, particularly how the loss of cross-sectional area due to deterioration affects the mechanical properties and load-bearing capacity of the joints. This analysis should consider different stages of decay and their corresponding impact on structural integrity.
- Advanced Imaging and Scanning: Employ advanced imaging and scanning techniques to assess the internal condition of the joints, focusing on areas susceptible to decay. This technology can provide a more accurate assessment of the extent of decay and its spatial distribution within the joint.
- Material Property Assessment: Analyze how the deterioration of material properties due to decay influences the overall behavior of the joints. This involves studying changes in the wood's mechanical properties such as elasticity, strength, and toughness as the material loses mass and integrity.
- Load Redistribution Analysis: Explore how the deterioration and loss of material in one part of the joint affect the load redistribution across the entire joint structure. Understanding this redistribution is crucial for predicting failure modes and for planning appropriate maintenance or reinforcement strategies.

5. Snow Load Impact Studies:
   Future models should incorporate dynamic climate data to assess the impact of changing snow load patterns on timber structures. This involves collaboration with climatologists to obtain accurate, predictive climate models for snowfall and temperature variations.
6. Targeted Research on Partial Decay of Structural Components:
   Investigate the partial decay phenomena in timber components, focusing on differential decay patterns due to varied environmental exposures. Implement localized treatment and maintenance strategies that include partial replacements or localized strengthening techniques in the framework.
7. Analysis of Structural Deflection Under Load:
   Implement sensors and monitoring technologies to study how timber structures deflect under various load cases. This data can help refine the predictive models used in MARL to better anticipate and mitigate potential failures.
8. Exploration of Advanced Inspection and Maintenance Techniques:

   Explore and integrate advanced NDT methods that utilize emerging technologies in AI and machine learning to improve the detection and analysis of structural weaknesses without damaging the material. The more precise the data gathered from these methods, the more robust the reinforcement learning framework will become.

9. Development of Innovative Maintenance Approaches:

Research the effectiveness of adding redundant structures or reinforcements that do not require dismantling the original timber framework. Such studies would provide alternatives that preserve structural integrity while maintaining the historical authenticity of the structure.

10. Exploration of Diverse Reinforcement Learning Methods:
Investigate the potential of different reinforcement learning configurations, including Deep Reinforcement Learning and hybrid models, to handle complex decision-making environments more effectively. This could enhance the adaptability and efficiency of maintenance planning for historical structures under varied and changing conditions.

Societal and Ethical Implications

1. Potential Societal Impact: If broadly implemented, the MARL method could revolutionize the maintenance of historical timber structures worldwide, potentially extending their lifespan and reducing maintenance costs. This would have significant cultural and economic benefits by preserving heritage structures in a more sustainable manner. Moreover, a deeper understanding of the factors that affect timber's structural strength can enhance the use of timber in modern buildings. This knowledge can improve the efficiency and resilience of modern timber construction, supporting the broader adoption of timber as a sustainable building material.
2. Ethical Considerations: The use of advanced technologies in historical conservation raises ethical questions, particularly regarding the potential for technology to replace traditional practices and skills, which are cultural heritages in their own right. There is a need to balance technological advancement with the preservation of traditional crafts and techniques. As the understanding of timber's properties improves, it is vital to consider how these technologies can complement rather than replace the craftsmanship that defines many cultural heritage structures.
3. Sustainability and Environmental Impact: The project aligns with sustainable development goals by promoting the longevity of materials and reducing the frequency of invasive maintenance procedures, which can be both resource-intensive and environmentally taxing. Enhanced knowledge and application of timber's strength factors not only benefit the conservation of historical structures but also pave the way for more sustainable practices in contemporary architecture. By demonstrating the viability and durability of timber, the research supports its wider use as a sustainable material in the construction industry, potentially reducing reliance on more environmentally harmful materials.

References

Aghayere A, V. J. (2007). Structural Wood Design a Practice-Oriented Approach Using the Asd Method.

Andriotis, C. P., & Papakonstantinou, K. G. (2019). Managing engineering systems with large state and action spaces through deep reinforcement learning. *Reliability Engineering & System Safety*, *191*, 106483. https://doi.org/https://doi.org/10.1016/j.ress.2019.04.036

C.H. Wang, R. H. L., M.N. Nguyen. (2008a). *Manual 4 - Decay above-ground*.

C.H. Wang, R. H. L., M.N. Nguyen. (2008b). *Manual 9 – Models for timber protected in building envelope*.

Carll, C. G. (2009). *Decay Hazard (Scheffer) Index Values Calculated from 1971–2000 Climate Normal Data*.

Cruz, H., Jones, D., & Nunes, L. (2015). Wood. In M. C. Gonçalves & F. Margarido (Eds.), *Materials for Construction and Civil Engineering: Science, Processing, and Design* (pp. 557-583). Springer International Publishing. https://doi.org/10.1007/978-3-319-08236-3_12

Csébfalvi, A., & Len, A. (2020). THE CLIMATE IMPACT ON TIMBER STRUCTURES. *Iran University of Science & Technology*, *11*, 143-154.

EN 1995-1-1 Eurocode 5: Design of timber structures - Part 1-1: General-Common rules and rules for buildings, (2004).

Gedeon, G. (1999). *Wood handbook--Wood as an engineering material*.

IPCC. (2023a). *Climate Change 2023: Synthesis Report* (Contribution of Working Groups I, II and III to the Sixth Assessment Report of the Intergovernmental Panel on Climate Change, Issue.

IPCC. (2023b). *Synthesis Report (SYR) Glossary*.

Museum, T. C. T. (2014). Permanent Exhibitions Catalog. In T. C. T. Museum (Ed.).

Nasir, V., Fathi, H., Fallah, A., Kazemirad, S., Sassani, F., & Antov, P. (2021). Prediction of Mechanical Properties of Artificially Weathered Wood by Color Change and Machine Learning. *Materials*, *14*(21), 6314. https://www.mdpi.com/1996-1944/14/21/6314

Neves, L., & Frangopol, D. (2005). Condition, safety and cost profiles for deteriorating structures with emphasis on bridges. *Reliability Engineering [?] System Safety*, 185-198. https://doi.org/10.1016/j.ress.2004.08.018

Niemz, P., Sonderegger, W., Gustafsson, P. J., Kasal, B., & Polocoşer, T. (2023). Strength Properties of Wood and Wood-Based Materials. In P. Niemz, A. Teischinger, & D. Sandberg (Eds.), *Springer Handbook of Wood Science and Technology* (pp. 441-505). Springer International Publishing. https://doi.org/10.1007/978-3-030-81315-4_9

Office of Cultural Assets Preservation, t. B. o. E. i. N. P. (2009). *Toshodai-ji Kondo (Golden Hall)*. B. o. E. Nara Prefecture.

Office of Cultural Assets Preservation, t. B. o. E. i. N. P. (2009). *Report on the Restoration Work at the TOSHODAI-JI KONDO, a National Treasure*. B. o. E. Nara Prefecture.

Pablo G. Morato, C. P. A., Konstantinos G. Papakonstantinou, Philippe Rigo. (2022). Inference and dynamic decision-making for deteriorating systems with probabilistic dependencies through Bayesian networks and deep reinforcement learning. *Reliability Engineering and System Safety* https://doi.org/10.48550/arxiv.2209.01092

Pascal Leroy, P. G. M., Jonathan Pisane, Athanasios Kolios, Damien Ernst. (2023). IMP-MARL: a Suite of Environments for Large-scale Infrastructure Management Planning via MARL. https://doi.org/https://doi.org/10.48550/arXiv.2306.11551

Pierre Berard, P. Y., Hidefumi Yamauchi, Kenji Umemura, Shuichi Kawai. (2011). Modeling of a cylindrical laminated veneer lumber I: mechanical properties of hinoki (Chamaecyparis obtusa) and the reliability of a nonlinear finite element model of a four-point bending test. *The Japan Wood Research Society*, *57*, 100-106. https://doi.org/10.1007/s10086-010-1150-1

Richard S. Sutton, A. G. B. (2018). *Reinforcement Learning: an Introduction* (Second edition ed.). The MIT Press.
Roszyk, E. (2013). The effect of ultrastructure and moisture content on mechanical parameters of pine wood (Pinus sylvestris L.) upon tensile stress along the grains. *Turkish Journal of Agriculture and Forestry*, *38*, 413-419. https://doi.org/10.3906/tar-1306-81
van Nimwegen, S. E., & Latteur, P. (2023). A state-of-the-art review of carpentry connections: From traditional designs to emerging trends in wood-wood structural joints. *Journal of Building Engineering*, *78*, 107089. https://doi.org/https://doi.org/10.1016/j.jobe.2023.107089
van Noortwijk, J. M. (2009). A survey of the application of gamma processes in maintenance. *Reliability Engineering & System Safety*, *94*(1), 2-21. https://doi.org/https://doi.org/10.1016/j.ress.2007.03.019
Verbist, M., Nunes, L., Jones, D., & Branco, J. M. (2019). 11 - Service life design of timber structures. In B. Ghiassi & P. B. Lourenço (Eds.), *Long-term Performance and Durability of Masonry Structures* (pp. 311-336). Woodhead Publishing. https://doi.org/https://doi.org/10.1016/B978-0-08-102110-1.00011-X
Xin, Z., Ke, D., Zhang, H., Yu, Y., & Liu, F. (2022). Non-destructive evaluating the density and mechanical properties of ancient timber members based on machine learning approach. *Construction and Building Materials*, *341*, 127855. https://doi.org/https://doi.org/10.1016/j.conbuildmat.2022.127855